UNIVERSIDADE FEDERAL DE SANTA CATARINA

PROGRAMA DE PÓS-GRADUAÇÃO EM

ENGENHARIA MECÂNICA

DISPOSITIVO DE PROTEÇÃO CONTRA SOBRECARGAS PARA MOTORES TRIFÁSICOS OPERANDO EM REGIME CONTÍNUO

Dissertação submetida à

UNIVERSIDADE FEDERAL DE SANTA CATARINA

para a obtenção do grau de

MESTRE EM ENGENHARIA MECÂNICA

REINALDO STUART JÚNIOR

Florianópolis, março de 2005

Livros Grátis

UNIVERSIDADE FEDERAL DE SANTA CATARINA
PROGRAMA DE PÓS-GRADUAÇÃO EM
ENGENHARIA MECÂNICA

DISPOSITIVO DE PROTEÇÃO CONTRA SOBRECARGAS PARA MOTORES
TRIFÁSICOS OPERANDO EM REGIME CONTÍNUO

REINALDO STUART JÚNIOR

Esta dissertação foi julgada adequada para a obtenção do título de

MESTRE EM ENGENHARIA
ESPECIALIDADE ENGENHARIA MECÂNICA

sendo aprovada em sua forma final.

_____
Prof. Carlos Alberto Martin, Dr.-Ing. – Orientador

_____
Prof. Dr.-Ing. Frank Berger – Co-orientador

_____
Prof. José Antônio Bellini da Cunha Neto, Dr. - Coordenador do Curso

BANCA EXAMINADORA

_____
Prof. Walter Lindolfo Weingaertner, Dr.-Ing. - Presidente

_____
Prof. Edison Bazzo, Dr.Eng.

_____
Prof. Hari Bruno Mohr, Dr. Eng.

MY GRATITUTE

SUMMARY

LIST OF SIMBOLS AND ABBRE VIATIONS

A	area normal to the heat flow direction	$[m^2]$
A.C.	alternating current	[A]
CSA	Canadian Standards Association	
C_p	specific heat of mass	[J/Kkg]
C_t	thermal capacitance	[J/K]
C_T	calibration time	[s]
$d_{FI\,int}$	bimetal free displacement at I_{int}	[mm]
$d_{F\,Im\,ax}$	bimetal free displacement at I_{max}	[mm]
$d_{F\,Im\,in}$	bimetal free displacement at I_{min}	[mm]
$d_{TI\,int}$	bimetals tripping displacement at I_{int}	[mm]
$d_{T\,Im\,ax}$	bimetals tripping displacement at I_{max}	[mm]
$d_{T\,Im\,in}$	bimetals tripping displacement at I_{min}	[mm]
D.O.L.	direct-on-line a.c. motor starter	
IEEE	The Institute of Electrical and Electronics Engineers	
IEC	International Electrotechnical commission	
I_{int}	intermediary current setting	[A]
I_{lim}	current limit value	[p.u.]
$\bar{I}_{lim}$	average value for I_{lim}	[p.u.]
I_{max}	maximum current setting	[A]
I_{min}	minimum current setting	[A]
I_{rated}	rated current of an electric motor	[A]
$I_{setting}$	current value that has been set at the overload release dial	[A]
I_{start}	starting current of an electric motor	[A]
I_{trip}	current value that has tripped the overload release	[A]
I^2R	Joule losses in electric conductors	[W]
k_I	relation factor between applied current and rated current.	[dimensionless]
k_T	relation factor between applied torque and rated torque	[dimensionless]
k_v	relation factor between applied voltage and rated voltage	[dimensionless]
$k_{\Delta T}$	correction factor for ΔT_{rated} based on power losses	[dimensionless]

k_{fT}	index for power factor = f (applied torque)	[dimensionless]
k_{fv}	index for power factor = f (applied voltage)	[dimensionless]
l	length in the flow direction	[m]
m	mass of system	[kg]
MPW25	motor protective circuit breakers for motors up to 11 kW/400 V (25A)	
n	rotation	[rpm]
NEC	National Electrical Code	
NEMA	National Electrical Manufacturers Association	
p.p.m.	parts per million	
P	active power	[W]
P_f	fixed power losses at a different value of load and voltage	[W]
$P_{f\,rated}$	fixed power losses at rated load and voltage	
	(obtained by tests or calculation)	[W]
P_p	process capability index	[dimensionless]
PTC	positive temperature coefficient thermistors	
PT100	type of platinum resistance thermometer	
P_v	variable power losses at a different value of load and voltage	[W]
$P_{v\,rated}$	variable power losses at rated load and voltage	
	(obtained by tests or calculation)	[W]
Q	reactive power	[kVAr]
q'	heat flow	[W]
R_t	thermal resistance	[K/W]
s	standard deviation	
S	apparent power	[kVA]
SF	service factor	
t_{lim}	corresponding time to reach ΔT_{lim} supposing the motor	
	was previously operating at rated conditions.	[s]
T	load torque	[Nm]
T.E.A.M.	thermal, electrical, ambient and mechanical stresses	
TEFC	Totally Enclosed Fan-Cooled (electric motor)	
T.F.	tolerance field	[mm]

T.L.C.	thermal limit curves	
$T_{\max\,ambient}$	maximum allowable ambient air temperature	[ºC]
$T_{\max\,transient}$	maximum allowable temperature for motor windings at transient conditions	[ºC]
T_p	tripping time	[s]
UL	Underwriters Laboratories	
U_L	upper limit of specifications	
L_L	lower limit of specifications	

a_1	calibration angle range available at MPW25 setting dial cam	[º]
a_2	setting angle range available at MPW25 setting dial cam	[º]
Δd	gap necessary for calibration operation of MPW25	[mm]
ΔT	temperature rise	[K]
$\Delta T_{\lim}$	temperature rise limits for stator windings operating under transient conditions	[K]
$\Delta T_{\max}$	maximum temperature rise	[K]
$\Delta T_{overload}$	temperature rise for stator windings when the motor is submitted to overload conditions	[K]
ΔT_{rated}	temperature rise when the electric motor is submitted to overload conditions	[K]
s_c	thermal conductivity	[W/Km]
t	thermal time constant for heating conditions	[s]

ABSTRACT

Electric motors endurance depends on the strength of the different components employed for manufacturing them. Motor windings are one of the most sensible parts among these components. Their endurance is affected by many factors, among them, their operating temperatures.

This research proposes a thermal model for predicting motors temperature rise when they are submitted to different values of overload currents.

The model is further applied for calculating thermal limit curves for 11 kW electric motors.

One 11 kW motor is subsequently submitted to different overload current tests for validating the proposed model.

Electric motors may be protected against overloads by many different types of devices. Motor protective circuit breakers are employed very often for it. The limits of operation of their overload releases are specified by international standards.

This research also compares these limits of operation, required by the standards, to previously obtained thermal limit curves, for confirming the effectiveness of overload protection provided.

One type of motor protective circuit breaker, applicable for motors up to 11 kW, is further analysed. Test data about their overload releases are compared to the limits of operation required by the standards. Tripping repeatability of these overload releases is subsequently tested and analysed.

Finally, some improvements are recommended for both the analysed motor protective circuit breakers and for the design and quality management procedures nowadays employed for developing and implementing switchgears in a Brazilian company.

RESUMO

A durabilidade dos motores elétricos depende da resistência dos diversos componentes utilizados na sua fabricação. Entre os componentes empregados, enrolamentos de motores são considerados uma das partes mais sensíveis. Sua durabilidade é afetada por diversos fatores, entre os quais a temperatura de operação.

Esta pesquisa propõe um modelo térmico para prever a elevação de temperatura de motores elétricos quando submetidos a diferentes valores de corrente de sobrecarga.

Em seguida, o modelo é utilizado para calcular curvas de limite térmico para motores elétricos de 11 kW.

Subseqüentemente, um motor de 11 kW é submetido a diferentes testes de corrente de sobrecarga para validar o modelo proposto.

Motores elétricos podem ser protegidos contra sobrecargas por muitos tipos diferentes de dispositivos de proteção. Disjuntores para comando e proteção de motores freqüentemente são empregados para este fim. Os limites de operação dos seus disparadores de sobrecarga são especificados por normas internacionais.

Esta pesquisa também compara estes limites de operação, exigidos pelas normas, às curvas de limite térmico obtidas previamente, para confirmar a eficácia da proteção contra sobrecarga que é obtida.

Um tipo de disjuntor, aplicável para comando e proteção de motores elétricos até 11 kW, é adicionalmente analisado. Dados de testes sobre os seus disparadores de sobrecarga são comparados aos limites de operação especificados pelas normas. Posteriormente, a repetibilidade de atuação dos disparadores de sobrecarga é testada e analisada.

Finalmente, recomenda-se algumas melhorias, tanto para os disjuntores analisados, quanto para os procedimentos de projeto e de garantia da qualidade empregados atualmente para o desenvolvimento e implementação de dispositivos de comando, manobra e proteção elétrica em uma empresa brasileira.

CHAPTER 1

INTRODUCTION

This chapter gives an overview about electric motors and about motor control and protection. The text further explains how this research is related to the design of a new motor protective circuit breaker by WEG.

It also explains the objectives of this research and shows the basic structure of the following text.

1.1 – Overview about electric motors and WEG

Electric motors are employed in all human activities. They can be seen installed in home appliances, agriculture, mining activities, ships, industries, shopping centers, leisure centers, etc.

Due to the diversity of applications, there are many different types of electric motors (Figure 1.1).
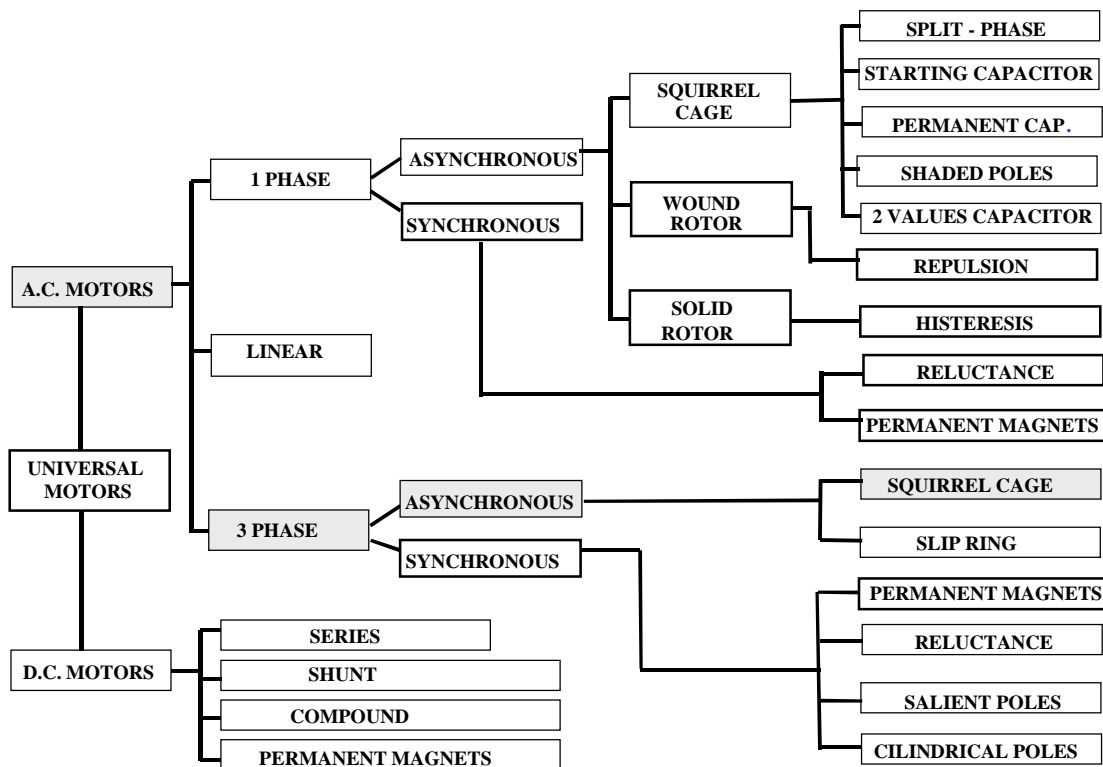
Figure 1.1 – Types of electric motors available in the market /1/

Among these different types, squirrel cage asynchronous three-phase A.C. motors are largely used in industrial applications. The reason for it is this kind of electric motor is simple, robust and has low manufacturing costs /1/.

Squirrel cage asynchronous three-phase A.C. motors may be environmentally protected and cooled in many different ways. A very well known construction is the Totally Enclosed Fan-Cooled (TEFC) motor (Figure 1.2).

This kind of construction has the following advantages for industrial applications:

- Protection for personnel;
- Protection against liquids and solid particles;
- Simple installation and maintenance.
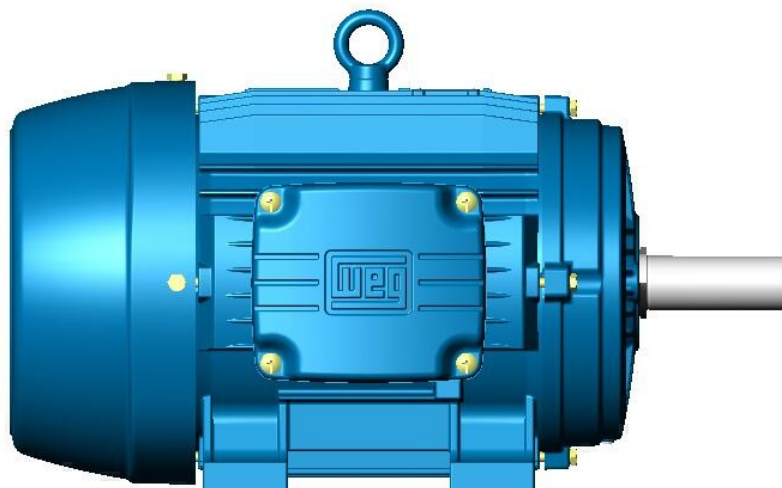
Figure 1.2 – Typical 3 phase squirrel cage TEFC asynchronous motor manufactured by WEG

WEG is a Brazilian company specialized on manufacturing industrial electric systems that includes electric motors and other rotating machines (Figure 1.3).
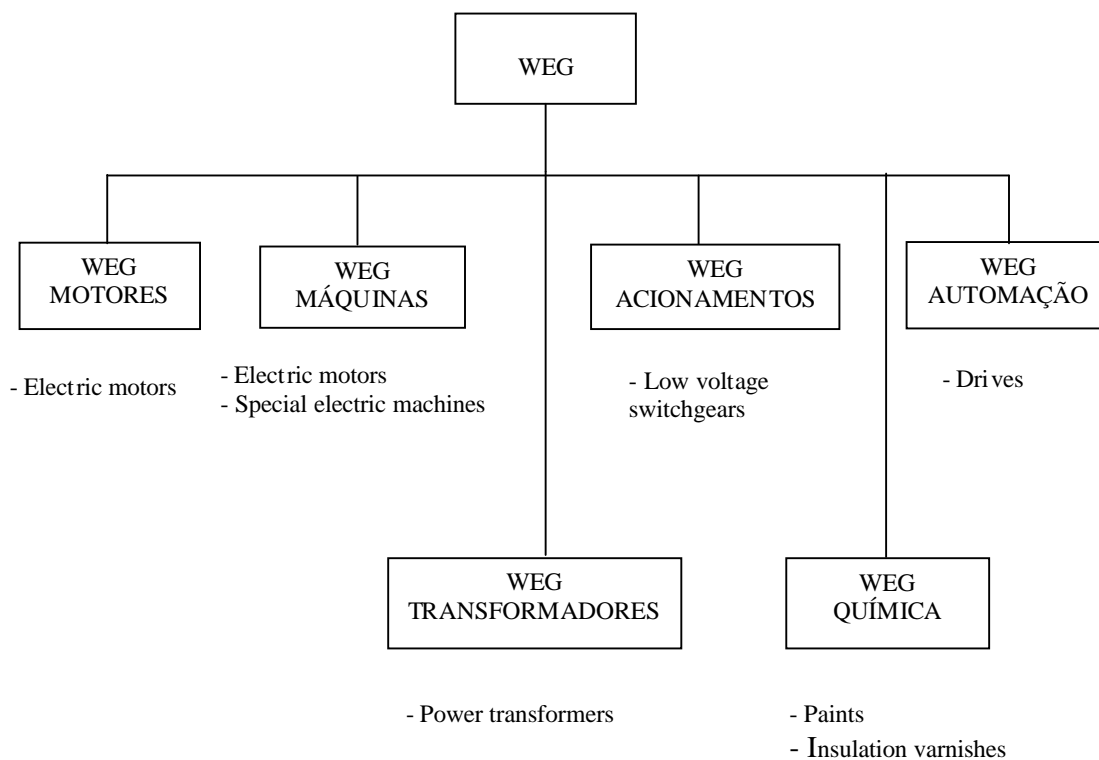
Figure 1.3 – Main divisions of WEG group and their products

The production of rotating electric machines at WEG is split between WEG MOTORES and WEG MAQUINAS as showed at figure 1.4.
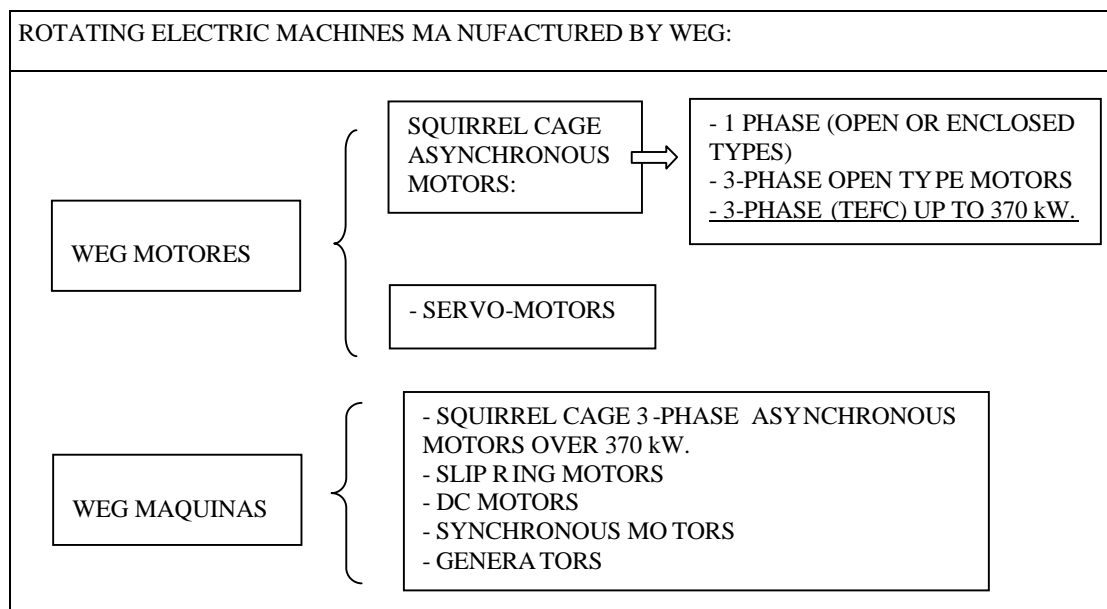
Figure 1.4 – Types of rotating electric machines produced by WEG

Most industrial type electric motors supplied by WEG are 3 phase squirrel cage TEFC asynchronous electric machines up to 370 kW.

Due to it, this research will concentrate on this type and range of electric motors.

In this text, these specific electric machines will be named just as electric motors or motors.

1.2 – Overview about motor control and protection

The proper operation of an electric motor requires the use of a motor starter. These equipments are employed for controlling and protecting electric motors (Figure 1.5).

```
┌─────────────────────┐
│   POWER SUPPLY      │
└─────────────────────┘
          ⇓
┌─────────────────────┐
│ MOTOR STARTER       │      ┌──────────────────────┐
│                     │      │ POWER SWITCHING      │
│  - CONTROL    ⇒     │      └──────────────────────┘
│                     │
│                     │  ┌──────────────────────────┐    ┌──────────────────────┐
│                     │  │ BASICALLY AGAINST:       │    │ RISKS AND DAMAGES    │
│  - PROTECTION ⇒     │  │ - SHORT CIRCUIT CURRENTS │ ⇒  │ FOR:                 │
│                     │  │ - THERMAL OVERLOADS      │    │                      │
│                     │  └──────────────────────────┘    │ - PERSONNEL          │
└─────────────────────┘                                  │ - EQUIPMENTS         │
          ⇓                                               │ - BUILDINGS AND      │
        ╱────╲                                            │   INSTALLATIONS      │
       │  M   │                                           └──────────────────────┘
       │  3 ~ │
        ╲────╱
```
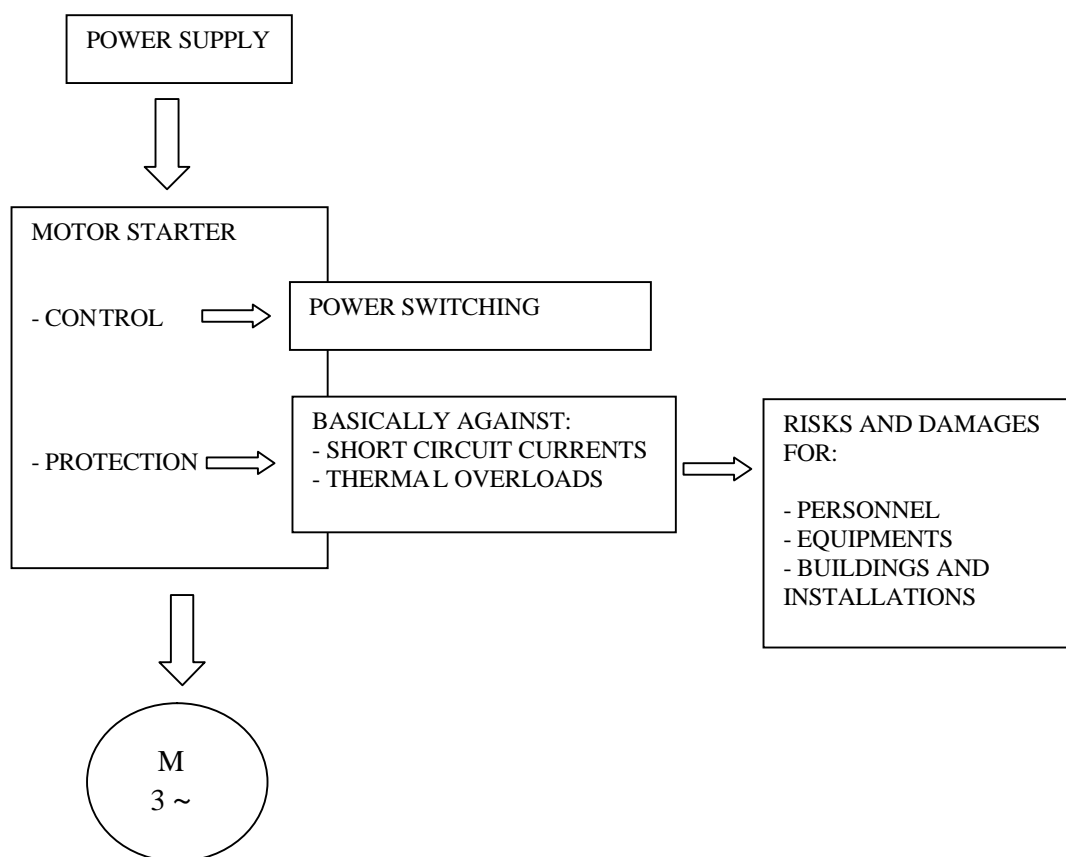
Figure 1.5 – Basic functions of a motor starter

Electric motors endurance depends on the durability of their different components.

Motor windings are one of the most sensible parts among the different components used to build an electric motor. Their durability is affected by thermal, electrical, ambient and mechanical stresses, also called T.E.A.M. stresses (Figure 1.6).
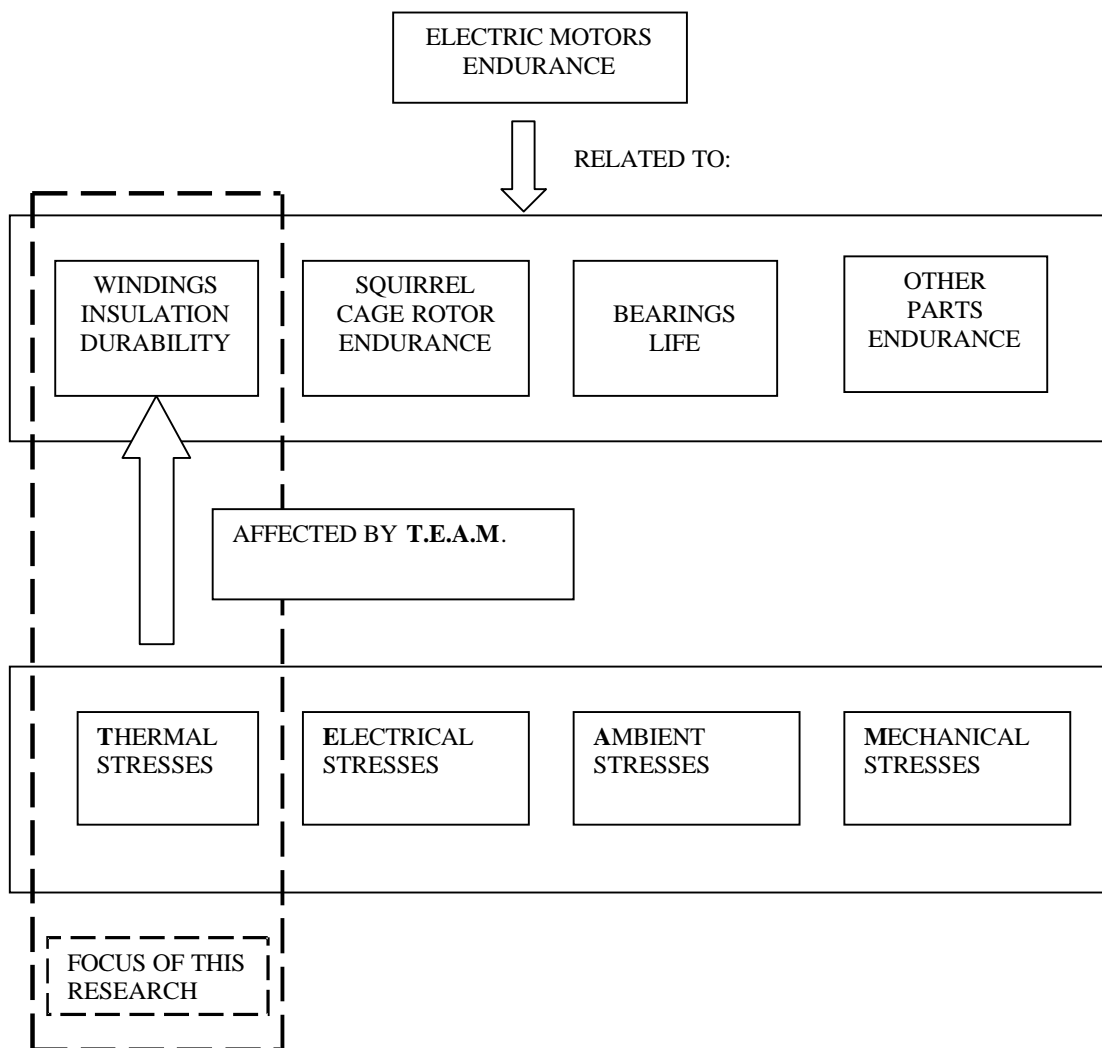
Figure 1.6 – Main influences on electric motors windings endurance

Thermal stresses (or thermal overloads) are a frequent reason of damages on electric motors windings.

Due to it this research will focus on thermal overload protection for motor windings.

Figure 1.7 shows the main causes of thermal overloads and their effects on motor windings endurance.

```
┌──────────────────────────────────────────────────────────────────────────┐
│  POSSIBLE THERMAL OVERLOADS:                                               │
│                                                                            │
│  ┌────────────────────────────────┐    ┌────────────────────────────────┐ │
│  │ - MECHANICAL OVERLOADS         │    │ - IRREGULAR LOADS              │ │
│  │ - STARTING / STOPPING CONDITIONS│    │ - SWITCHING FREQUENCY          │ │
│  │ - POWER SUPPLY FLUCTUATIONS /  │    │ - AMBIENT TEMPERATURE          │ │
│  │ FAILURES.                      │    │                                │ │
│  └────────────────────────────────┘    └────────────────────────────────┘ │
└──────────────────────────────────────────────────────────────────────────┘
```

EFFECT

INCREASE ON ELECTRIC
MOTOR CURRENT

EFFECT

EFFECT

INCREASE ON STATOR
WINDINGS
TEMPERATURE

EFFECT

DECREASE OF WINDING ENDURANCE
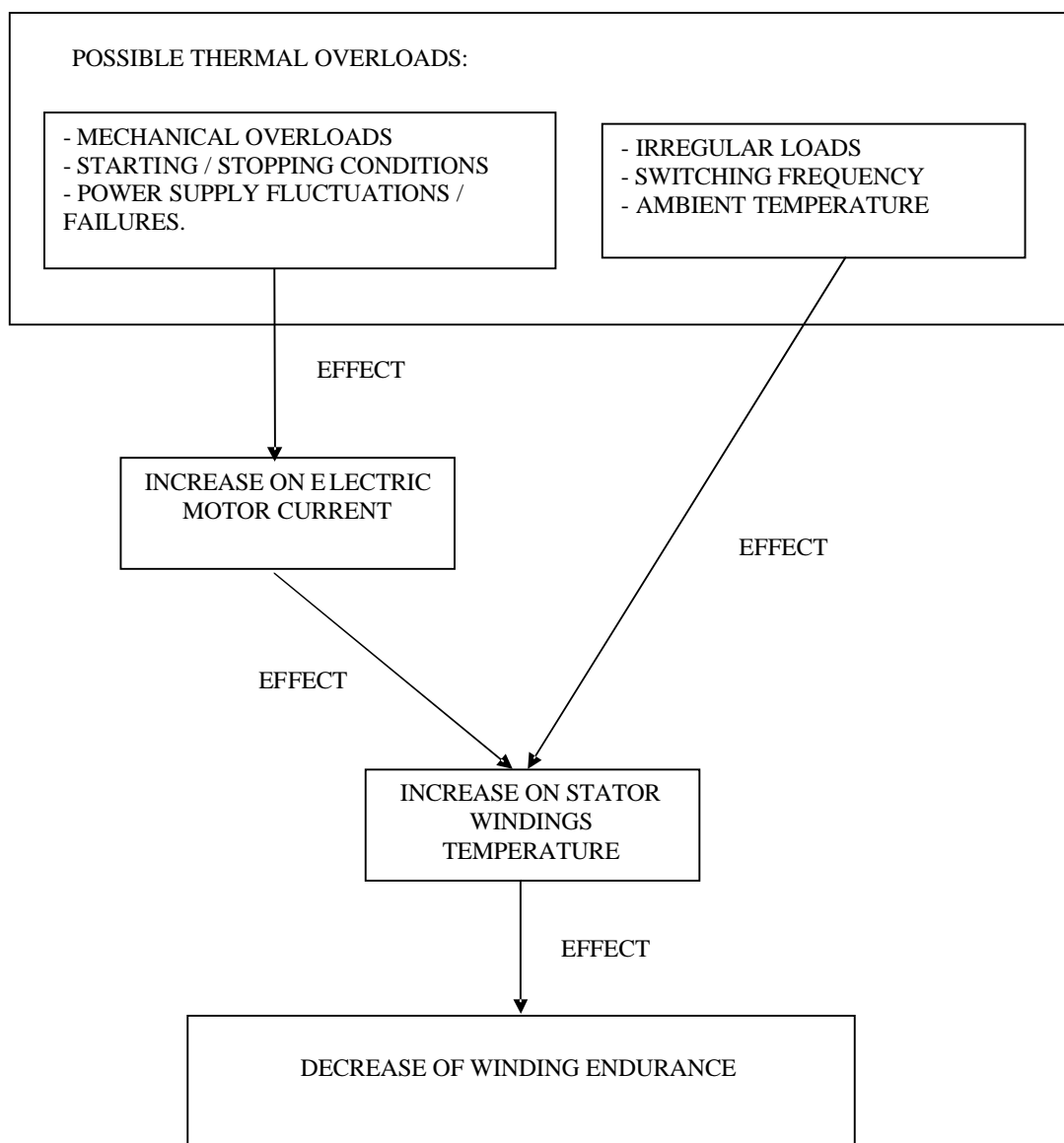
Figure 1.7 – Thermal overloads and their effects

Thermal overload protection can be provided by different types of devices (Figure 1.8).

Current dependent devices are a widespread solution employed for providing thermal overload protection.

The protection features of these devices are represented by their current-time characteristics.

On the other hand, the maximum allowed time an electric motor can operate under different current values might be represented by their thermal limit curves.

OVERLOAD PROTECTION DEVICES IN THE MARKET:	
CURRENT DEPENDENT DEVICES	→
TEMPERATURE SENSITIVE DEVICES	
TEMPERATURE AND CURRENT SENSITIVE DEVICES	

SOLUTIONS OFFERED BY **WEG ACIONAMENTOS**:

- OVERLOAD RELAYS FOR R ATED CURRENTS UP TO 840 A.

- **MPW25**: MOTOR PROTECTIVE CIRCUIT BREAKERS FOR MOTORS UP TO 11 kW / 400V (25 A).

LAUNCHED IN THE MARKET IN 2001
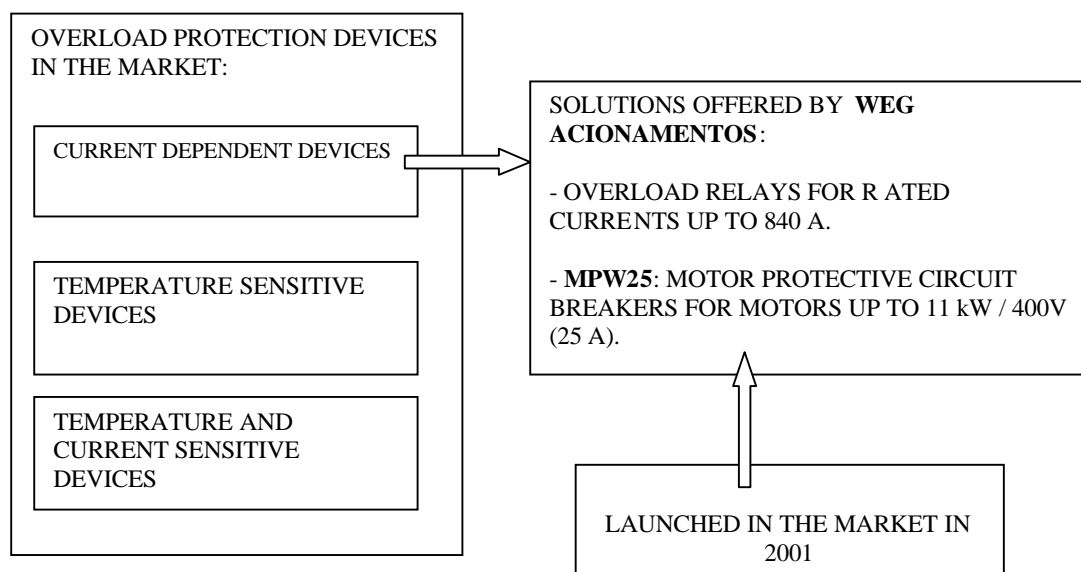
Figure 1.8 – Overload protection devices available in the market

A proper thermal protection depends on the matching between these two curves (Figure 1.9).

This research will analyse thermal overload protection for motor windings provided by WEG's motor protective circuit breakers due to the following reasons:

- Overload relays and motor protective circuit breakers are a widespread solution used for providing thermal protection for industrial motors;

- Overload relays and motor protective circuit breakers manufactured by WEG have an important market share;

- WEG's motor protective circuit breakers went recently to the market and their performance must be further analysed.
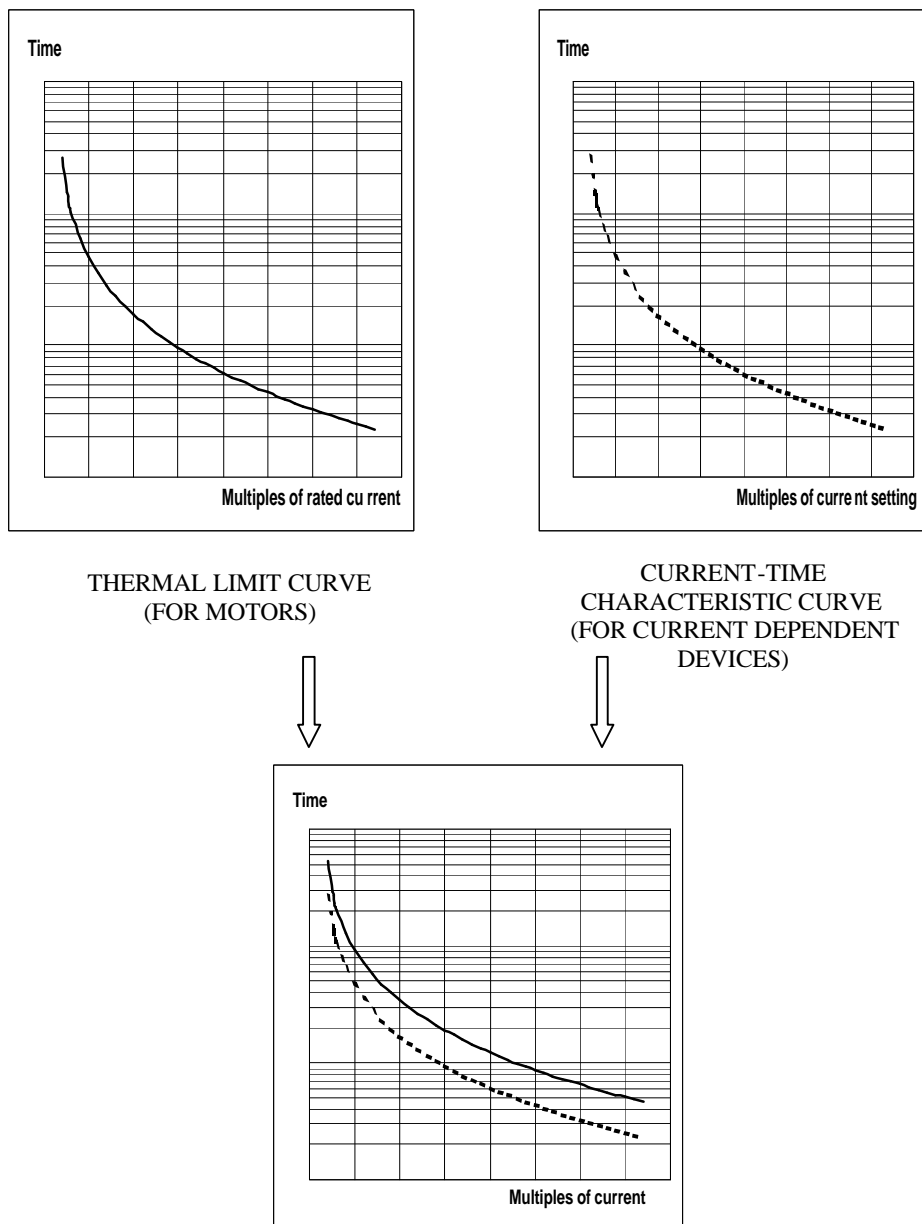
Figure 1.9 – Matching thermal limit curves and current-time characteristic curves

1.3 – Context of this research

WEG was founded in 1961 and has become one of the world leaders in electric motors manufacture.

In 1980 the company decided to diversify its products portfolio.

Based on a technology transfer agreement with a German company WEG started

producing electric components for motor control and protection (low voltage switchgears). Due to this starting conditions the company had not implemented a design center for these products until 1996.

In 1996 it was established a partnership with Technischen Universität Dresden (Germany) to develop the complete design for a new motor protective circuit breaker up to 11 kW to be manufactured by WEG.

Besides that, the partnership should train WEG's engineers in order they would continue the next developments of the company.

The new product, based on international standards, was launched in the market in 2001.

WEG engineers have continued their qualification via a master program at UFSC and by new researches and developments at the company.

This research aims on answering some remaining questions about electric motors thermal behaviour and how effective is the protection provided by thermo-magnetic motor protective circuit breakers.

It also aims on obtaining practical knowledge that can be implemented immediately in the company for:

- Improving currently available products performance;
- Predicting and avoiding failures on similar switchgears to be developed and implemented by the company in the future.

1.4 – Objectives

This research has the following objectives:

- Analyse how operating temperatures affect electric motors windings endurance;
- Define a thermal model that is able to predict electric motors temperature rise when they are submitted to different operating currents due to thermal overloads;
- Use the obtained model for calculating thermal limit curves for electric motors;
- Validate the calculated thermal limit curves through tests on electric motors manufactured by WEG MOTORES;

- Summarize standards requirements applicable for current dependent overload protection devices. Compare these requirements to obtained thermal limit curves for confirming the effectiveness of overload protection;

- Discuss adjustment and calibration processes employed by WEG for manufacturing MPW25 overload releases;

- Test MPW25 overload releases actual performance and compare test data to standards requirements;

- In case of standards requirements are not fulfilled, propose improvements on MPW25 overload releases. Validate the proposed improvements by testing and implement them;

- Obtain practical knowledge that could be used for further improvements on MPW25 overload releases quality;

- Obtain practical knowledge that could be used for improving the quality of new designs for switchgears. This knowledge should lead to new design and quality management procedures for predicting quality problems and implementing improvements during the early stages of design and manufacturing.

1.5 – Structure of the text

The research results are presented according to the following structure:

- Chapter 1 gives an overview about electric motors and their control and protection, explains how this research is inserted in a broader task related to the development of a new motor protective circuit breaker, and explains the objectives of this research;

- Chapter 2 explains the working principle of electric motors and how the durability of their insulation systems are related to the temperatures they are submitted during their operating life. The concept of temperature rise is also explained. The method for measuring the temperature rise on motor windings, based on the change in resistance, is detailed;

- Chapter 3 introduces the concept of power losses in electric motors and shows a basic mathematical model that can be used to explain their thermal behaviour. The text also explains the meaning of electric motors thermal limiting curves and the procedure to calculate and plot them;

- Chapter 4 introduces the concept of maximum permissible temperature for motor windings under transient conditions and shows the calculation of three different thermal limit curves for an 11 kW electric motor. Furthermore, one electric motor of this power is taken from the assembly line and submitted to overload tests. Temperature rise is measured at different parts of this electric motor. Measured values are compared to the values predicted by the calculated thermal limit curves;

- Chapter 5 explains basic control and protection functions provided by motor starters. Different types of overload protective devices are also described. Standards requirements for overload relays and releases are further detailed;

- Chapter 6 describes MPW25 main features. Besides it the text thoroughly explains design parameters for its overload releases. The procedures for adjusting and calibrating MPW25 overload releases are further discussed;

- Chapter 7 starts detailing the test procedures employed for evaluating the accuracy of overload releases operation. It also shows actual performance of currently produced devices. Tripping repeatability is thoroughly analysed. Improvements on design and process parameters are proposed. Finally, an experiment is conducted to confirm if proposed improvements are really effective;

- Chapter 8 presents the main conclusions obtained from this research including proposals for improving WEG's quality management system for next developments of switchgears. This chapter also includes proposals for next researches to be developed in the field of low voltage switchgears.

The text structure can be further explained by figure 1.10.
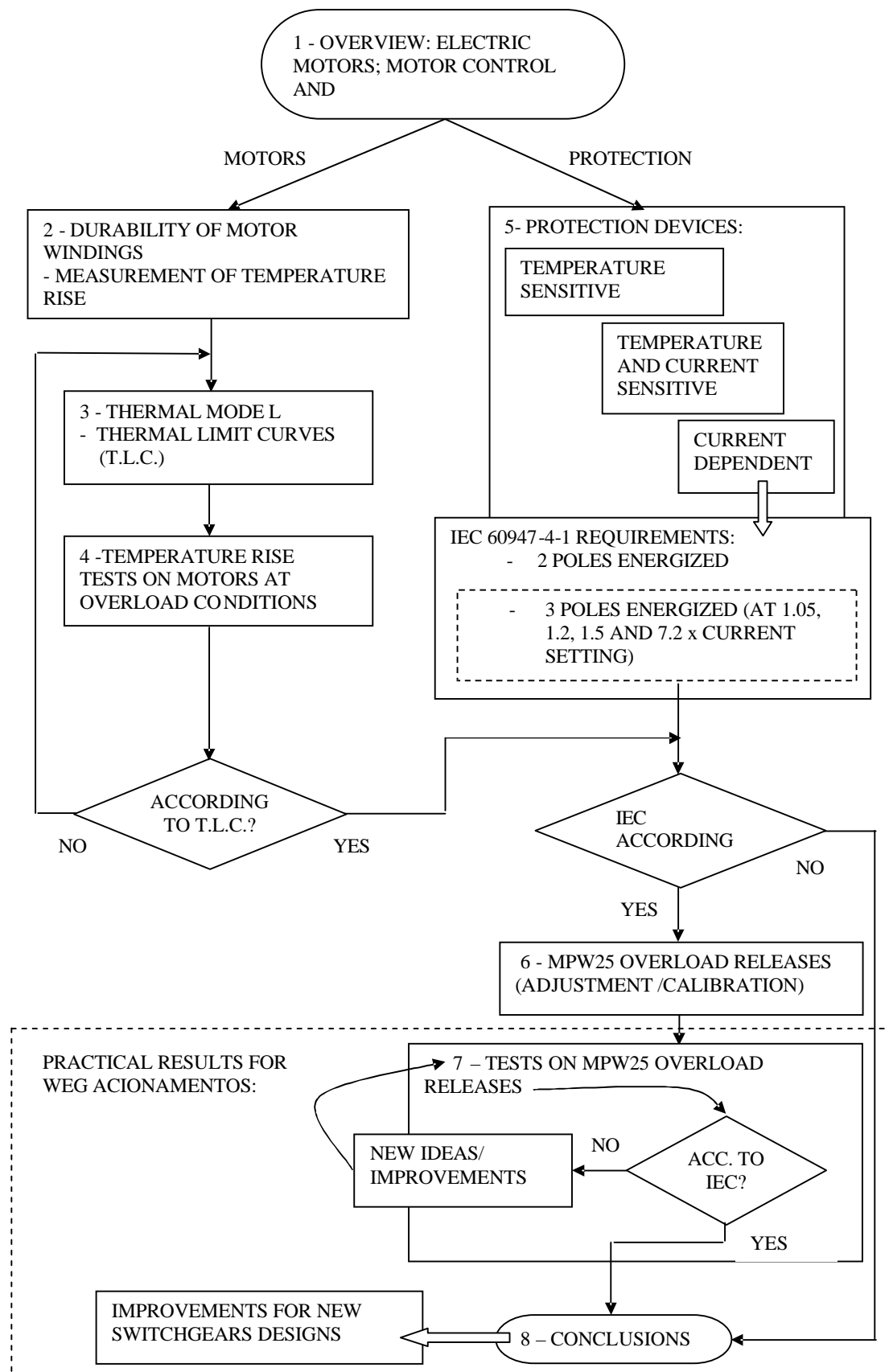
Figure 1.10 – Overview about the text structure

CHAPTER 2
TEMPERATURE RISE OF ELECTRIC MOTORS

This chapter starts presenting a brief description about the working principle of three-phase induction motors and follows discussing the durability of insulation systems employed in motor windings.

In the sequence, temperature rise limits for motor windings are discussed. It is also explained the method for measuring temperature rise on motor windings based on the change in the resistance.

Additionally, some temperature rise measurements, performed at motors manufactured by WEG, are reported.

2. 1 – Working principle of three-phase induction motors

Squirrel cage three-phase induction motors basically are built as showed at figure 2.1.
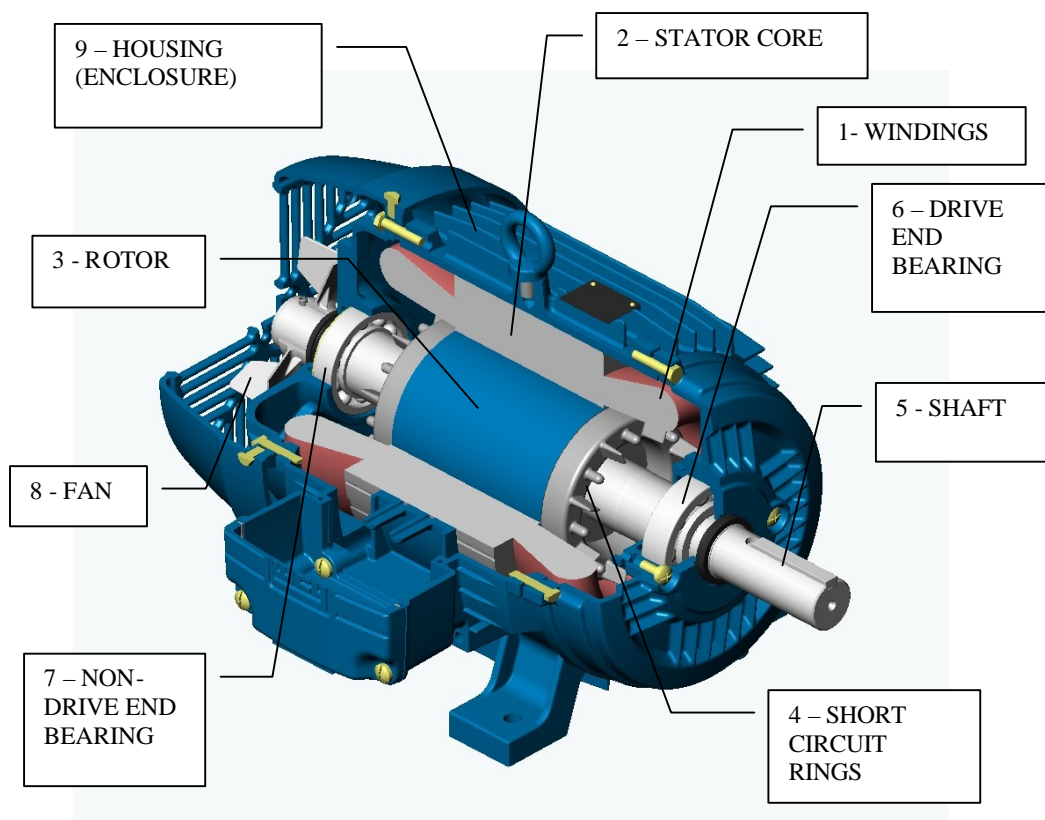
Figure 2.1- Basic construction of electric motors

The most important parts for this research are: stator windings (1), stator core (2), squirrel cage rotor (3) and rotor bars/short circuit rings (4). Temperature rise measurements of these parts will be reported in chapter 4. Temperature rise measurements on stator windings will be thoroughly discussed in the same chapter.

Whenever current flows through three-phase windings, it is generated a rotating magnetic field in the stator.

This rotating magnetic field cuts the squirrel cage rotor bars inducing electric currents in it. Therefore there is a magnetic field in the rotor too. The polarity of this magnetic field is opposite to the one generated in the stator. Consequently there is an attraction between the two magnetic fields and the rotor magnetic field follows the stator field. As a result there is a torque in the rotor, which can be applied for moving mechanical loads coupled to motor shaft /1/.

2.2– Electric motors endurance

Electric motors are robust machines. Motors endurance is affected by the lifetime of different components employed to build them. Among these components, motor windings are considered to be one of the most sensible parts /1/. As showed at figure 1.6 windings insulation durability is affected by thermal, electrical, ambient and mechanical stresses. This research will be focused on motor windings endurance and will analyse only the influence of thermal stresses on this component.

Windings insulation endurance is in inverse proportion to their operating temperatures (equation 2.1):

$$\text{WINDING ENDURANCE} \propto \frac{1}{(operating\ temperature)} \qquad (2.1)$$

According to IEC 60085 /2/, insulation systems for motor windings are classified according to thermal classes. Every thermal class has assigned temperatures as indicated at table 2.1. These figures are the maximum permissible steady state temperatures motor windings may be submitted.

Insulation systems are designed and tested to withstand their thermal class temperature for a long time without significant decrease in their mechanical and electrical properties.

These tests are performed on special samples called "motorettes", which are dummy windings representing electric motors windings /3/, /4/, /5/.

Table 2.1 – Most common thermal classes for electric
machines insulation systems /2/.

Thermal class	Assigned temperature (ºC)
A	105
B	130
F	155
H	180

Figure 2.2 shows a "typical thermal endurance evaluation for a class B insulation system, produced by plotting test results at high temperatures (the solid line) and extrapolating them back to lower operating temperatures (the dashed line)." /6/
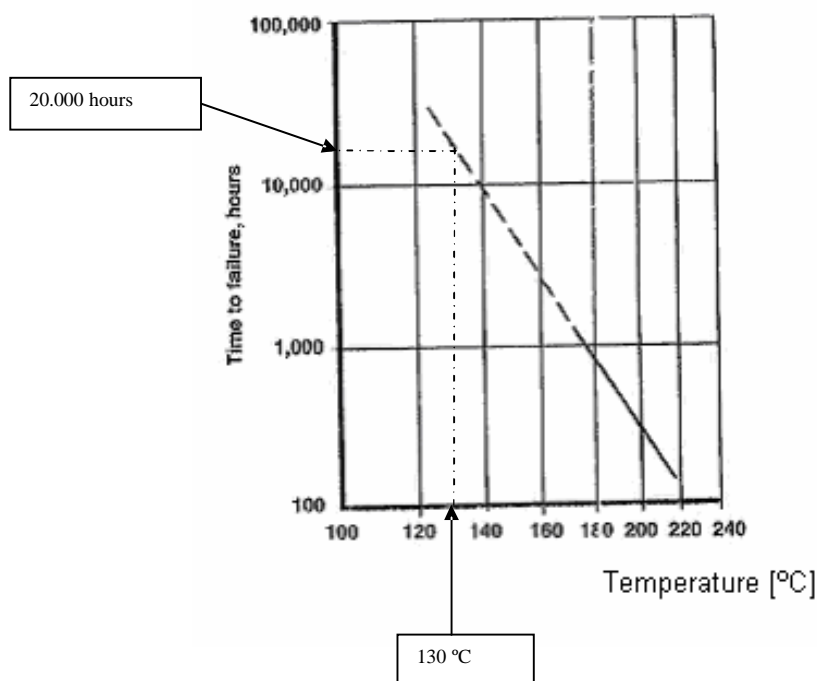
Figure 2.2 – Endurance evaluation for a class B insulation system /6/.

Figure 2.2 also shows that when this insulation system is subjected to a temperature equal to 130ºC its endurance will be approximately 20.000 hours.

Practice shows that such insulation system, when applied at electric motors used under normal service conditions, can endure some decades /6/, /7/, /8/, /9/ and /10/.

According to North American literature /9/ the following rule of thumb can be applied: "insulation life will be doubled for each 10 degrees of unused insulation temperature capabil-

ity…the same ten-degree rule also applies to motors operating at above rated temperature. In this case, insulation life is halved for each 10ºC of over temperature." This behaviour can also be predicted by observing figure 2.2, where an increase on operating temperature from 130 ºC to 140 ºC is likely to reduce expected endurance from 20.000 hours to 10.000 hours.

On the other hand, according to Berger /11/, "basic is the law of Montsinger, who has researched that oil/cellulose insulation paper durability will be halved for each additional 7 ºC; for class A insulation systems it is known, that a temperature rise of 8 ºC leads to half endurance."

The main conclusion here is that winding insulation systems have a decrease on their endurance when operating at temperatures above their thermal classes.

Next sections will explain the procedures for measuring motor windings temperatures and how international standards specify limits of operating temperatures for electric motors.

2.3– Temperature rise of a part of a machine

The mechanical power available at motor's shaft is lower than the electric power absorbed from the power supply.

Part of the supplied energy is converted into power losses that are responsible for heating motor components.

This heat must be dissipated to the environment in order to avoid excessive temperatures in the electric motor.

Standards /12/, /13/ use to limit electric motors temperatures according to maximum allowed temperature rise.

Temperature rise (ΔT) is defined according to equation 2.2 /12/:

$$\Delta T = \text{Temperature of the part } - \text{Temperature of the coolant} \tag{2.2}$$

The concept of temperature rise for a motor winding is further explained by figure 2.3 where can be observed the following important temperatures:

A - The winding hottest spot.

AB - Temperature drop due to the thermal resistance between the hottest spot and the external wires of the winding.

B - Temperature drop due to the thermal resistance between the winding and its insulation film.

BC - Temperature drop due to the thermal resistance of the core plates.

C   - Temperature drop due to the thermal resistance between the core plates and the motor housing (air gaps).

CD - Temperature drop due to the thermal resistance of the housing width.
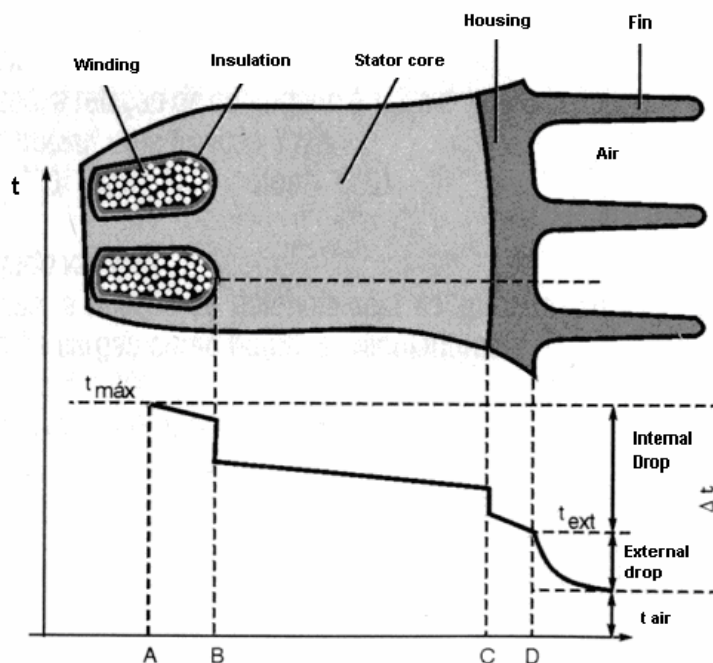
Figure 2.3 – Temperature gradient in electric motors /1/.

2.4 – Temperature rise limits for electric motors - according to IEC 60034-1 /12/

Table 2.2 summarizes the temperature rise limits for alternating current (AC) windings operating at continuous running duty and under ambient conditions as follows:

- Altitude $\leq$ 1000 m above sea level
- Maximum ambient air temperature $\leq$ 40°C
- Minimum ambient air temperature $\geq$ -15°C

Thermal class temperatures, according to table 2.1, can be obtained just adding the temperature rise limits showed at table 2.2 to the maximum allowed ambient temperature (40°C) plus the hottest spot temperature (10°C for a $\leq$ 370 kW rated output electric motor).

Table 2.2 – Temperature rise limits (K) for AC windings

Rated output	Insulation thermal class			Method of measurement
	B	F	H	
≤ 370 kW	80	105	125	By change in resistance
< 600 W	85	110	130	

The main conclusion here is: IEC 60034-1 requires that, when an electric motor is submitted to its rated load and is operating under continuous running duty, the maximum allowed temperature rise of its windings shall be according to table 2.2.

2.5 – Temperature rise limits for electric motors - according to NEMA MG 1 /13/ (See also appendix 1)

2.5.1 – Temperature rise limits for small motors

The temperature rise "for each of the various parts of the motor" shall not exceed the values given in table 2.3 when tested in accordance with the rating (based on a maximum ambient temperature of 40ºC and operation at altitudes ≤ 1000 m). For motors "having a service factor greater then 1.0, the temperature rise shall not exceed the values given" in the same table when tested at the service factor load.

Table 2.3 – Temperature rise limits (K) for small motors

	Class of insulation		
	B	F	H
TEFC motors, including variations thereof- measurement by resistance or thermocouple.	85	110	135

2.5.2 – Temperature rise limits for medium polyphase induction motors

The temperature rise for the windings shall not exceed the values given in table 2.4 when tested in accordance to the rating, "except that for motors having a service factor 1.15 or higher" where the tests shall be performed at the service factor load. Temperature measurements shall be performed according to the resistance method; ambient temperature ≤ 40 ºC and altitude ≤ 1000 m.

"The temperatures attained by cores, squirrel-cage windings, and miscellaneous parts (such as brush holders, brushes, pole tips, etc.) shall not injure the insulation or the machine in any respect." /13/

Table 2.4 – Temperature rise limits (K) for medium motors

	Class of insulation		
	B	F	H
Motors with 1.0 service factor	80	105	125
All motors with 1.15 or higher service factor	90	115	…

2.5.3– Temperature rise limits for large machines

The temperature rise at the windings "under rated-load conditions, …shall not exceed the values given in" tables 2.5 and 2.6. Temperature for external air $\leq$ 40 ºC. Temperature measurements shall be performed according to the resistance method.

Table 2.5 - Machines with a 1.0 SF at rated load (K)

	Class of insulation		
	B	F	H
All horsepower ratings	80	105	125

Table 2.6 - Machines with a 1.15 SF at service factor load (K)

	Class of insulation		
	B	F	H
All horsepower ratings	90	115	135

"The temperatures attained by cores, squirrel-cage windings, collector rings, and miscellaneous parts (such as brushholders and brushes, etc.) shall not injure the insulation or the machine in any respect." /13/

The main conclusion for sections 2.5.1, 2.5.2, and 2.5.3 is: NEMA MG 1 requires that, when an electric motor is submitted to its rated load (SF equal to 1) and is operating under continuous running duty, the maximum allowed temperature rise of its windings shall be according to table 2.3, 2.4, and 2.5.

2.6– Temperature rise measurement by change in resistance

"A commonly used method for determining the average temperature of a winding is to measure the resistance of the winding at the unknown temperature and to compare this value with the resistance at a known temperature."/14/

Experiments have showed conductors have a linear relationship between resistance and temperature over a considerable range. /14/

It is also possible to experimentally extrapolate the temperature value for zero resistance for specific conductors.

These relationships are showed at figure 2.4:
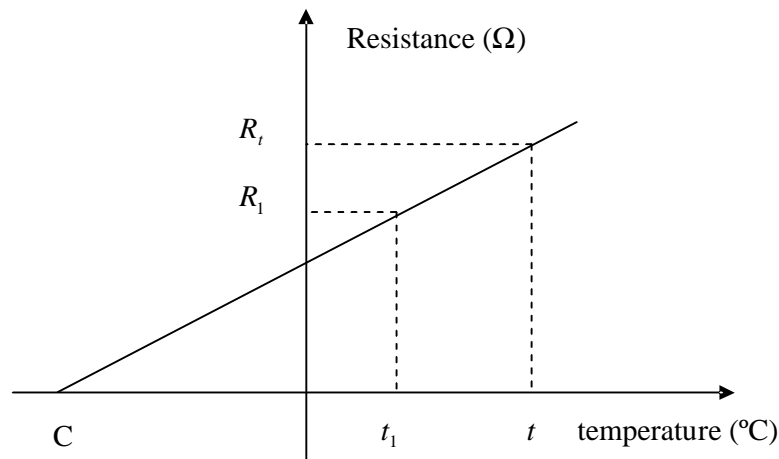
Figure 2.4 – Relationship between temperature and electrical resistance

Where

t = unknown temperature (°C)

t_1 = known temperature (°C)

R_t = measured resistance at t

R_1 = measured resistance at t_1

C = extrapolated temperature for zero resistance. For annealed copper C = 235 °C /14/.

"The proportionality of corresponding sides of similar triangles permit the relationship" between resistance and temperature to be expressed as follows /14/:

$$\frac{t + C}{t_1 + C} = \frac{R_t}{R_1} \tag{2.3}$$

After re-arranging the terms of equation 2.3, equation 2.4 is obtained, which is considered valid for commercial purposes /12/, /15/.

$$t - t_1 = \left(\frac{R_t}{R_1} - 1\right)(t_1 + C) \tag{2.4}$$

Kelvin bridges are recommended for accurate low value resistance measurements. See table 2.7 below.

Table 2.7 – Low resistance measuring methods; extract from /14/

Resistance to be measured	Accuracy required	Bridge methods
Low resistance ($< 5\ \Omega$)	Greater than 0.1%	Kelvin or current comparator
	0.1% - 1%	Kelvin
	Less than 1%	Any bridge type circuit

2.7 – Actual temperature rise for standard motors manufactured by WEG

WEG has a large quantity of type test reports available.

The company's data bank was surveyed for three different powers of standard electric motors. For each power, fifteen reports were analysed and actual temperature rise results were computed /16/. Table 2.8 presents a summary of this survey.

Table 2.8– Actual temperature rise for standard motors (4 pole, 380V/60Hz)

Power (HP)	WEG's plant number	Thermal class	Temperature rise (K)		Remarks
			Average	Standard deviation	
2	I	B ($\Delta T \leq 80$ K)	40.6	3.0	Temperature rise values are very below their corresponding insulation thermal class.
20	IV		64.4	4.9	
200	III	F ($\Delta T \leq 105$ K)	70.6	5.3	

All motors reported above could be said to be operating in a "cold state", i.e. the temperature rise of their windings is far bellow the thermal class limits of their insulation systems (Table 2.2). Nevertheless, due to economic reasons, the whole motors population could show specimens with temperature rise values equal to the maximum allowed temperature rise for the thermal class of their insulation systems (the worst case).

Chapters 3 and 4 will analyse motor windings temperature rise when electric motors are submitted to overload conditions. The motors will be supposed to have been previously submitted to their rated loads and their windings have reached steady state temperature rise (ΔT_{rated}). The worst case for steady state temperature rise will be considered, i.e., motor windings will be considered to have reached the maximum allowed temperature rise for the thermal class of their insulation system (i.e., ΔT_{rated} equal to thermal class limits according to Table 2.2).

After it the electric motor will be submitted to overload conditions that will make its winding temperature rise reach values above the thermal class limit.

Motor windings are expected to be submitted to such conditions only for a short time, till overload protection devices trip and protect electric motors.

Therefore, it will be also necessary to define temperature rise limits for stator windings operating under transient conditions ($\Delta T_{\lim}$).

These operating conditions are further explained by figure 2.5.
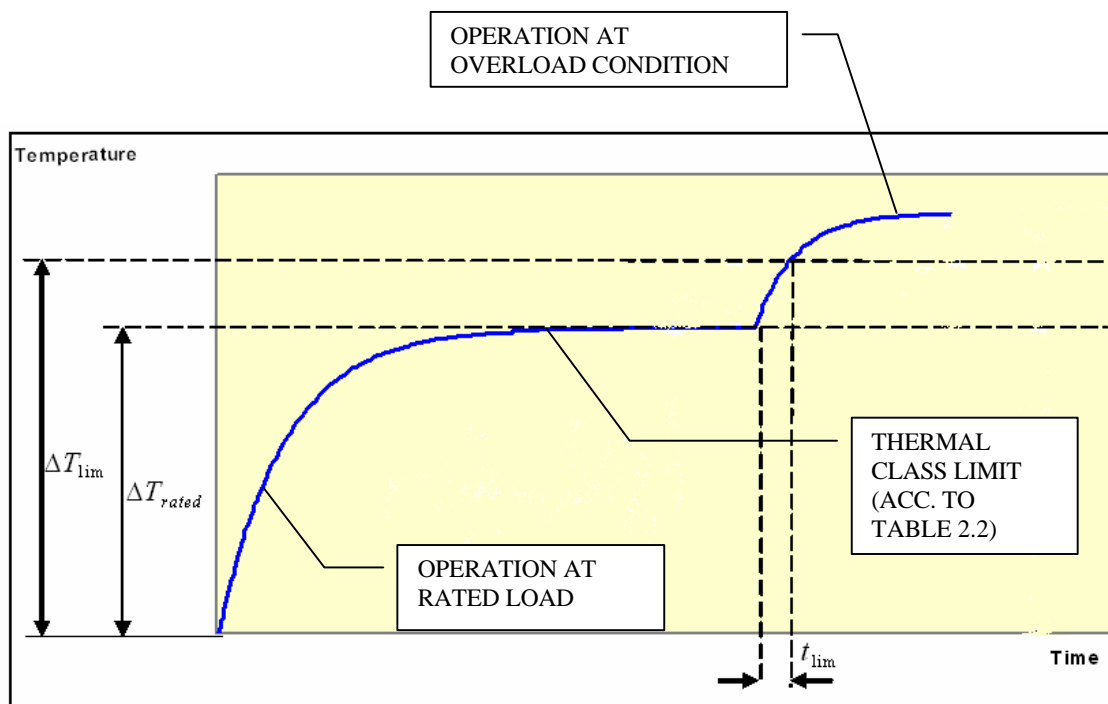
Figure 2.5 – Temperature rise at different loads

2.8 – Main conclusions for chapter 2

- Electric motors endurance is mainly dependent on their insulation systems durability;

- Insulation systems durability is in inverse proportion to their operating temperatures;

- Insulation systems are classified according to thermal classes. Each thermal class has an assigned temperature that means the maximum permissible temperature the insulation system may be submitted continuously;

- Standards use to limit motor windings temperature according to maximum allowed temperature rise, when the motors are submitted to their rated load, under continuous running duty;

- Motors can be supplied with their windings operating at the maximum allowed temperature rise (according to the standards). Therefore, in case such motors are subsequently submitted to overload conditions, their windings will reach temperature values higher than the maximum allowed temperature rise. This condition will continue until protection devices switch off the electric motor. Next chapters will discuss temperature rise limits for motor windings operating under transient conditions. They will also analyse, how long motor windings could operate at overload conditions.

CHAPTER 3

THERMAL LIMIT CURVES FOR ELECTRIC MOTORS

This chapter discusses an analytical method for calculating temperature rise in motor windings when the motor is submitted to overload conditions ($\Delta T_{overload}$). The method is subsequently employed for calculating thermal limit curves for electric motors. Thermal limit curves are graphs showing the maximum time a motor can operate with various values of current.

The structure of this chapter is further explained by figure 3.1.
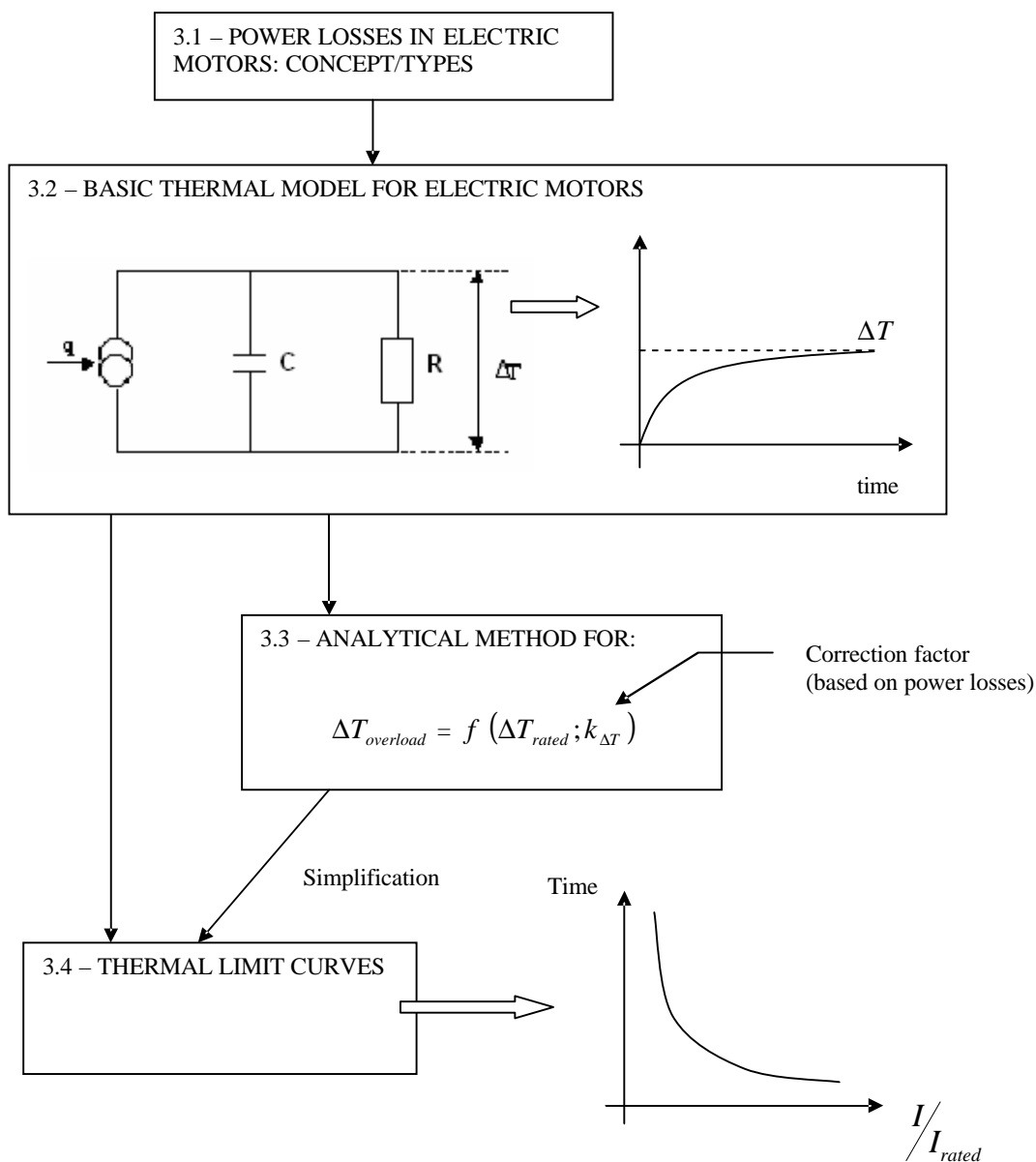
Figure 3.1 – Structure of chapter 3

3.1 – Power losses in electric motors

According to the energy conservation principle, electric energy supplied for electric motors is converted into different forms of energy according to equation 3.1 /17/.

$$
\left(\begin{array}{l}\text{Electri-}\\ \text{cal}\\ \text{energy}\\ \text{input}\end{array}\right) = \left(\begin{array}{l}\text{Mechani-}\\ \text{cal}\\ \text{energy}\\ \text{output}\end{array}\right) + \left(\begin{array}{l}\text{Increase on}\\ \text{energy stored}\\ \text{in coupling}\\ \text{fields}\end{array}\right) + \left(\begin{array}{l}\text{Energy}\\ \text{converted}\\ \text{into heat}\end{array}\right) \qquad (3.1)
$$

Figure 3.2 extends the understanding about the way electric power is converted in electric motors. The apparent power (S) supplied by the electric network is split into reactive power (Q) and active power (P). The reactive power is used to establish and maintain the magnetic fields in the motor windings. The active power is consumed partly to provide the mechanical power output supplied by the motor shaft and the remaining power is transformed into heat (losses).
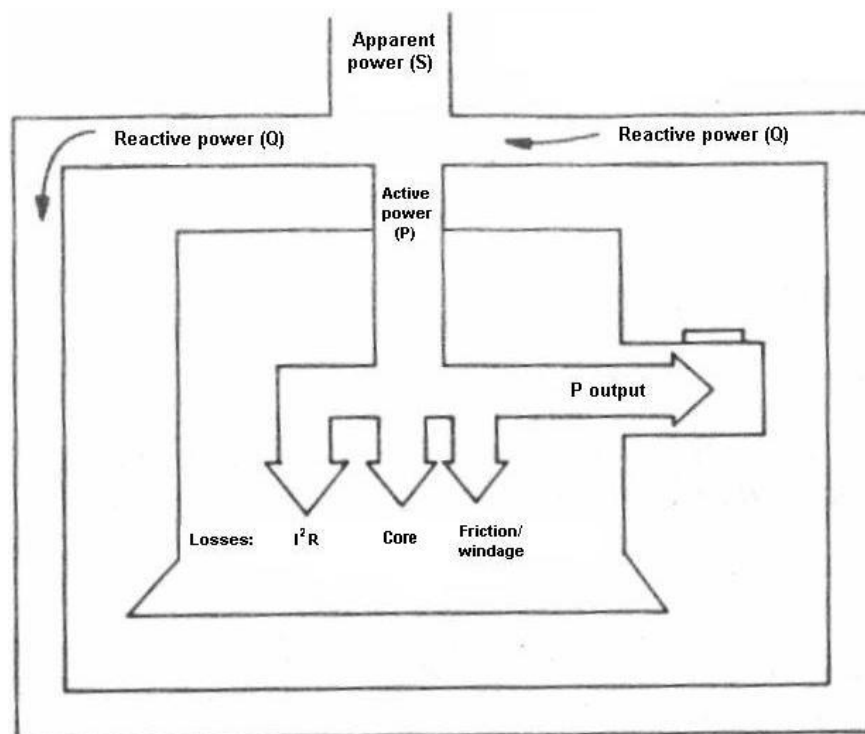
Figure 3.2 – Overview about power input, power output and power losses /18/.

Power losses in electric motors are further detailed at table 3.1. It also shows the relationship between the terms used by IEEE 112 /15/ and the physical heat sources distributed in electric motors. The different types of power losses may be understood as different heat sources distributed inside the electric motors.

As an example of actual power losses presented by an electric motor, table 3.2 summarises the results of a loss segregation test performed in a standard 11 kW motor manufactured by WEG (detailed measurement results at appendix 2).

Table 3.2 also shows that the efficiency of such specimen is 87.7 % and the main contributions for power losses inside this motor are stator I^2R losses and core losses.

Appendix 2 shows that the temperature rise of this motor sample, is 75.2 K; therefore, according to previous definition: $\Delta T_{rated} = 75.2$ K.

Table 3.1 – Classification of power losses in electric motors

Physical heat sources / Types of losses (1)	I^2R losses in electric conductors	Iron losses		Friction	
		Hysteresis	Eddy current	Bearings	Fans
- Variable losses (dependent on motor current)					
- Stator I^2R losses	x				
- Rotor I^2R losses	x				
- Stray-load losses (2)		x	x		
- Fixed losses (not dependent on motor current)					
- Core losses		x	x		
- Friction and windage losses				x	x
Notes: (1) According to WEG /19/ and IEEE 112 /15/. (2) Due to pulsating flux between stator and rotor slots (also known as zigzag flux) and stray flux in motor frame and shaft.					

Table 3.2 – Power losses in an 11 kW motor (segregation loss
tests in one sample according to IEEE 112 /15/)

	Measured values (W)	% of active power
Active power supplied	12,588.21	100.0
- Stator I^2R losses	627.79	4.9
- Rotor I^2R losses	297.77	2.4
- Stray-load losses	109.35	0.9
Σ variable losses	1,034.91	8.2
- Core losses	396.92	3.2
- Friction and windage losses	116.32	0.9
Σ fixed losses	513.24	4.1
Σ losses	1,548.15	12.3
Mechanical power output	11,040.06	87.7 (Efficiency)

3.2 – Basic thermal model for electric motors

Literature presents different thermal models for electric motors /20/, /21/, and /22/.
A simple one is shown at figure 3.3 (motor parameters are lumped /23/), and it is based on the
following restrictions:

- All power losses are concentrated in only one heat source, represented by q';
- There are no thermal resistances between the heat source and the thermal capacitance;
- Heat is stored in just one single and homogeneous mass, represented by C_t;
- Heat transfers only to the environment by a thermal resistance, represented by R_t.
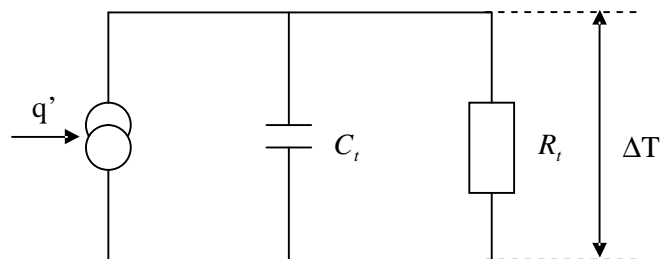
q' = heat flow [W]
R_t = thermal resistance [K/W]
C_t = thermal capacitance [J/K]
ΔT = temperature rise [K]

Figure 3.3 – Thermal model for electric motors

An ideal thermal resistance is defined according to Fourier equation (considering conductive heat transfer is happening) /24/:

$$R_t = \frac{l}{s_c \cdot A} \tag{3.2}$$

Where:

$l =$ length in the flow direction [m]

$s_c =$ thermal conductivity [W/Km]

$A =$ area normal to the heat flow direction [m^2]

And thermal capacitance is defined according to equation 3.3 /24/:

$$C_t = C_p \cdot m \tag{3.3}$$

Where:

$C_p =$ specific heat of mass [J/Kkg]

$m =$ mass of system [kg]

The differential equation that represents the behaviour of the above presented thermal model is:

$$q' = C_t \frac{d\Delta T(t)}{dt} + \frac{\Delta T(t)}{R_t} \tag{3.4}$$

According to Valenzuela et al /20/ and supposing the electric machine was previously in thermal equilibrium with the environment, the solution for equation 3.4 is:

$$\Delta T(t) = \Delta T_{max} \left(1 - e^{\left(-t/t\right)} \right) \tag{3.5}$$

Where:

$t = R_t \cdot C_t =$ Thermal time constant for heating conditions [s]

And:

$$\Delta T_{max} = R_t \cdot q' = \text{Maximum temperature rise} \tag{3.6}$$

Making $t = \mathsf{t}$ in equation 3.5, one obtains $\Delta T_{(t=\mathsf{t})} = 0.632 \Delta T_{max}$. Additionally, making $t = 3 \cdot \mathsf{t}$, one obtains $\Delta T_{(t=3\mathsf{t})} = 0.95 \Delta T_{max}$; that means after a time lag $t = 3 \cdot \mathsf{t}$ the temperature rise ($\Delta T(t)$) reaches 95 % of its final value.

Equation 3.7 describes temperature behaviour during cooling, i.e., making q = 0 and $\Delta T_{(t=0)} = \Delta T_{max}$, which means the heat source was removed after the maximum temperature has been reached.

$$\Delta T(t) = \Delta T_{max} \cdot e^{\left(-t/\mathsf{t}_{COOLING}\right)} \tag{3.7}$$

The thermal time constant (for heating conditions) for the motor which tests were reported at appendix 2 can be estimated considering all power losses reported at table 3.2 concentrated in just one heat source.

$$R_t = \frac{\Delta T_{max}}{q'} = \frac{75.2K}{1,548.15W} = 0.05 \frac{K}{W} \tag{3.8}$$

$$C_t = C_{pfe} \cdot m_{fe} + C_{pcu} \cdot m_{cu} = 32622.7 \frac{J}{K} \tag{3.9}$$

Where:

$C_{pcu} = 383.02$ J/kgK, /25/

$m_{cu} = 5.5$ kg (obtained from WEG data bank)

$C_{pfe} = 452.09$ J/kgK, /25/

$m_{fe} = (73 - 5.5) = 67.5$ kg /1/

Therefore, the thermal time constant for this motor (for heating conditions) could be estimated as $\mathsf{t} = 1631.1 \ s \sim 27 \ \text{minutes}$.

It is also known most heat dissipation from electric motors occurs via forced convection due to the operation of fan coolers coupled to motor shafts.

Figure 3.4 shows the heating curve for this motor based on equation 3.5 and taking $t = 27$ minutes, $\Delta T_{max} = 75.2K$ and $\Delta T_0 = 0$.
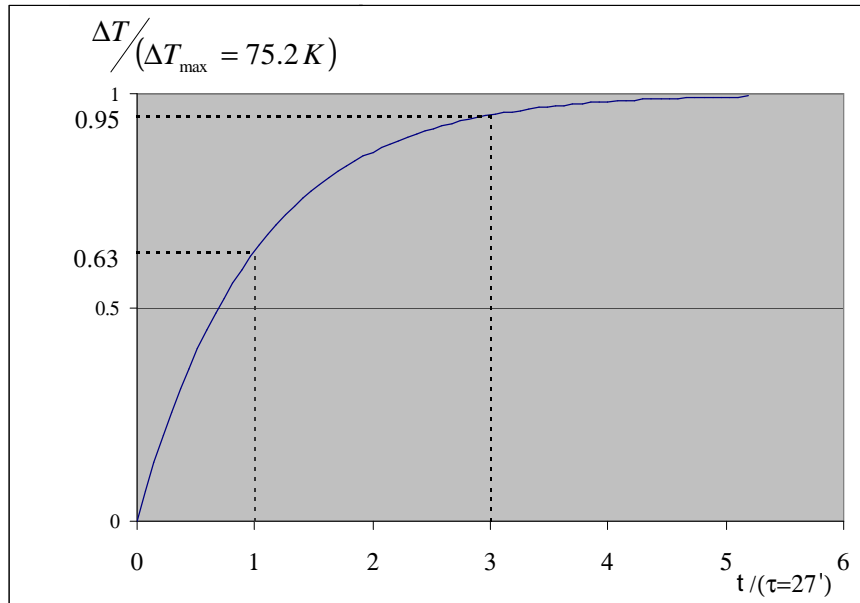
Figure 3.4 – Simulated heating curve for an 11 kW electric motor

3.3 – Method for estimating the temperature rise of electric motors

This section discusses an analytical method, developed by WEG /19/, for estimating temperature rise of electric motor windings when motors are submitted to the following conditions:

- Operating voltage is different of rated voltage;
- Operating load is different of rated load.

The method is subsequently simplified for a special case where the motor is considered to be submitted to small overload conditions but the operating voltage is equal to rated voltage. After it, the method is employed for calculating an example: the temperature rise of motor windings for an 11 kW motor. The structure of this section is further explained by figure 3.5.
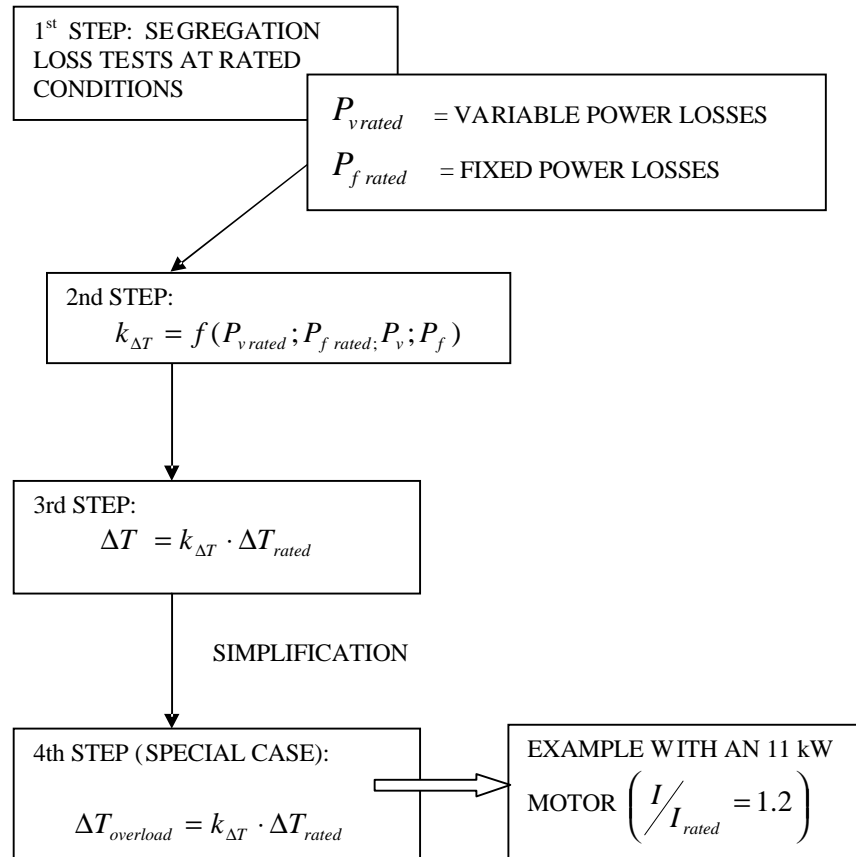
Figure 3.5 – Structure of section 3.3.

Equation 3.6 and reference /19/ show temperature rise (ΔT) is proportional to power losses (q') in the electric motor. So, it is possible to re-write equation 3.6 as follows:

$$\frac{\Delta T_{rated}}{q'_{rated}} = \frac{\Delta T}{q'} = R_t \tag{3.10}$$

Where:

ΔT_{rated} = temperature rise at rated load and voltage (steady state)

q'_{rated} = power losses at rated load and voltage, considering all power losses are concentrated in one single heat source;

ΔT = temperature rise when the motor is operating at a different value of load and voltage (steady state).

q' = power losses when the motor is operating at a different value of load and voltage, considering all power losses are concentrated in one single heat source;

R_t = thermal resistance, a fixed parameter of the thermal circuit.

After re-arranging equation 3.10 and eliminating R_t, the following equation is obtained:

$$\Delta T = \left(\frac{q'}{q'_{rated}}\right)\Delta T_{rated} \tag{3.11}$$

Equation 3.11 can also be written as follows /19/:

$$\Delta T = k_{\Delta T} \cdot \Delta T_{rated} \tag{3.12}$$

Where:

$k_{\Delta T} \Rightarrow$ Correction factor for ΔT_{rated} based on power losses and calculated according to the following equation /19/:

$$k_{\Delta T} = \frac{P_v + P_f}{P_{v\,rated} + P_{f\,rated}} \tag{3.13}$$

Where:

$P_{v\,rated}$ = variable power losses at rated load and voltage (obtained by tests or calculation);

$P_{f\,rated}$ = fixed power losses at rated load and voltage (obtained by tests or calculation);

P_v = variable power losses at a different value of load and voltage;

P_f = fixed power losses at a different value of load and voltage.

According to the proposed method, P_f and P_v can be calculated according to equations 3.14 and 3.15, and were validated, by WEG, for voltages and loads ranging between 85% and 115% of their rated values /19/.

$$P_f = \left(k_v\right)^n \cdot P_{f\,rated} \tag{3.14}$$

$$P_v = \frac{P_{v\,rated} \cdot \left(\dfrac{k_T}{k_{fT}}\right)^2}{\left(k_v \cdot k_{fv}\right)^2} \tag{3.15}$$

Where:

$k_v \Rightarrow$ Relation factor between applied voltage and rated voltage

$$k_v = \frac{V}{V_{rated}} = \frac{Actual\ operating\ voltage}{Rated\ voltage} \tag{3.16}$$

$n \Rightarrow$ Exponent for the variation of fixed losses $= f$ (core losses; applied voltage)

$k_T \Rightarrow$ Relation factor between applied torque and rated torque

$$k_T = \frac{T}{T_{rated}} = \frac{Torque\ at\ a\ different\ load}{Rated\ Torque} \tag{3.17}$$

$k_{fT} \Rightarrow$ Index for power factor $= f$ (applied torque):

$$k_{fT} = \frac{Cos f = f(k_T)}{Cos f_{rated}} \tag{3.18}$$

$k_{fv} \Rightarrow$ Index for power factor $= f$ (applied voltage):

$$k_{fv} = \frac{Cos f = f(k_v)}{Cos f_{rated}} \tag{3.19}$$

Considering that $V = V_{rated}$, than $k_v = 1$ and equations 3.14 and 3.15 are simplified as follows:

$$P_f = P_{f\,rated} \tag{3.20}$$

$$P_v = P_{v\,rated} \cdot \left(\frac{k_T}{k_{fT}} \right)^2 \tag{3.21}$$

Based on equation 3.22, it is possible to say power output is directly proportional to load torque, when electric motors are submitted to small overloads /1/.

$$T = \frac{9555 \times P}{n} \tag{3.22}$$

Where:

T = load torque [Nm]

P = power output [kW]

n = rotation [rpm]

According to the above information and based on curve D, appendix 3, it is possible to say that when an 11 kW motor is submitted to a torque equal to 1.2 times its rated torque (i.e. $k_T = 1.2$), its operating current is approximately equal to 1.2 times the rated current.

Now it may be introduced the following equation:

$$k_I = \frac{I}{I_{rated}} \tag{3.23}$$

Where:

$k_I \Rightarrow$ Is a relation factor between applied current and rated current. When $k_I = 1.2$, it means the actual current absorbed by the motor is 1.2 times the rated current.

Based on curve B of the graph presented in appendix 3, is possible to say that $k_{fT} = 1.0$ when the analysed motor is submitted to 20 % overload, i.e., $k_T = k_I = 1.2$.

Therefore, for the above described conditions, it is possible to re-write equation 3.21 as follows:

$$P_v = P_{v\,rated} \cdot (k_I)^2 \tag{3.24}$$

And equations 3.12 and 3.13 can be re-written, for this special case, as follows:

$$\Delta T_{overload} = k_{\Delta T} \cdot \Delta T_{rated} \qquad (3.25)$$

$$k_{\Delta T} = \frac{(k_I)^2 P_{v\,rated} + P_{f\,rated}}{P_{v\,rated} + P_{f\,rated}} \qquad (3.26)$$

As an example of this special case, $k_{\Delta T}$ and $\Delta T_{overload}$ were calculated for an 11 kW motor (loss segregation tests summarized at table 3.2), supposing the following conditions:

- $V = V_{rated}$; Therefore $P_f = P_{f\,rated} = 513.24$ W

- $k_T \sim k_I = 1.2$

- $k_{fT} \sim 1$

- $P_{v\,rated} = 1{,}034.91$ W

- $\Delta T_{rated} = 75.2$ K (obtained from loss segregation test report presented in appendix 3)

Results:

$k_{\Delta T} = 1.29$

$\Delta T_{overload} \sim 1.29 \times 75.2 K \sim 97 K$.

Section 3.4 discusses the method employed by WEG for calculating thermal limit curves for electric motors. The method requires the calculation of $\Delta T_{overload}$ values for various values of motor current.

It will be showed $\Delta T_{overload}$ values for thermal limit curves are calculated using an equation that is an additional simplification of equations 3.25 and 3.26.

3.4 – Thermal limit curves used by WEG

Thermal limit curves, also known as thermal damage or thermal capability curves, are plots showing "the time during which different values of motor current can be allowed to flow without undue loss of life in the stator or rotor due to thermal stress…The higher the current, the shorter the allowable time." /26/

They are useful for properly selecting protective devices for electric motors /26/.

Figure 3.6 shows a typical thermal limit curve used by WEG.
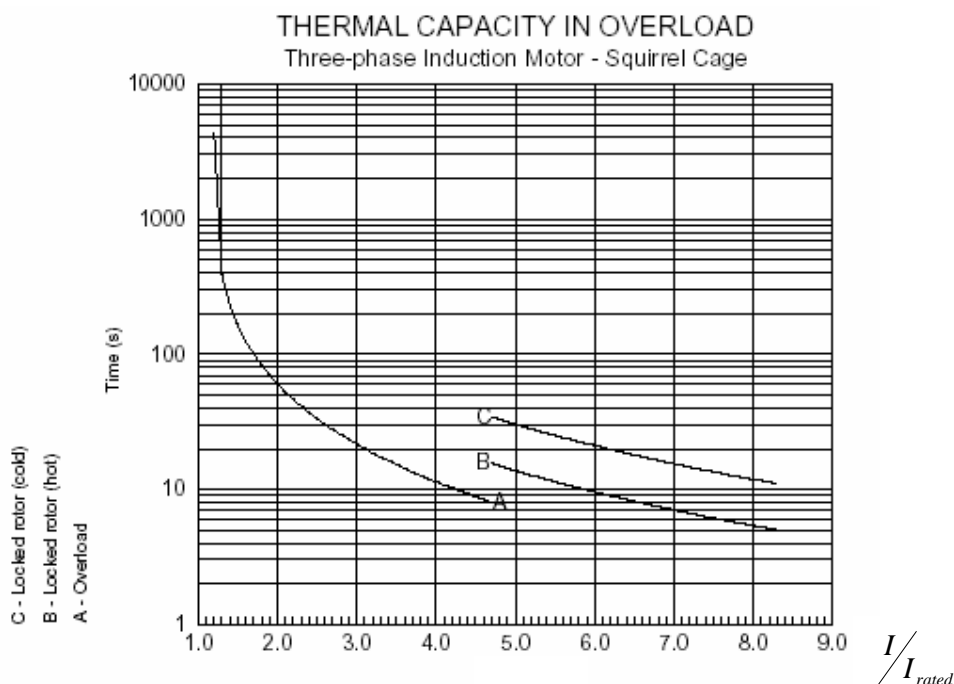
Figure 3.6 –Thermal capacity curve (WEG)

Segment A of the plot is known as the running overload portion /26/ of the thermal limit curve. This part of the plot considers the motor was initially at a hot state. It means the motor had already reached its steady state temperature while operating at its rated conditions. After it, the motor is subsequently overloaded and the thermal limit curve shows the maximum allowed time the motor can withstand at different over current values /27/.

This segment starts at rated current, where the electric motor can operate for its whole life, and the current increases up to reaching a value slightly below the current related to the motor breakdown torque. Beyond this point the motor operation becomes instable and its rotation reduces suddenly up to a complete stop. /26/

Segment B is the locked rotor region and plots allowable current x time during motor starting. Different values of locked rotor current can happen due to "frequent occurrence of voltage drops at motor terminals during starting." In case the voltage decreases locked rotor current drops proportionally. Segment B "shows locked rotor points for a range of voltages from the rated value down to the minimum expected during motor starting" and is applicable for motors at hot state. /26/

Segment C has the same meaning as the segment B, but it is applicable for motors at cold state.

This research will analyse stator temperature rise according to segment A of WEG's thermal limit curves.

Figure 3.7 explains the method used for calculating each point of segment A of WEG's thermal limit curve.
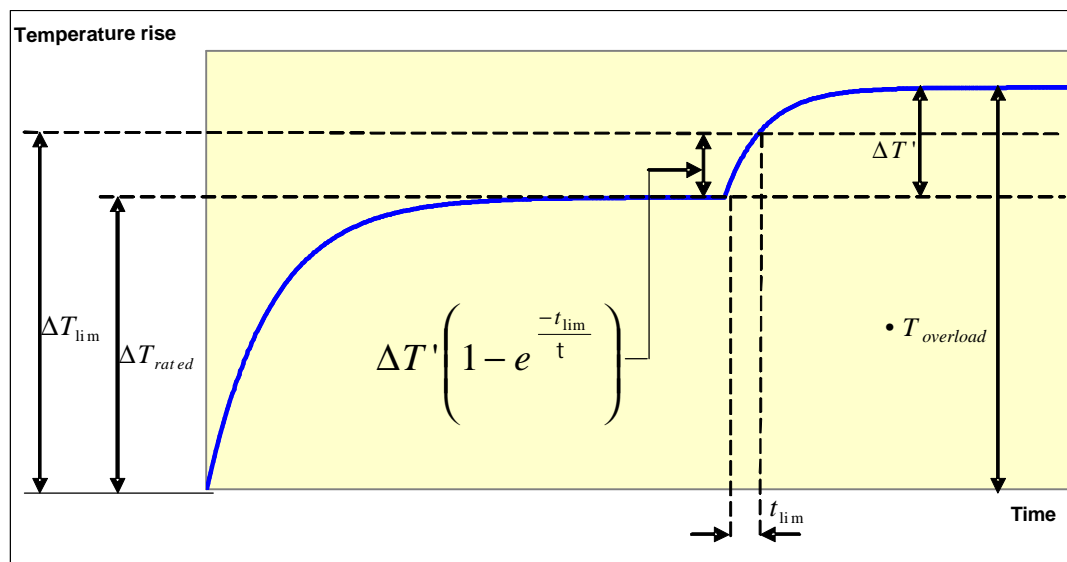
Figure 3.7 – Method for calculating thermal limit curves

ΔT_{rated} is the stator temperature rise when the motor is operating at rated load and voltage (experimental data).

$\Delta T_{overload}$ is the stator temperature rise when the motor is submitted to an overload and its value is estimated according to the following equation /27/:

$$\Delta T_{overload} \sim (k_I)^2 \cdot \Delta T_{rated}$$

(3.27)

Equation 3.27 is a simplification of equations 3.25 and 3.26 and takes

$$k_{\Delta T} \sim \frac{P_v}{P_{v\,rated}} \sim \frac{P_{v\,rated}\,(k_I)^2}{P_{v\,rated}} \sim (k_I)^2 .$$

Considering $k_I = 1.2$ and $\Delta T_{rated} = 75.2$ K, than $\Delta T_{overload} \sim (1.2)^2 \times 75.2 \sim 108K$. This value is 11 % higher than $\Delta T_{overload} = 97$ K obtained at the example presented at section 3.3 before.

Therefore, $\Delta T_{overload}$ estimated by equation 3.27 is higher than the value obtained by equation 3.25 and therefore safer for protection purposes.

$\Delta T'$ is obtained according to the following equation:

$$\Delta T' = \Delta T_{overload} - \Delta T_{rated} \tag{3.28}$$

Equations 3.27 and 3.28 can be grouped as follows:

$$\Delta T' = \Delta T_{rated}\left[(k_I)^2 - 1\right] \tag{3.29}$$

ΔT_{lim} is the temperature rise limit for the stator windings under transient conditions.

And t_{lim} is the corresponding time to reach ΔT_{lim} supposing the motor was previously operating at rated conditions.

According to figure 3.7, ΔT_{lim} and t_{lim} can be related as follows:

$$\Delta T_{lim} = \Delta T_{rated} + \Delta T' \cdot \left(1 - (e)^{-\frac{t_{lim}}{t}}\right) \tag{3.30}$$

Finally, equations 3.29 and 3.30 are joined and re-arranged as follows:

$$t_{lim} = -t \cdot \ln\left[1 - \frac{(\Delta T_{lim} - \Delta T_{rated})}{\Delta T_{rated}\left((k_I)^2 - 1\right)}\right] \tag{3.31}$$

Figure 3.8 is a partial thermal limit curve (segment A only) for a standard 11 kW motor, applying the following parameters in equation 3.31:

- $\Delta T_{rated} = 75.2$ K;
- $\Delta T_{lim} = 90$ K. This value is the maximum allowed temperature rise for thermal class B (80 K) + 10 K that is the additional temperature rise allowed by NEMA standards for motors operating at service factor > 1 (Tables 2.4 and 2.6).
- t = 27 min;
- $k_I = 1.0$ up to 4.7.
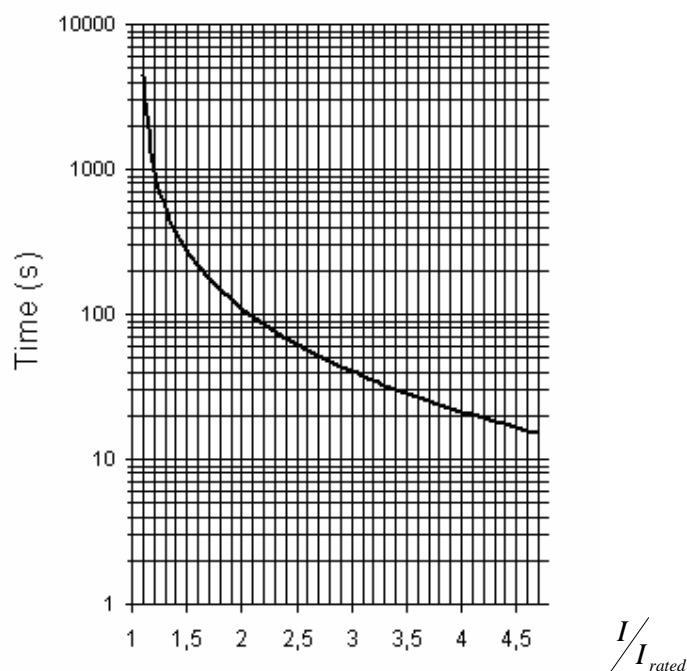
Figure 3.8 – Thermal limit curve for an 11 kW motor (segment A)

According to the above thermal limit curve is possible to state this motor would withstand an overload equal to $1.2 \times I_{rated}$ for just 15min. These parameters do not match to standards specifications for motor protective overload relays and releases to be discussed at chapter 5. New values for ΔT_{lim} must be defined.

3.5 – Main conclusions for chapter 3

- Thermal limit curves show the maximum time various values of over current can be allowed to flow through electric motors without reduction of their lives;

- The thermal limit curve showed at figure 3.8 informs the analysed motor could be submitted to an over current value equal to $1.2 \times I_{rated}$ during 15 minutes;

- This time lag is too small when compared to operating limits specified for overload relays and releases (detailed at chapter 5);

- Therefore, this thermal curve must be revised. It is necessary to define better values for temperature rise limits for stator windings under transient conditions (ΔT_{lim}). Chapter 4 will discuss different values for ΔT_{lim} that can be found in available literature. Besides that, new thermal limit curves will be calculated and tests will be performed in an 11 kW electric motor. Test results will be employed for validating obtained thermal limit curves.

CHAPTER 4

TEMPERATURE RISE TESTS AT OVERLOAD CONDITIONS

In this chapter it is introduced the concept of maximum allowable temperature for motor windings at transient conditions ($T_{\text{max transient}}$). This parameter will be employed for obtaining temperature rise limits for stator windings under transient conditions (ΔT_{lim}).

Based on this concept, three different thermal limit curves for an 11 kW motor are calculated and plotted.

Tests on an 11 kW motor at overload conditions are also reported.

Temperature rise values obtained by measurements are compared to calculated thermal limit curves.

4.1 – Maximum allowable temperatures for a.c. windings under transient conditions

Table 2.1 has presented the maximum acceptable temperatures for electric motors insulation systems, operating under continuous running duty.

It was also shown, at chapter 3, the calculation of thermal limit curves requires the consideration of a ΔT_{lim}, i.e., the temperature rise limit for the stator windings under transient conditions.

ΔT_{lim} can be calculated according to equation 4.1:

$$\Delta T_{\text{lim}} = T_{\text{max transient}} - T_{\text{max ambient}} \tag{4.1}$$

Where:

$T_{\text{max transient}}$ = Maximum allowable temperature for a part under transient conditions.

$T_{\text{max ambient}}$ = Maximum allowable ambient air temperature (= 40ºC).

Boothman, et al, /28/ claim that values for $T_{\text{max transient}}$ are not precisely defined and present some different data, as reproduced in table 4.1.

Table 4.1 - $T_{\max\ transient}$ data (According to Boothman)

	$T_{\max\ transient}$ values according to:		
	A 1961 poll with ten leading motor manufacturers	Informal polling of designers within GE	Published data by insulation material manufacturers
Class B stator winding	135 to 220ºC	180ºC	180ºC
Rotor bars	190 to 640ºC		

Values for $T_{\max\ transient}$ can also be established based on standards requirements for thermal protection for electric motors.

NEMA /13/ requires "the protector in a thermally protected medium motor shall limit the winding temperature" according to table 4.2 below. See also definitions in appendix 1.

Table 4.2 – Winding temperatures for running load (1) /13/

Insulation system class	Max winding temperature (2) (ºC)
A	140
B	165
F	190
H	215
(1) Running load: overload condition not including locked -rotor conditions. (2) Measuring procedure: resistance method. Thermocouple method is also accepted for motors rated $\leq$ 15 Hp.	

According to IEC /29/, built-in thermal protectors shall limit motor windings tempera-tures to the values presented in table 4.3.

These values are valid for thermal overloads with slow variation. See also appendix 4.

Table 4.3 – Maximum allowable temperature (ºC) according to IEC /29/

Insulation class	A	E	B	F	H
Thermal protection category 1	125	140	145	170	195
Thermal protection category 2	140	155	165	190	215
Measuring procedure: resistance method. Thermocouple meth od may be used for ma-chines rated $\leq$ 11 KW.					

IEC standard also claims "category 1 and 2 may both give satisfactory protection to a machine. The choice of category is normally made by the machine manufacturer and depends upon many factors…" /29/

4.2 – Calculated thermal limit curves for a standard electric motor

Figure 4.1 presents three different thermal limit curves calculated for standard 4 poles - 11 kW motors (frame 132). The curves were plotted only for the so-called running overload portion (segment A of figure 3.6). The electric motor winding was supposed to have a class B insulation system and ΔT_{rated} = 90 K (80 K for thermal class limit + 10 K for the hottest spot); i.e. worst case. The thermal time constant for heating was considered to be t = 20.64 minutes, based on appendix 5.
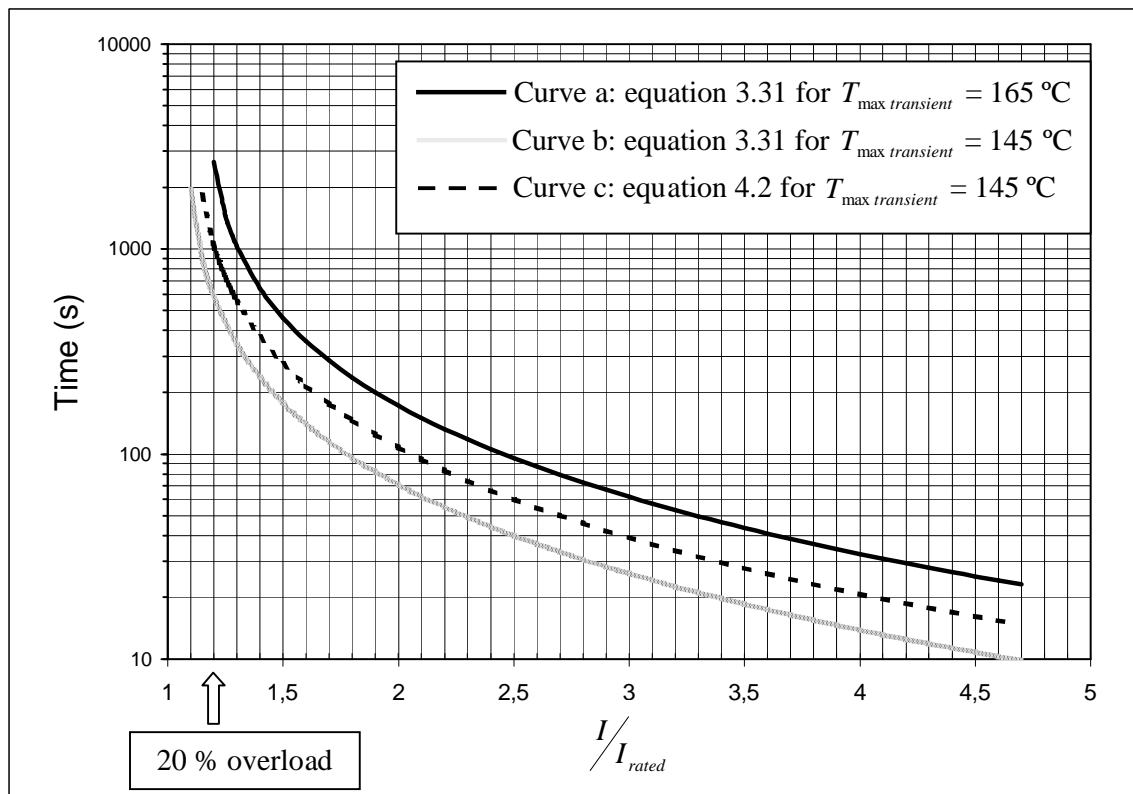
Figure 4.1 – Calculated thermal limit curves for standard 4 poles 11 kW motors

- Curve "a" was calculated according to equation 3.31, considering $T_{max\ transient} = 165°C$ (table 4.3, category 2). Therefore $\Delta T_{lim} = 165 - 40 = 125$ K.

  According to the plot is possible to say that for $I/I_{rated} = 1.2$, $t_{lim} \sim 2700$ s (~ 45 minutes).

- Curve "b" was also calculated according to equation 3.31, considering $T_{max\ transient} = 145°C$ (table 4.3, category 1). Therefore $\Delta T_{lim} = 145 - 40 = 105$ K.

  According to the plot is possible to say that for $I/I_{rated} = 1.2$, $t_{lim} \sim 600$ s (~ 10 minutes).

- Curve "c" was calculated according to equation 4.2, which is based on equations 3.12 and 3.31,

$$t_{lim} = -t \cdot \ln\left[1 - \frac{(\Delta T_{lim} - \Delta T_{rated})}{\Delta T_{rated}(k_{\Delta T} - 1)}\right] \tag{4.2}$$

where power losses values were obtained from table 3.2 and $k_{\Delta T}$ was calculated according to equations 3.20 and 3.21 and the subsequently presented example (in chapter 3). $\Delta T_{lim} = 105$ K (like for curve 2).

According to the plot is possible to say that for $I/I_{rated} = 1.2$, $t_{lim} \sim 1000$ s (~ 17 minutes).

4.3 – Temperature rise tests on a motor sample

A standard four poles three phase 11 kW motor, class B insulation system, 380 V/60 Hz was prepared for temperature rise measurements according to figure 4.2.
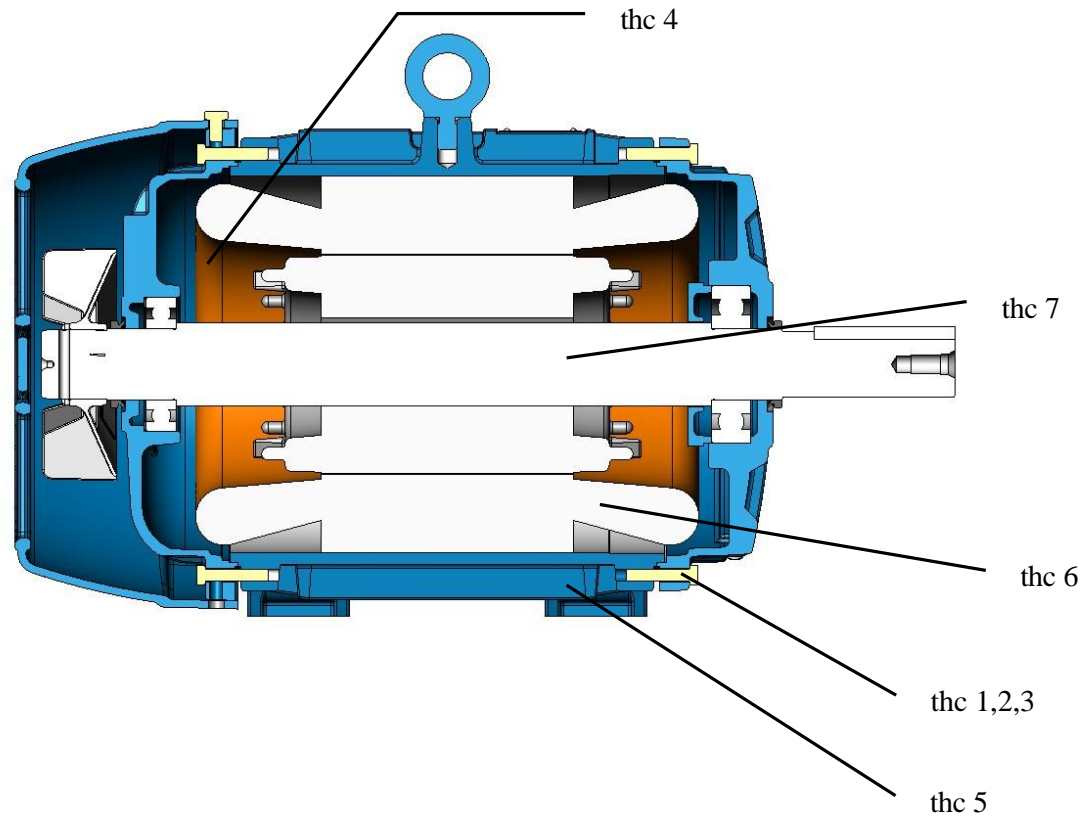
Figure 4.2 – Installation of thermocouples

Thermocouples 1,2 and 3 were placed in the drive-end overhangs (one thermocouple per phase) and thermocouple 4 in one of the non drive-end overhangs.

Thermocouples 5 and 7 were installed in holes machined respectively in the drive-end stator core and the drive-end rotor core.

Thermocouple 6 was placed in the drive-end of the rotor short circuit ring. One additional thermocouple (number 8) was provided for ambient temperature measurements.

4.3.1 – Tests at rated load conditions

The electric motor was operated at rated conditions [torque = 59.8 Nm (6.1 kgfm) and current = 22.7 A] until reaching steady state temperature.

Temperature rise measured by resistance method = 78.3 K

The maximum temperature rise measured by each thermocouple is presented in table 4.4

Table 4.4 – Temperature rise figures for $1 \times I_{rated}$

STEP 1xI $_{rated}$				
Measurement Point	Maximum Temperature (ºC)	• T (K)	t$_{lim1}$ Time to 105K (min)	t$_{lim2}$ Time to 125K (min)
Drive-end overhang 1	115.7	89.0		
Drive-end overhang 2	117.6	90.9	-	-
Drive-end overhang 3	117.2	90.5		-
Non drive-end overhang	114.1	87.4		
Drive-end stator core	92.9	66.2		
Drive-end short circuit ring	132.4	105.7		
Drive-end rotor core	130.5	103.8		
		Ambient Temperature (ºC)		26.7

Figure 4.3 shows the temperature rise plot detected in the drive end overhang 2.
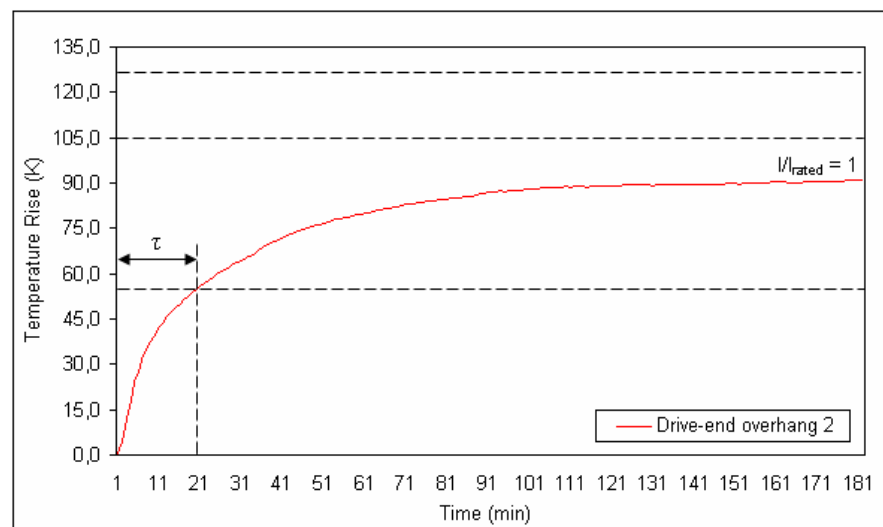
Figure 4.3 – Temperature rise measured by thermocouple 2 $\left(\dfrac{I}{I_{rated}} = 1.0 \right)$

Main conclusions obtained from the above test results:

- The temperature rise value measured by resistance method (78.3 K) is close to the limit of temperature rise for class B insulation systems (ΔT_{max} = 80 K).

- The maximum temperature rise value measured by thermocouples in the windings was 90.9 K (at drive-end overhang 2). This value is close to the hot spot temperature value considered in the calculation of thermal limit curves presented in item 4.2 before.

- The thermal time constant $t = 20$ minutes is close to the value obtained from appendix 5.

4.3.2 – Tests at small overload conditions

After the previous tests and measurements, the motor had cooled down to temperature values below to the steady state temperature reached at rated load operation. The motor was switched on again at rated load conditions as described in item 4.3.1. This load condition was kept until the motor reached steady state temperature again. The torque was subsequently raised in a way $I/I_{rated} = 1.1$ and this load was kept until motor reached steady state temperature.

Temperature rise measured by each thermocouple is presented in table 4.5.

Table 4.5 – Temperature rise figures for $1.1 \times I_{rated}$

STEP 1.1xI$_{rated}$				
Measurement Point	Maximum Temperature (ºC)	• T (K)	t$_{lim1}$ Time to 105K (min)	t$_{lim2}$ Time to 125K (min)
Drive-end overhang 1	133.0	108.6		
Drive-end overhang 2	134.8	110.4		
Drive-end overhang 3	135.4	111.0	42	-
Non drive-end overhang	131.5	107.1		
Drive-end stator core	105.0	80.6		
Drive-end short circuit ring	151.7	127.3		
Drive-end rotor core	150.6	126.2		
Ambient Temperature (ºC)				24.4

The highest temperature rise was measured at the drive-end overhang 3, which reached $\Delta T_{lim} = 105$ K in 42 minutes. Figure 4.4 shows the temperature rise plot detected in the drive end overhang 3.
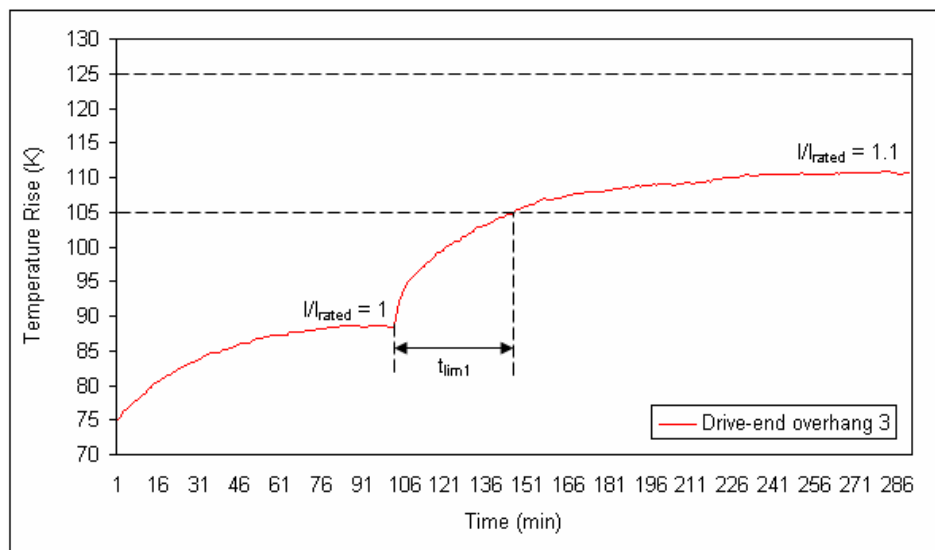
Figure 4.4 - Temperature rise measured by thermocouple 3 $\left(\dfrac{I}{I_{rated}} = 1.1 \right)$

The previous test sequence was repeated for overloads providing $\dfrac{I}{I_{rated}}$ = 1.2 and 1.3.

Tests results for $1.2 \times I_{rated}$ are presented at table 4.6 and figure 4.5.

Table 4.6 – Temperature rise figures for $1.2 \times I_{rated}$

STEP 1.2xI_rated				
Measurement Point	Maximum Temperature (ºC)	• T (K)	t_{lim1} Time to 105K (min)	t_{lim2} Time to 125K (min)
Drive-end overhang 1	154.8	129.3		
Drive-end overhang 2	158.5	133.0	6	43
Drive-end overhang 3	157.7	132.2		
Non drive-end overhang	153.7	128.2		
Drive-end stator core	119.5	94.0		
Drive-end short circuit ring	34.5	9.0		
Drive-end rotor core	31.9	6.4		
Ambient Temperature (ºC)				25.5
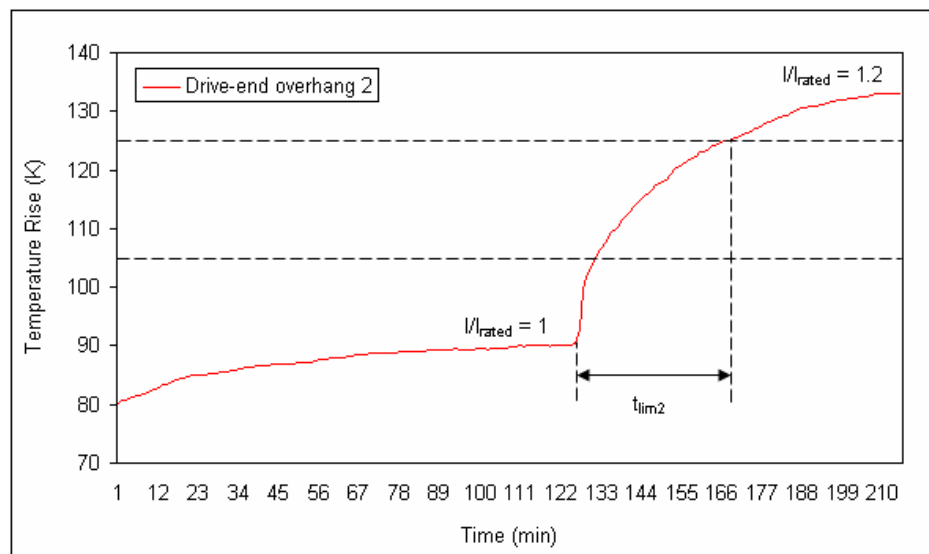
Figure 4.5 - Temperature rise measured by thermocouple 2 $\left(\dfrac{I}{I_{rated}} = 1.2 \right)$

Tests results for $1.3 \times I_{rated}$ are presented at table 4.7 and figure 4.6.

Table 4.7 – Temperature rise figures for $1.3 \times I_{rated}$

| STEP 1.3xI_{rated}				
Measurement Point	Maximum Temperature (ºC)	• T (K)	t_{lim1} Time to 105K (min)	t_{lim2} Time to 125K (min)
Drive-end overhang 1	185.3	161.7		
Drive-end overhang 2	188.7	165.1	3	16
Drive-end overhang 3	187.2	163.6		
Non drive-end overhang	181.9	158.3		
Drive-end stator core	138.3	114.7		
Drive-end short circuit ring	205.1	181.5		
Drive-end rotor core	207.3	183.7		
Ambient Temperature (ºC)				23.6
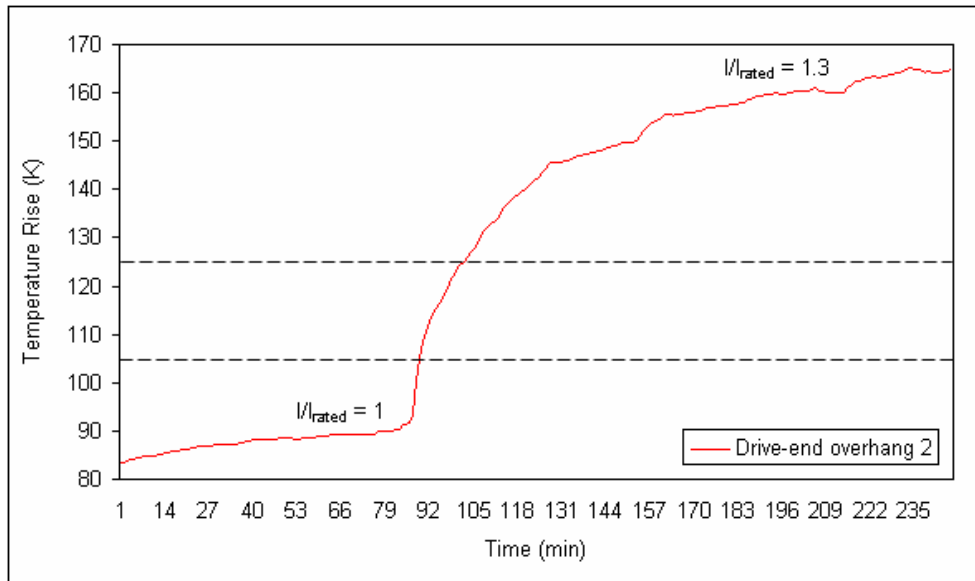
Figure 4.6 - Temperature rise measured by thermocouple 2 $\left(\dfrac{I}{I_{rated}} = 1.3 \right)$

The main conclusions here are:

- $\Delta T_{\lim} = 105$ K is quickly reached for overloads = 1.2 and 1.3 x I_{rated}. Even for overloads = 1.1 x I_{rated} this limit is reached in less than 1 hour (42 minutes). Due to it actual thermal limit curves for $\Delta T_{\lim} = 105$ K will not be considered in this research.

- When an overload providing $\dfrac{I}{I_{rated}} = 1.2$ was applied, $\Delta T_{\lim} = 125$ K was reached in 43 minutes.

- When an overload providing $\dfrac{I}{I_{rated}} = 1.3$ was applied, $\Delta T_{\lim} = 125$ K was reached in 16 minutes.

4.3.3 – Tests at higher overloads

The test sequence described in item 4.3.2 was repeated for overloads providing $\dfrac{I}{I_{rated}} = 1.5$, 2 and 3. These overloads were kept until the windings reached temperatures close to 170 ºC.

Test results for $1.5 \times I_{rated}$ are presented at table 4.8 and figure 4.7.

Table 4.8– Temperature rise figures for $1.5 \times I_{rated}$

STEP 1.5xI$_{rated}$				
Measurement Point	Maximum Temperature (ºC)	• T (K)	t$_{lim1}$ Time to 105K (min)	t$_{lim2}$ Time to 125K (min)
Drive-end overhang 1	161.4	137.4		
Drive-end overhang 2	167.1	143.1	1.6	4
Drive-end overhang 3	164.7	140.7		
Non drive-end overhang	165.5	141.5		
Drive-end stator core	109.8	85.8		
Drive-end short circuit ring	152.4	128.4		
Drive-end rotor core	150.2	126.2		
Ambient Temperature (ºC)				24.0
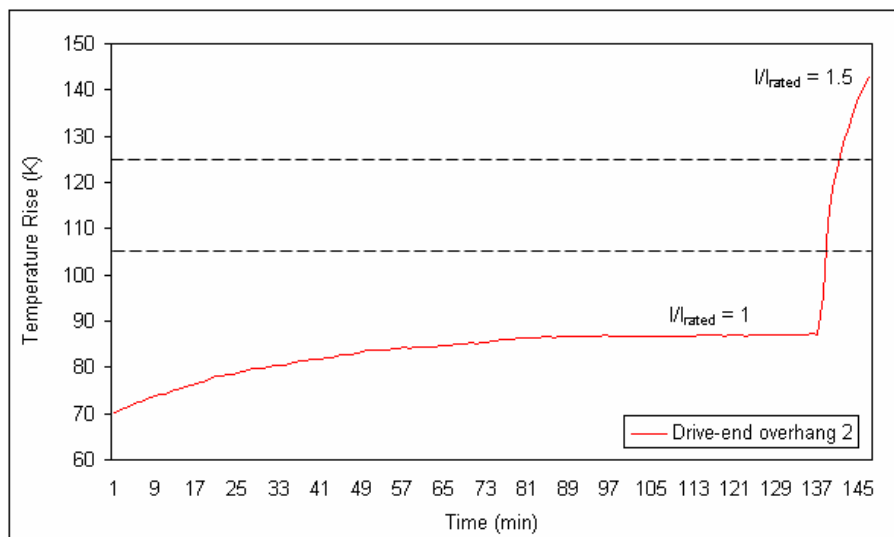
Figure 4.7 - Temperature rise measured by thermocouple 2 $\left(\dfrac{I}{I_{rated}} = 1.5 \right)$

For this load condition ($1.5 \times I_{rated}$), the drive-end overhang 2 reached $\Delta T_{\lim} = 125$ K in four (4) minutes. This value is according to IEC 60034-1 /12/, which requires the motor shall "withstand a current equal to 1.5 times the rated current for not less than 2 minutes."

For loads providing $\dfrac{I}{I_{rated}} = 2$ and 3, $\Delta T_{\lim} = 125$ K was reached in less than 1.5 minutes.

4.4 – Tests summary and main conclusions for chapter 4

Test results for temperature rise at motor windings (worst case: drive –end overhang 2) were summarized in table 4.9.

Table 4.9 – Limits for each value of I/I_{rated}

I/I$_{rated}$	t$_{lim1}$	
	Time to 125K	
	(min)	**(s)**
1.0	-	-
1.1	-	-
1.2	43.0	2580
1.3	16.0	960
1.5	4.0	240
2.0	1.5	90
3.0	0.4	24

The values from table 4.9 were subsequently plotted in an actual thermal limit curve and compared to the calculated one. The plot for the calculated thermal limit curve was obtained from item 4.2, curve 1.
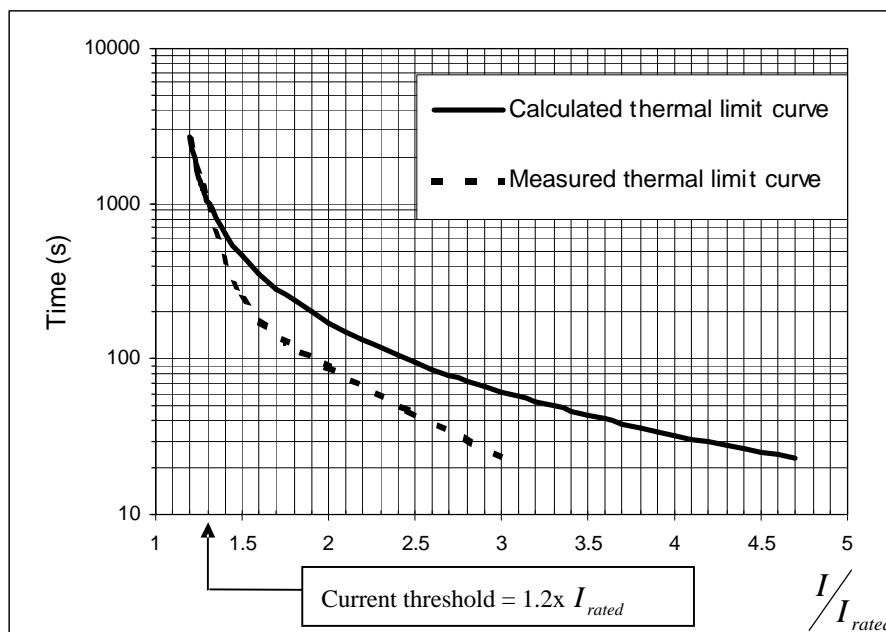
Figure 4.8 – Measured and calculated thermal limit curves for the tested motor ($\Delta T_{lim} = 125$ K)

Test results for temperature rise at stator core, short circuit ring and rotor core were not analysed here and remain available for future researches.

Main conclusions after analysing thermal limit curves at figure 4.8:

- Measured thermal limit curve for the 11 kW motor sample is quite similar to the calculated thermal limit curve up to $I/I_{rated} = 1.3$;

- For I/I_{rated} higher than 1.3 the calculated thermal limit curve no longer agrees to the measured thermal limit curve. The electric motor is heating faster than predicted by the mathematical model. Anyway, the proposed thermal model was considered acceptable because the main concern of this research is to analyse the performance of overload protection devices for overloads up to 1.2 x I_{rated} ;

- Thermal limit curves employed by WEG should be based on an better thermal model;

- When $I/I_{rated} = 1.2$, $\Delta T_{lim} = 125$ K is reached in approximately 43 minutes (see item 4.3.2). $I/I_{rated} = 1.2$ must be considered an important current threshold (Figure 4.8) in order to avoid thermal damages in motor windings insulation;

- Therefore, current dependent protection devices should be designed for tripping when the electric motor is submitted to over current values ≥ 1.2 times their rated current. This conclusion is in accordance to the limits of operation required by IEC 60947-4-1 for overload relays and releases (informed at chapter 5 – Table 5.2).

CHAPTER 5
BASICS ABOUT MOTOR CONTROL AND PROTECTION

This chapter starts presenting the main functions provided by motor starters, among them overload protection. The main operating conditions that can make an electric motor become thermally overloaded, are also discussed.

Additionally, different types of overload protective devices are described and classified according to their sensing principle.

As informed in chapter 1, chapters 6 and 7 will analyse thermal overload protection provided by WEG's motor protective circuit breakers. These devices employ bimetal overload releases for providing overload protection for electric motors. Due to it, bimetal overload relays and releases are presented in a detailed way, in chapter 5, including working principle, standard requirements and application procedures.

5.1 – Motor starters
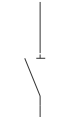
Motor starters are equipments providing all components necessary to properly switch and protect electric motors.

A typical direct-on-line (D.O.L.) a.c. motor starter /30/, /31/, /32/, /33/ is assembled with devices providing the following control and protection functions:

- Isolating function: for disconnecting (separating) the electrical equipment from the power supply for safety reasons (e.g. for work on a machine/electrical equipment) /34/, /35/.

- Short-circuit protection: for detecting and breaking over currents arising from short-circuits.

- Power switching function: "which allows the supply to be switched on and off, to start and stop the motor" /31/. The control of such function can be either manual (local) or remote /32/.

- Overload protection: to avoid operating conditions, which can cause excessive heating in motor components and associated electric circuits.

One possible solution for assembling a D.O.L. motor starter is showed at Table 5.1.

Table 5.1 – Circuit diagrams for a typical D.O.L motor starter

Function	Device	Circuit diagrams	
		IEC symbols	ANSI/CSA symbols
Isolation	Switch-disconnector		
Short circuit protection	Fuses		
Power switching	Contactor		
Overload protection	Thermal over-load relays		
Electric motor			

Electric motors present special operating features /32/ such as:

- Heavy start-up current (see figure 5.1) that can cause important voltage drops in the power supply circuit.
- Number and frequency of start-up operations are generally high.

Motor starters components must be able to properly perform their functions under these special operating conditions.

$$I'' = 8 \ to \ 12 \times I_{rated}$$
$$I_{start} = 5 \ to \ 8 \times I_{rated}$$
$$I_{rated} = \text{Motor rated current}$$
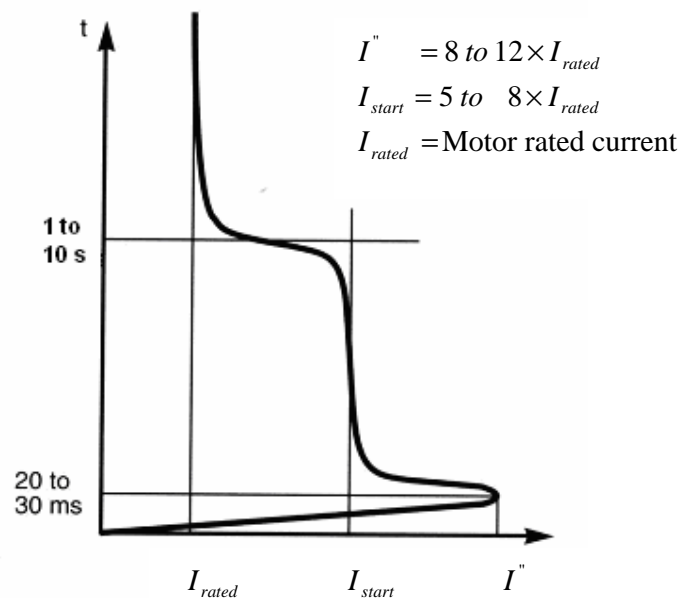
Figure 5.1 – Typical direct on line starting current of electric motors /32/

5.2 – Overload protection

Electric motors can become thermally overloaded due to the following operating conditions /36/, /37/:

- Continuous mechanical overloads;
- Locked rotor conditions;
- Extended starting and stopping (caused by a too high moment of inertia of load);
- Voltage and frequency fluctuations;
- Phase unbalance/single phasing;
- High switching frequency;
- Irregular intermittent duty (when the motor is continuously operating but the load is irregularly applied);
- Increased ambient temperature;
- Restricted cooling.

IEC 60204-1 /34/ requires the use of overload protection for each motor rated at more than 0.5 kW. The same standard claims this protection can be provided by overload protective devices, temperature-sensing devices or current-limiting devices.

Notes:

1 - "Overload protective devices detect the time-current relationships in a circuit that are in excess of the rated full load…and initiate appropriate control responses."/34/

2 - In practice, current-limiting devices are applied only for short circuit protection where high prospective short circuit currents are expected.

National Electrical Code (NEC) /38/ explains the meaning of overload in electrical apparatus as follows: "…an operating overcurrent that, when it persists for a sufficient length of time, would cause damage or dangerous overheating of the apparatus. It does not include short circuits or ground faults."

Besides that, NEC /38/ requires that each continuous-duty motor shall be protected against overloads by one of the following means:

- An overload device responsive to motor current;
- "A thermal protector integral with the motor, approved for use with the motor it protects" and capable of protecting it against overloads and failure to start. A thermal protector is a temperature-sensing device installed in the motor. (See also appendix 1);
- "A protective device integral with the motor that will protect the motor against damage due to failure to start …if the motor is part of an approved assembly that does not normally subject the motor to overloads;"
- "For motors larger than 1500 hp, a protective device having embedded temperature detectors…" that interrupts the current when the motor reaches a temperature rise higher than the value marked on the nameplate.

NEC also states that motors under intermittent operation conditions "shall be permitted to be protected against overload by the branch-circuit short circuit and ground-fault protective device…"

Figure 5.2 illustrates and classifies the main overload protection devices available in the market.

```
                        ┌─────────────────┐
                        │ Overload protec- │
                        │  tion devices   │
                        └─────────────────┘
```

Current dependent protection devices	Thermal detectors* (temperature sensitive devices)	Thermal protectors* (temp. and current sensitive devices)

| Electromechanical devices | PTC thermistors | Phenolic motor protectors |

| Bimetal overload relays and releases (**) | Thermostats | Thermostats |

| Eutectic alloy relays | Platinum resistance thermometers | |

| Electronic overload relays |

| Analogue relays |

| Microprocessor based relays |

(*) Terms and definitions according to
IEC 60034-11 /30/
(**) Type of overload protection devices manufac-
tured by WEG Acionamentos.

Figure 5.2 – Main overload protection devices available in the market

5.3 – Bimetal overload relays and releases

5.3.1 – Working principle

An overload relay is an electric device designed to sense currents passing through its main

circuit. In case an over current is detected it opens an auxiliary contact that can be series connected to a contactor coil. As a consequence, the contactor opens its main contacts interrupting the current that flows though the circuit and protecting the motor. On the other hand, an overload release can be defined as a "device, mechanically connected to a mechanical switching device, which releases the holding means and permits the opening …of the switching device." /35/

Figure 5.3 illustrates a basic design for a three-pole bimetal overload relay. These devices have three bimetal strips (6) that are indirectly heated by the motor current which flows through the heater windings (7).

1 Manual/automatic reset selector (reclosing lock-out)	5 Tripping bar
2 Reset button	6 Bimetal strip
3 Tripping lever	7 Heater winding
4 Ambient temperature compensation strip	8 Test button
	9 Setting screw
	10 Switch rocker
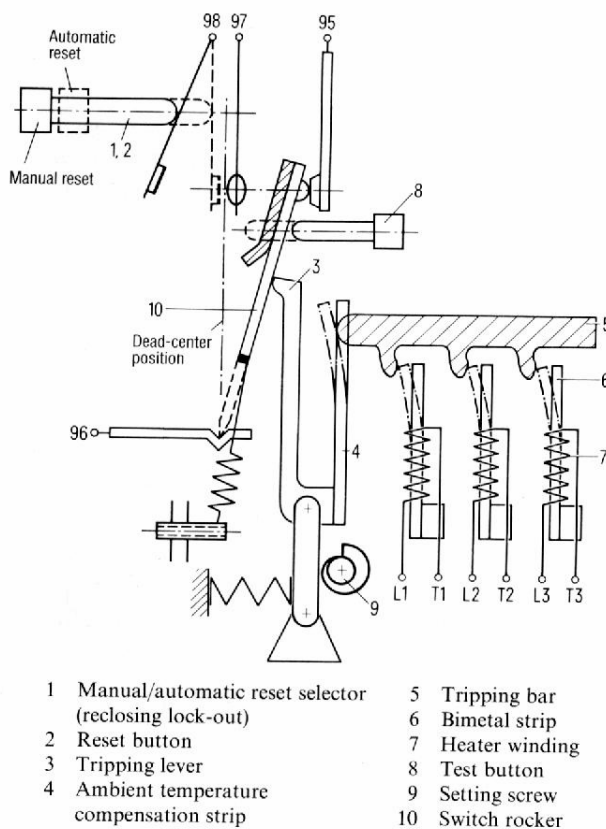
Figure 5.3 – Working principle of a bimetal overload relay /36/

Due to the temperature rise the bimetal strips bend and move the tripping bar (5) and the tripping lever (3). In the event of an overload, the bimetals movement is enough to make the snap-action moveable contact (10) change its position, opening the normally closed (NC) contact (95/96) and closing the normally open (NO) contact (97/98).

The reset operation can be either manual or automatic depending on the chosen position for the reset selector/button (1,2).

Bimetal overload relays also have a setting dial (9), which allows the current setting according to the motor full load current.

The bimetal strips deflection depends also on the ambient temperature. The compensation strip (4) is used to "reduce the effect of the ambient temperature on the tripping behaviour of the overload relay." /36/

The above description considers the same current value simultaneously heats all three bimetal strips. In case there is a phase loss, one bimetal will deflect less and the other two would

have to provide the necessary force for tripping the overload relay. A trip delay would happen and the electric motor could not be properly protected.

A solution for this matter is the use of an additional differential tripping bar (II) as showed at figure 5.4. For an operational three pole symmetrical overload all three bimetal strips bend by the same amount (a +b). "If phase L1, for example, is disconnected during operation then the respective bimetal strip will cool down and its end will return to the cold position. This will cause the differential tripping bar II and the lower hinged point of the differential lever to be moved to their original positions as well. The heated bimetal strips L2 and L3, on the other hand, continue to force the tripping bar I in the direction of the tripping point. Due to this differential movement of the tripping bars, the differential lever turns around its lower hinged point, and its end moves towards the tripping point (a + b) at a greater rate determined by the leverage ratio." /36/

Figure 5.5 shows a typical current-time characteristic curve for a three-pole overload relay. It "gives the tripping time as a function of the operating current I_r, which is expressed as a multiple of the current setting. They are usually provided for symmetrical three-pole and for 2-pole loading" /36/ starting from the cold state. In case the overload relay has already reached steady state, tripping times obtained from curve will be reduced to around 25 % of the cold state values /36/.

IEC 60079-14 /39/ specifies the tolerance field for current-time characteristic curves for overload relays and releases applied for protecting increased safety motors (used in explo-

sive gas atmospheres). This standard requires tripping times shall be according to the values obtained in the supplied characteristic curves within a tolerance field equal to +/- 20 %, for current values higher than $3 \times I_r$.

Due to low production costs, high availability and ease to install, bimetal overload relays and releases are widespread used in regular industrial applications.
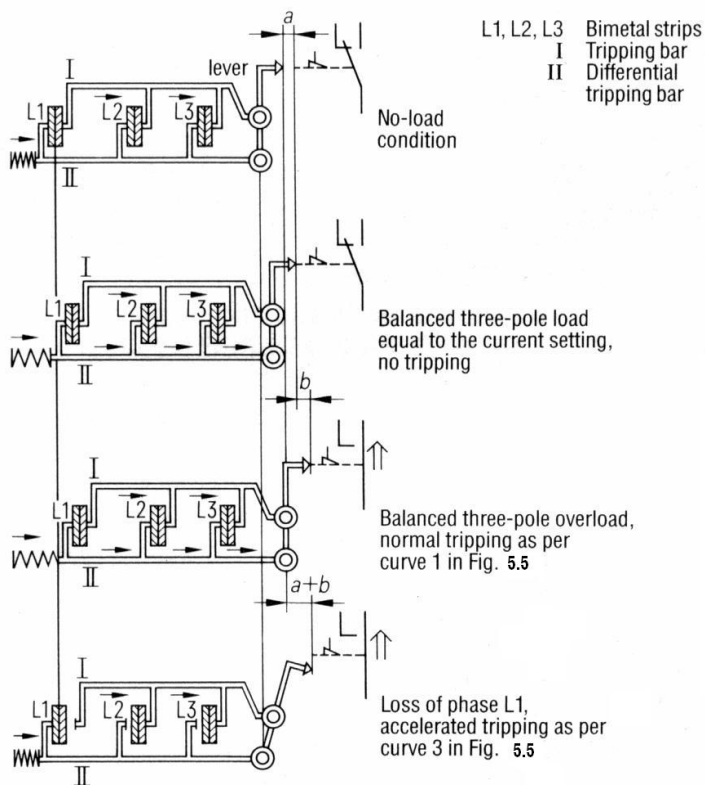
Figure 5.4 – Working principle of phase-loss sensitivity feature /36/

1 Symmetrical three-pole loading from the cold state
2 Two-pole loading from the cold state, relay without phase failure sensitivity
3 Two-pole loading from the cold state, relay with phase failure sensitivity
I_r Current setting of the overload relay
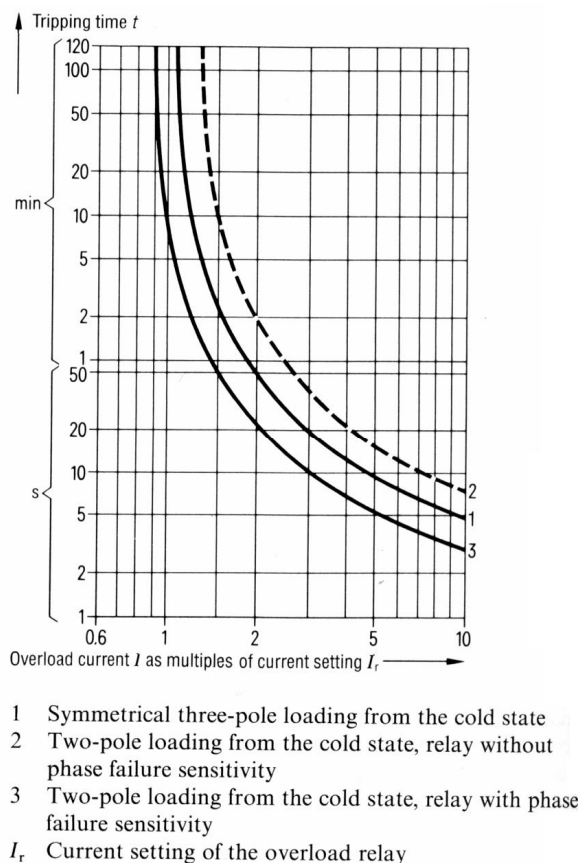
Figure 5.5 – Current-time characteristic curve /36/

5.3.2 – Standard requirements for three-pole overload relays and releases

IEC 60947-4-1 /40/ requires overload relays and releases operate as follows, when all poles are energized (refer to table 5.2):

a) "At A times the current setting, tripping shall not occur in less than 2 h starting from the cold state…" In practice, thermal equilibrium is reached before 2 hours and the devices shall never trip with such small multiple of current setting;

b) "When the current is subsequently raised to B times the current setting, tripping shall occur in less than 2 h;" This limit of operation is in accordance to current threshold highlighted at figure 4.8 – thermal limit curves for an 11 kW motor. The additional limits of operation discussed below will not be compared to thermal limit curves showed at chapter 4. The reason for it is this research is focused on the adjustment and calibration of bimetal overload releases for motor protective circuit breakers. It

will be showed in chapter 6 these protection devices are calibrated for tripping when carrying current values between 1.05 and 1.2 times their current settings.

c) When the relay or release is energized at C times the current setting, tripping shall occur in less than 2, 4, 8 or 12 minutes (according to the tripping class), starting from thermal equilibrium;

d) "At D times the current setting, tripping shall occur within the limits given in" table 5.2 (according to the trip class), " starting from the cold state."

In case only two poles are energized, the limits of operation must be as follows (refer to table 5.3): "with the relay or release energized on three poles, at A times the current setting, tripping shall not occur in less than 2 h, starting from the cold state. Moreover, when the value of the current flowing in the two poles carrying the higher current is increased to B times the current setting, and the third pole is de-energized, tripping shall occur in less than 2 h."

Devices with a current setting range must comply with the above mentioned limits "when…carrying the current associated with the maximum setting and also when…carrying the current associated with the minimum setting."

Table 5.2 – Limits of operation when all poles are energized (IEC 60947-4-1)

Type of over-load relay	Multiple of current setting I_r						Reference ambient temperature
	A $T_p > 2\,h$	B $T_p \leq 2\,h$	C Tripping class	T_p (minutes)	D Tripping class	T_p (seconds)	
			10 A	≤ 2	10A	$2 < T_p \leq 10$	
			10	≤ 4	10	$4 < T_p \leq 10$	
			20	≤ 8	20	$6 < T_p \leq 20$	
			30	≤ 12	30	$9 < T_p \leq 30$	
Not compensated for ambient air temperature variations	1.0	1.2	1.5			7.2	+ 40 ℃
Compensated for ambient air temperature variations	1.05	1.2	1.5			7.2	+ 20 ℃
T_p = Tripping time							

Table 5.3 – Limits of operation when energized on two poles only (IEC 60947-4-1)

Type of overload relay	Multiple of current setting				Reference ambient temperature
	A $T_p > 2$ h, starting from cold state of relay		B $T_p \leq 2$ h		
Compensated for ambient air temperature variations. Not phase loss sensitive.	3 poles	1.0	2 poles	1.32	+ 20 ℃
			1 pole	0	
Not compensated for ambient air temperature variations. Not phase loss sensitive.	3 poles	1.0	2 poles	1.25	+ 40 ℃
			1 pole	0	
Compensated for ambient air temperature variations. Phase loss sensitive	2 poles	1.0	2 poles	1.15	+ 20 ℃
	1 pole	0.9	1 pole	0	
T_p = Tripping time					

On the other hand, North American standards and codes /38/, /41 /, /42 / establish the limits of operation of overload relays as a function of motor service factor (table 5.4).

Table 5.4 – Limits of operation at 3 poles loading (NEC)

Motor Service Factor (SF)	Maximum tripping current
SF $\geq$ 1.15	1.25 x I_r
SF < 1.15	1.15 x I_r

This research will concentrate only on analysing overload releases performance according to IEC standards. It is recommended future researches may analyse how to set an IEC overload relay or release for protecting a NEMA type motor according to its service factor (SF).

5.3.3 – Basic application procedures

Overload relays and releases provide proper motor protection when their setting dials are set to the rated motor current. /37/

Most bimetal overload relays and releases available in the market are manufactured for tripping classes 10A and 10 /43/, /44/, /45/, /46/, /47/. Tripping classes 10A and 10 are appropriate for motors operating at normal starting conditions (most application cases).

In case of heavy starting conditions class 10A and 10 overload relays and releases are likely to trip before the motor reaches its running current. Typical examples of this application are "centrifuge pumps or high speed fans with large diameter and inertia, as well as ma-

chines which have to be started under load, such as conveyor belts or coal crushers." /36/ In such situation "it would be completely wrong to adjust an overload relay…to a current level higher than the rated motor current." /37/

There are three possible solutions for overload protection for heavy starting motors:

- Current transformer operated relays: It consists of using three saturating core current transformers for feeding a regular bimetal overload relay. "Up to two times current setting I_r, the transmission ratio I_1/I_2 of the saturating core current transformers is practically linear." For operating currents higher than two "the secondary current no longer grows in proportion to the primary current. This non-linear increase in the secondary current produces an extended tripping delay if over currents greater than twice the value of current setting occur, and hence permits longer starting times." /37/

- Overload relays having tripping classes from 15 up to 30: Normally, available only for electronic overload relays /43/, /44/ and /45/. (See also sections 5.5 and 5.6)

- Bridging of motor protection during starting: An additional contactor, parallel to the overload relay, is included in the motor starter. Due to this contactor, "the overload relay does not carry the full current during starting. Only when the motor has reached full speed the bridging contactor is switched off and the full motor current is then carried by the overload relay." Monitoring personnel is required during starting. /37/ This solution is specially recommended in case "the motor run-up time being longer than the tripping time associated with tripping class 30." /36/

Current dependent overload relays and releases may not provide proper protection when the winding temperature is not directly related to motor current /36/. These operating conditions are related bellow:

- High switching frequency;
- Irregular intermittent duty;
- Increased ambient temperature;
- Restricted cooling.

In these applications literature recommends the use of thermal detectors embedded ithe windings overhangs. The protection achieved using thermal detectors depends on whether the motor to be protected is stator critical or rotor critical /36/, /37/:

Stator critical motors can be defined as the ones that, under locked rotor conditions, the stator windings reach their permissible temperature limit quicker than the rotor. Three-phase induction motors up to approximately 15 kW are normally stator critical. In this case, a thermal detector alone fitted in the windings overhangs "ensures that the stator winding and the rotor are adequately protected even with a locked rotor". /37/

Rotor critical motors are electric machines that, under locked rotor conditions, the rotor reaches the permissible temperature limit earlier than the stator. Three-phase motors above 15 kW are usually rotor critical. Supposing a thermal detector alone is used to protect this motor, "the delayed temperature rise in the stator can lead to a delayed tripping" of the protecting device. "It is therefore advisable to supplement the protection of rotor critical motors by a conventional" current dependent overload relay or release. This supplementary device may present nuisance tripping in case the motor is operating under high switching frequency or under irregular intermittent duty. To avoid this undesired tripping the current dependent overload relay or release shall be set higher than the motor rated current. In this arrangement, the current dependent overload relay provides motor protection against locked rotor conditions; meanwhile, the thermal detector monitors the motor windings /38/.

Table 5.5 presents a summary of motor protection achieved by bimetal overload relays and thermal detectors (specifically thermistors here - see section 5.7).

5.4 – Eutectic alloy overload relays

"The eutectic alloy overload relay is designed with precision heater elements utilizing a eutectic alloy that liquefies at a predetermined temperature. When the eutectic liquefies, it releases a spindle mechanism and allows the overload relay to trip." / 48 / Figure 5.6.

Figure 5.7 and 5.8 show typical solutions for eutectic alloy overload relays and their respective heater elements. According to WEG's sales personnel in USA, this kind of overload relay has a decreasing market, even in North America.

Table 5.5 – Motor protection achieved by different devices /37/

MOTOR OPERATING COND ITIONS	Kind of motor protection		
	Bimetal relay	Thermistor	Bimetal relay and thermistor
Continuous mechanical overload	+	+	+
Locked rotor conditions (stator critical motor)	+	+	+
Locked rotor conditions (rotor critical motor)	(+)	(+)	(+) Better
Extended starting and stopping	(+)	+	+
Voltage and frequency fluctuations	+	+	+
Phase unbalance/single phasing	+	+	+
High switching frequency	-	+	+
Irregular intermittent duty	-	+	+
Increased ambient temperature	-	+	+
Restricted cooling	-	+	+
+ Full protection (+) Partial protection - No protection			
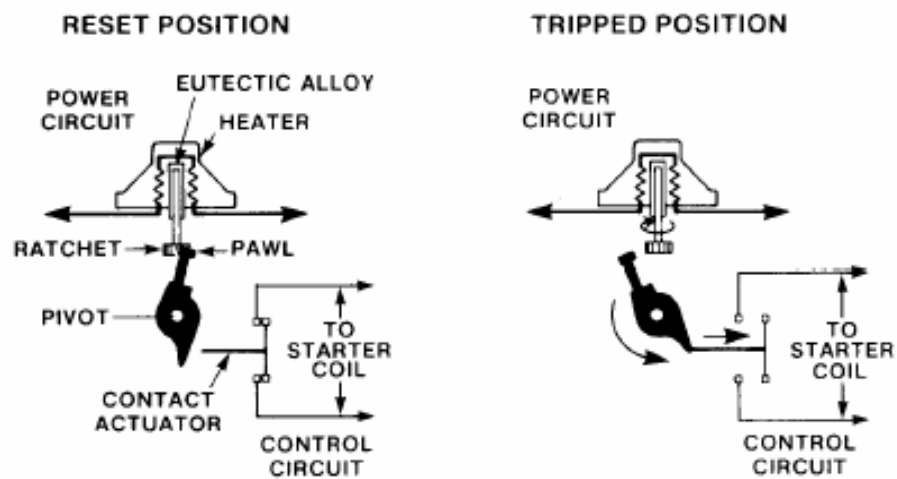
Figure 5.6 – Working principle of an eutectic alloy overload relay /48/
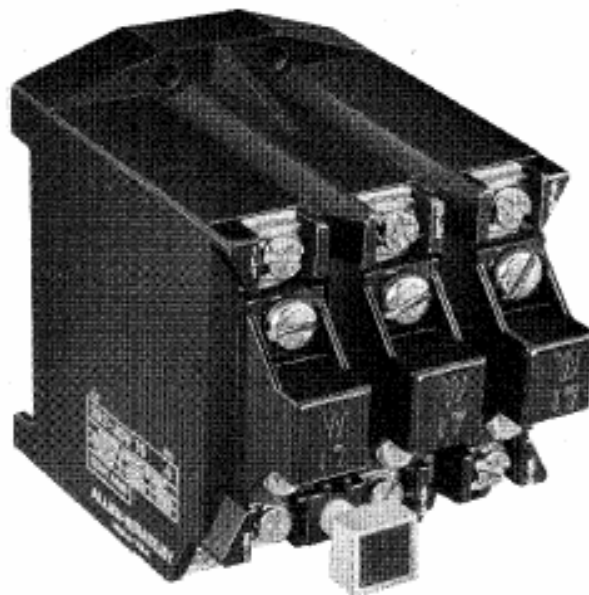
Figure 5.7 – Typical eutectic alloy overload relay /48/
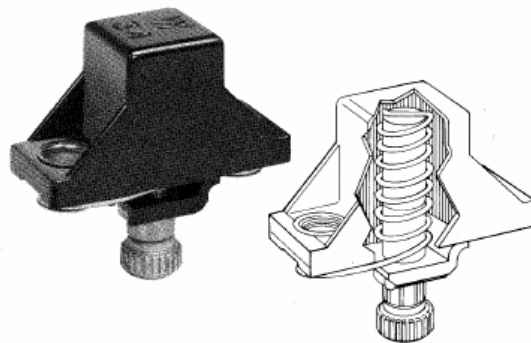
Figure 5.8 – Typical one-piece eutectic alloy heater element /48/

5.5 – Analogue electronic overload relays

Analogue electronic overload relays have one current transformer per phase. The secondary currents are fed to an electronic circuit where they are rectified.

The rectified signal is used both for self-powering the electronic circuit and as a proportional voltage signal for fault monitoring.

Figure 5.9 shows a diagram for an analogue electronic overload relay including its internal and external interfaces.

In case the electronic circuit detects a fault a capacitor is discharged over a tripping coil that makes a bi-stable magnetic armature change its position. Two moveable auxiliary contacts are directly assembled on the magnetic armature. The normally closed auxiliary contact is used for controlling the starter's power contactor, thus protecting the electric motor /33/, /49/.

Figure 5.10 gives an overview of a typical tripping mechanism employed in analogue electronic overload relays available in the market.

The main features presented by these devices are:

- Higher accuracy on overload tripping (tripping threshold = 1.15);
- Trip classes 10,15,20 and 30 available;
- Phase unbalance protection (40%; 3 seconds)
- Single phase protection (3 seconds);
- Low power consumption;
- Adjustment range 1:4;
- Higher production costs when compared to bimetal overload relays.

Mechanism		User/Operator
- trip free	Stop	
- stop function	Selection M/A	
- manual reset	Reset	
- selection manual / automatic reset		

M-Reset Force

Stop Force

Test

Indication

Adjustment Ie

Actuator/Contact System
- closing / opening contacts NO/NC
- stable positions
- trip indication
- test function

U_{trip}

U_{Reset}

Electronics
- self powered
- overload detection
- phase unbalance detection
- phase loss detection
- automatic Reset signal
- trip classes
- adjustment range

Electronic overload relay

Status NC

Status NO

Ia   Ib   Ic

3 phase power system

Contactor

Current sensors
- sensing
- provide power
- short circuit protection

3 phase motor

———— Mechanical interfaces   - - - - - - - Electrical interfaces

Figure 5.9 – Internal structure and interfaces of electronic overload relays /49/
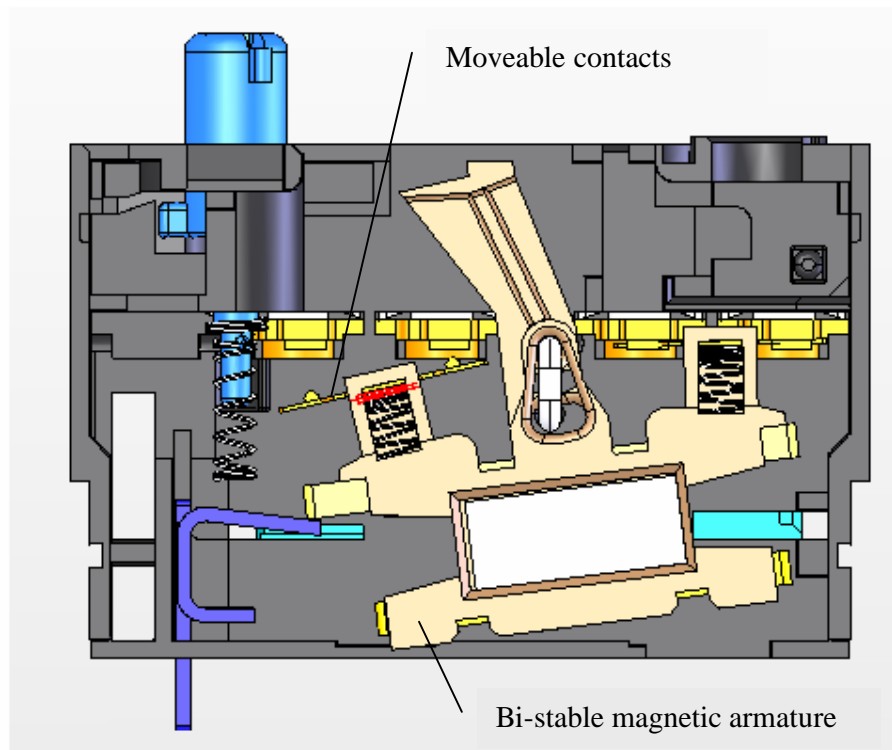
Figure 5.10 – Typical tripping mechanism of analogue electronic overload relays

5.6 – Microprocessor based overload relays

Electronic overload relays with microprocessors also have three current transformers used for measuring each motor phase current. The secondary currents are "converted to pro-portional voltages, rectified and fed to a microprocessor by means of an analogue-to-digital converter…The signal is processed in a corresponding" software, "and an impulse is given to output relays in the event of" a fault /36/.

Figure 5.11 presents a typical microprocessor based overload relay available on the market.

In relation to analogue relays, these devices present the following additional features:

- Possibility to connect PTC thermistors;
- Ground fault protection via internal or external ground fault sensors;
- Availability of analogue signal output indicating the motor current;
- Possibility to connect to industrial communication networks.

Figure 5.11 – Microprocessor based overload relay for current range = 50 to 205 A /50/

The simultaneous processing and analysis of three current signals and the inclusion of additional features require the use of high processing capacity microprocessors. Nowadays, these components have higher power consumption. Due to it these devices cannot be self-powered and require the use of external power supply.

5.7 – PTC thermistors (Positive Temperature Coefficient sensors)

PTC thermistors are semiconductor components that present "a very high positive resistance/temperature coefficient. For a temperature change of only 10 K around their rated operating temperature (TNF), their resistance increases more than ten fold (Figure 5.12)." /36/

PTC thermistors must be embedded in motor windings during manufacturing. Normally they are installed in the drive end overhangs of the motor windings (one per phase) and are connected in series (Figure 5.13). In case the temperature at one or more PTC thermistors exceeds their rated operating temperature (TNF), a separate electronic unit will detect the sharp resistance increase. As a consequence, the electronic unit will trip an internal electro-mechanical relay /36/, /51/. "This switching signal may be used to switch off the motor or to initiate an alarm." /36/

R   Resistance of detector circuit
ϑ Temperature
x_1 Tripping range of the tripping units
x_2 Resetting range of the tripping units
TNF   Rated operating temperature (tolerance limits in °C)
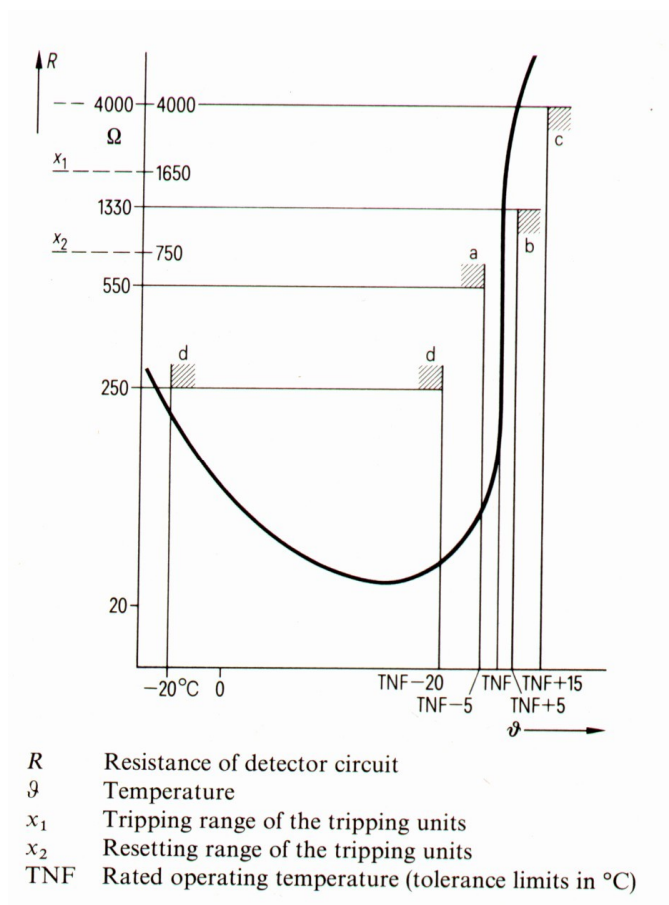
Figure 5.12 – Resistance/temperature characteristic of a PTC thermistor /36/
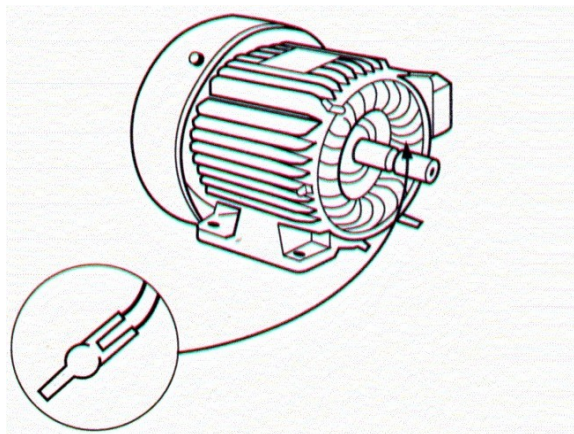
Figure 5.13 – Installation of PTC thermistors in motor windings /32/

5.8 –Thermostats

Thermostats have a bimetallic snap-acting element with electric contacts. This sensor-actuator element is assembled inside a sealed case, which provides protection against impregnation varnish and mechanical pressure (Figure 5.14). Due to these features and to their small dimensions thermostats "can be mounted directly on motor windings for fast detection of temperature changes." /52/
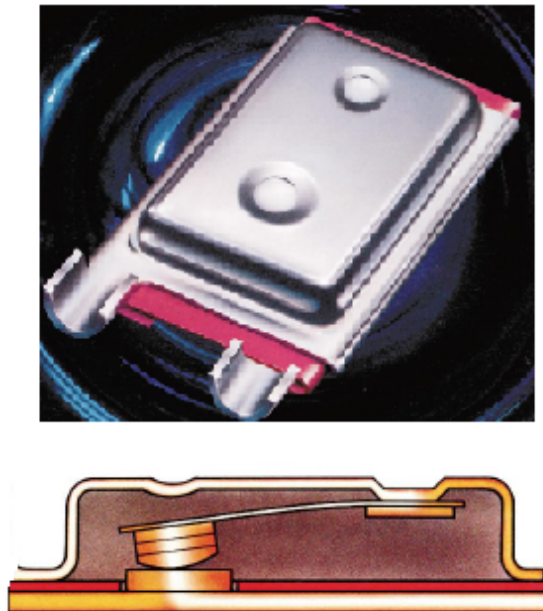
Figure 5.14 –Typical thermostat for motor protection -contacts closed

These devices can be applied in two different ways:

- <u>As a thermal protector</u>, i.e., as a "device sensitive to machine temperature and current…"/29/. In this case the bimetal element is series connected to motor windings and is actuated (opening the electric circuit) by the current passing through it and the heat conducted from the motor windings. After the windings have cooled the device resets automatically /53/. WEG normally uses this solution for single-phase fractional power motors for home appliances for North American market. Underwriters Laboratories (UL) and Canadian Standards Association (CSA) standards require the motor manufacturer to perform type tests to confirm the thermal protector really

match to the supplied motor. After test approvals the motor can be marked "thermally protected".

- <u>As a thermal detector</u>, i.e., as a "device sensitive to temperature only…" /29/. When requested by customers, WEG uses to apply this solution for protecting three-phase industrial motors (one thermostat per phase). The thermal detectors wire leads are series connected and subsequently connected to the motor starter control circuit. In case an overload is detected the thermal detector opens the control circuit, switching off the motor starter.

5.9 – Platinum resistance thermometers

The principle of operation of this kind of thermal detector is to measure the resistance of a platinum element that can be installed on motor windings. "The most common type (PT 100) has a resistance of 100 ohms at 0ºC and 138.4 ohms at 100 ºC. The relationship between temperature and resistance is approximately linear over a small temperature range…For precision measurements," it is necessary to apply suitable resistance versus temperature correction relationships /53/.

Platinum resistance thermometers must be connected to special control units that can provide tripping signals according to temperature limits preset by the machine user. In general, this solution is more common for large motors, especially medium voltage motors /22/.

5.10 – Motors with thermal detectors: sales figures by WEG

It was conducted a survey to obtain the quantity of industrial motors with thermal detectors sold by WEG during one year (from june/03 up to may/04). A summary for this survey is showed in tables 5.6 and 5.7.

Table 5.6 – Sales for Brazilian market

Plant/(motor power)	Motors with thermal detectors (%)	Kind of thermal detector (%)		
		PT100	Thermistor	Thermostat
Plant I/(up to 3.7 kW)	13.2	0.04	0.96	99.0
Plant IV/(4.5…30 kW)	5.3	4.1	15.0	80.9
Plant III/(37…370 kW)	20.2	10.9	51	38.1
Total	11.2	1.0	5.0	94.0

Main conclusions about Brazilian market (table 5.6):

- A relatively small quantity of motors from plant I and IV was supplied with thermal detectors (13.2% and 5.3 % respectively). Most thermal detectors used there were thermostats.
- For plant III, 20.2 % of the motors were supplied with thermal detectors. Most devices were thermistors.

Table 5.7 – Sales abroad

Plant/(motor power)	Motors with thermal detectors (%)	Kind of thermal detector (%)		
		PT100	Thermistor	Thermostat
Plant I/(up to 3.7 kW)	7.8	0.05	67.0	32.9
Plant IV/(4.5…30 kW)	18.2	3.4	80.7	15.9
Plant III/(37…370 kW)	97.9	2.0	95.5	2.3
Total	17.0	2.4	81.6	15.9

Main conclusions about sales abroad (Table 5.7):

- Only 7.8 % of plant I motors were supplied with thermal detectors.
- 18.2 % of plant IV motors were provided with thermal detectors.
- Most motors from plant III had thermal detectors.
- Most thermal detectors supplied were thermistors.

5.11 - Phenolic motor protectors (off-winding installed)

Phenolic motor protectors have a bimetallic snap-acting disc where electric contacts are mounted. They also have a resistance heater both assembled in a phenolic base (Figure 5.15).

Most applications, the phenolic motor protector is series connected to motor windings in a way motor current flows through both the snap-acting disc and the heater.

"If overheating conditions occur, the heating effect of the current flow through the bimetallic disc and the influence of motor heat will cause the disc temperature to rise. When the disc reaches the calibrated set point, the protector automatically opens and shuts down the motor, limiting the windings and shell temperature." After the motor has cooled the protector can be reset either manually or automatically. /54/

Resistance heater

Snap-acting disc and contacts

Phenolic base
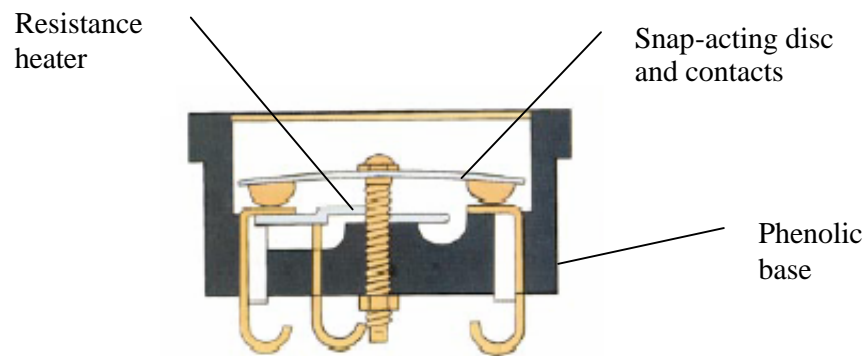
Figure 5.15 – Section view of a phenolic motor protector – contacts closed

WEG normally installs this kind of protector inside integral single-phase home appliance motors for North American market. The "thermally protected" mark (according to UL and CSA standards) can also be applied on motor nameplates after type tests approvals.

5.12 – Main conclusions for chapter 5

- According to IEC 60947-4-1, overload relays and releases must trip with current values between 1.05 and 1.20 times their current settings. These values are in accordance to the current threshold value highlighted at section 4.4 – thermal limit curves for an 11 kW electric motor.

- Therefore, classical thermo-mechanical overload relays and releases, manufactured according to IEC 60947-4-1, present a good performance for protecting electric motors;

- Table 5.8 presents a comparison between the different devices discussed in this chapter. It shows bimetal overload relays and releases are based on a well-known technology and present low manufacturing and installation costs. Their protection performance is not as accurate as the accuracy presented by electronic devices but they are still a cheaper solution. They are also a very well established method employed for protecting three-phase industrial motors. Due to these reasons WEG is still investing on the development of this technology. Next chapters will discuss the adjustment and calibration procedures, employed by WEG, for manufacturing bimetal overload releases.

WEG is also developing analogue electronic overload relays. These devices still have higher production costs when compared to bimetal overload relays and releases.

Table 5.8 – Comparison between the different protection solutions available in the market

Types of overload protection devices \ List of features	Availability of technology / Small risks with patents	Low manufacturing costs	Low installation costs	Protection performance	Frequently employed for industrial motors
1 – Bimetal overload relays and releases	+	+	+	(+)	+
2 – Eutectic alloy relays	+	+	(+)	(+)	-
3 – Analogue electronic overload relays	-	-	+	+	(+)
4 – Microprocessor based overload relays	-	-	(+)	+	(+)
5 – PTC thermistors	-	+	-	+	(+)
6 – Thermostats	+	+	(+)	+	(+)
7 – Platinum resistance thermometers	+	-	-	+	(+)
8 – Phenolic motor protectors	+	+	(+)	(+)	-
+ Good (+) Intermediary - Bad					

CHAPTER 6

DESIGN PARAMETERS FOR MPW25'S OVERLOAD RELEASES

MPW25 is a motor protective circuit breaker manufactured by WEG. This chapter gives an overview about MPW25 and presents the main design parameters for the overload release of this device. Overload release adjustment and calibration is discussed in a detailed manner.

6.1 – Main features of MPW25

MPW25 is applicable for motors up to 11 kW (4-pole motors @ 400V). The product is supplied in 13 different current ranges using the same housing which features 45 mm width.

Just one device provides all control and protection functions necessary to implement a direct-on-line motor starter as follows: isolation, short circuit protection, manual power switching and overload protection. In case a remote control is necessary, it is possible to provide it just connecting a contactor to MPW25 with the help of a special accessory.

Figure 6.1 highlights some parts of a MPW25 motor protective circuit breaker that are explained below:

- Rotating knob: used as a manual switch and as tripping indicator. Actuates directly over the lock mechanism, which moves the electric contacts.

- Overload release: provides protection against over currents up to 12 times the current setting. In case of an over current, the overload release actuates on the lock mechanism that opens the moveable contacts and makes the rotating knob move for a tripped position. The setting dial is used for adjusting the bimetal overload release operation to the rated current of the electric motor. The maximum setting range is 1:1.6 (detailed at figure 6.1).

- Magnetic over current release: which provides protection against short circuit currents (above 12 times the maximum current setting). This release also actuates on the lock mechanism providing contacts opening and tripping indication via rotating knob.

Setting dial

Calibration mark (drilled hole)

Engraved scale

Minimum current setting

CLASS 10   IEC 60947

MPW 25

1.6

1.3   1

TRIP

I9,2 A

TEST

weg

Lock mechanism

Housing

Rotating knob

Overload release (bi-metal + resistance winding)

Magnetic over current release

Electric contacts

Base
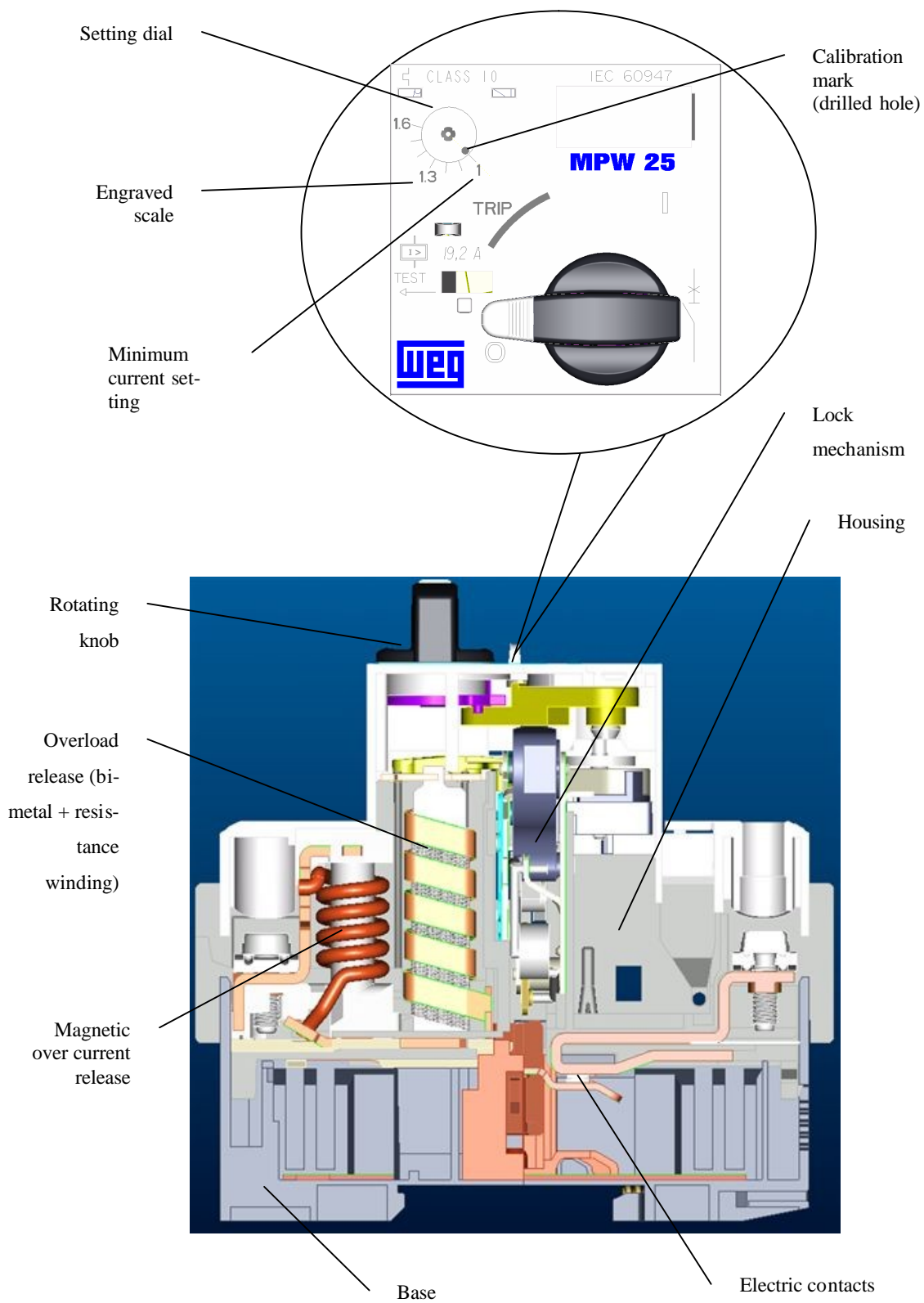
Figure 6.1 – MPW25: section view and detail of cover and setting dial

6.2 – Working principle of MPW25 overload releases

Figure 6.2 shows one bimetal assembly for MPW25 overload release. Electric current circulating as indicated heat the bimetal strip deflecting it in the direction of the reader.
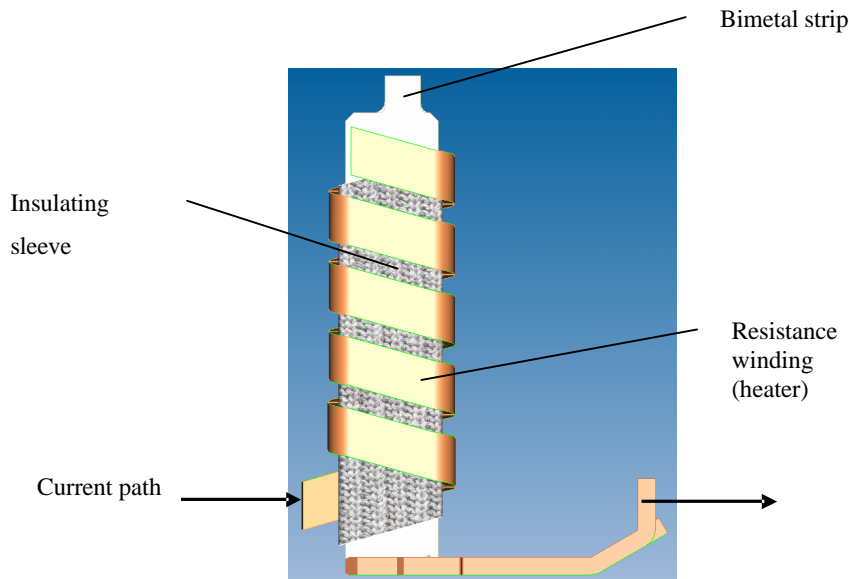
Figure 6.2 – Bimetal assembly for MPW25

Figures 6.3 and 6.4 present top views of MPW25's overload release. Current circulating through the three poles make the bimetal strips deflect to the left. This movement is transmitted to the differential lever by the tripping bars.

Due to this movement, the differential lever tip is pressed against the compensation strip. The resulting force is transmitted to lock mechanism trigger. In case of overload currents the displacement and force shall be enough for triggering the lock mechanism, which opens MPW25's contacts.

The overload release is adjusted and calibrated (detailed at section 6.4) at the assembly line at a reference temperature equal to 23º C. In case of operating at a higher ambient temperature, bimetal strips have a proportional displacement toward to left. Compensation strip have a similar behaviour thus compensating the effect of ambient temperature on overload release operation.

Phase loss operation follows the same working principle described at section 5.3.1 /55/.
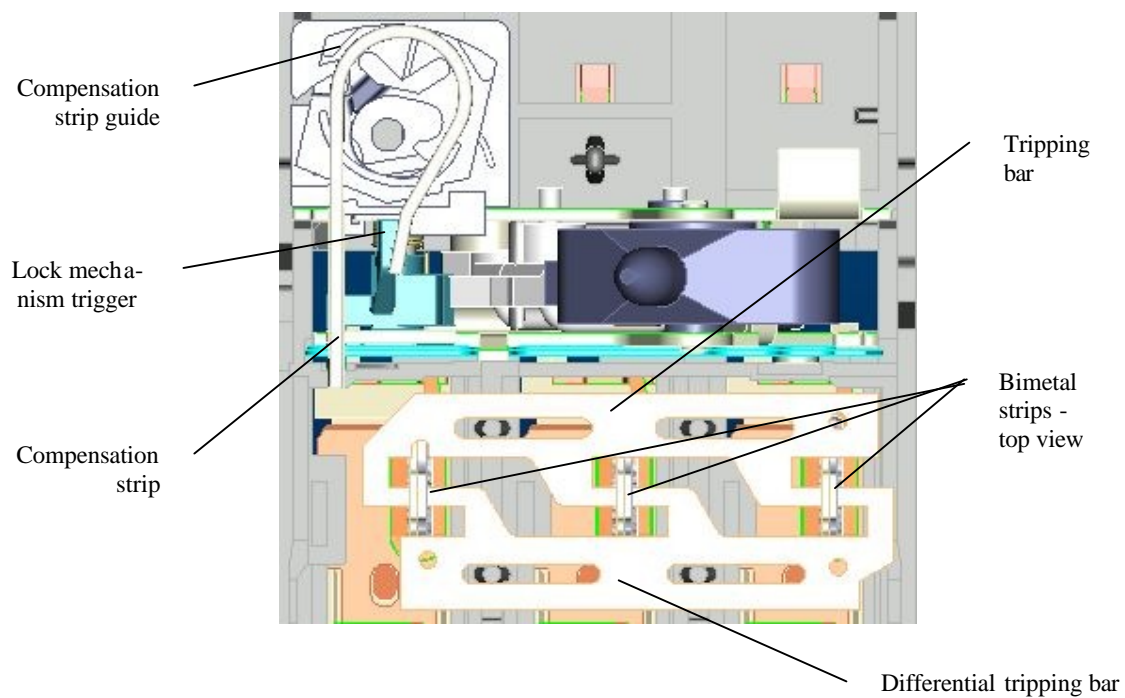
Figure 6.3 – MPW25 overload release. Setting dial and differential lever excluded
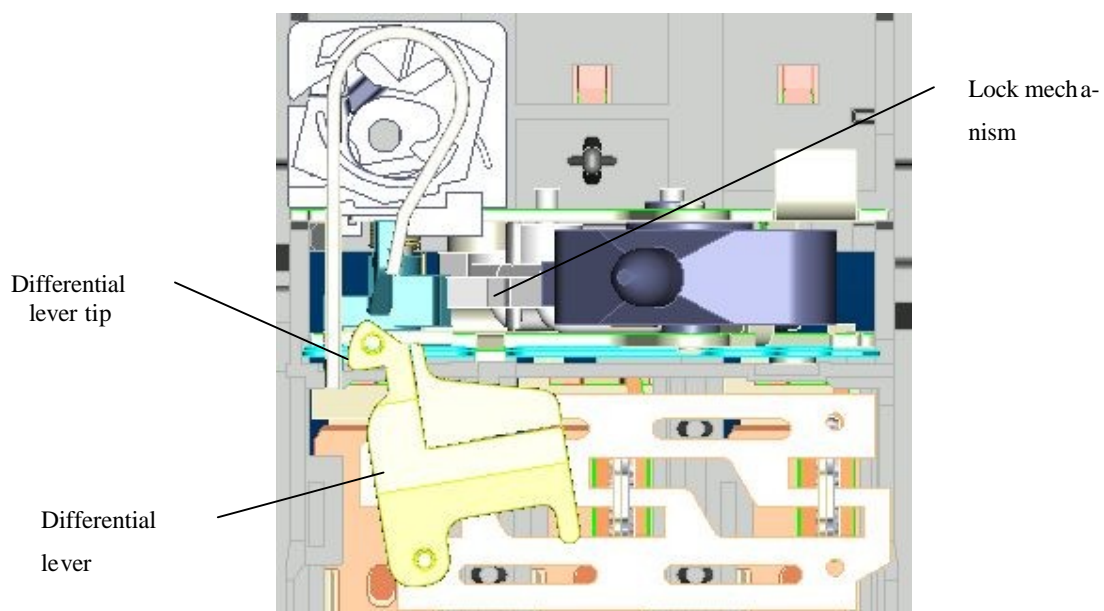
Figure 6.4 – MPW25 overload release. Setting dial excluded.

Figure 6.5 shows a displacement x force diagram for one bimetal of one motor protective circuit breaker available in the market.
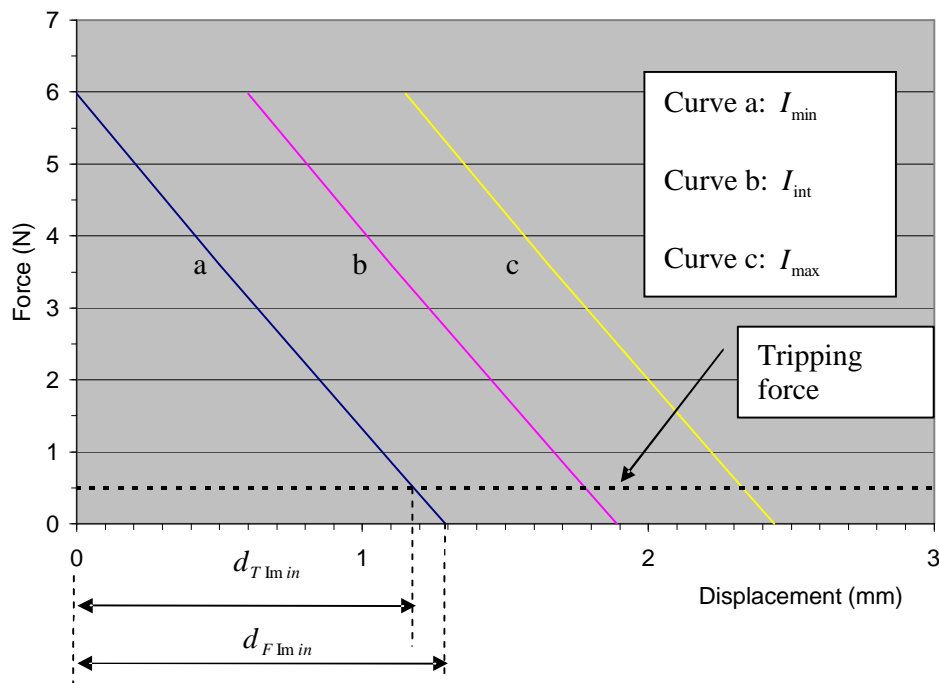
Figure 6.5 – Displacement x force diagram for one bimetal /57A/

For preparing this diagram, forces and displacements were measured at the tip of the first bimetal.

The test was started with the bimetal system without current (bimetal in cold state). A dynamometer and a digital scale were used for measuring the bimetal tip position.

After it, the overload release was submitted to a current value equal to the minimum current setting (I_{min}), until reaching steady state temperature. The dynamometer and the digital scale were subsequently moved against the bimetal tip in steps of 0.1 mm. This movement continued until bimetal tip was placed back to its initial position, i.e., at bimetal position in cold state. For each step, it was recorded a pair of values for displacement and force. The values were subsequently plotted in the presented diagram.

The above test sequence was repeated submitting the overload release to current values equal to intermediary current setting and maximum current setting respectively.

Curve a, represents the displacement x force values for the bimetal when the overload release was submitted to a current equal to its minimum current setting. Curves b and c repre-

sent the displacement x force values at intermediary current setting and maximum current setting respectively.

The crossings of these three lines with the horizontal axis show the free displacement of the bimetal for the corresponding current values ($d_{F\,lm\,in}$ representing bimetal free displacement at I_{min} is showed in the diagram).

On the other hand, the crossing of line I_{min} with vertical axis show the necessary force to be applied against the bimetal tip to completely avoid its movement when overload release is submitted to its minimum current setting.

Tripping force (equal to 0.5 N) represents the force that must be provided by the bimetal system in order to trip the lock mechanism. Due to this opposing force the bimetals tripping displacement ($d_{T\,lm\,in}$; $d_{TI\,int}$; $d_{T\,lm\,ax}$) is always smaller than their free displacement ($d_{F\,lm\,in}$; $d_{FI\,int}$; $d_{F\,lm\,ax}$).

The diagram also shows that higher current values make bimetal strips present larger displacements. This diagram was reported by Fraulob and Salmoria during the development of MPW25 /56/.

The setting dial (Figure 6.6 -a) is provided with a cam for adjusting the distance between the differential lever tip and the compensation strip according to operating current values. The clock wise movement of the cam makes the compensation strip rotate to the left allowing bimetals a larger displacement before trip occurs (Figure 6.6-b).

6.3 – Tolerance field for MPW25's overload release

As informed at section 5.3.2, overload releases must operate according to the limits required by IEC 60947-4-1 (Table 5.2 and 5.3) at each marked value of current scale. The limits of operation at 1.05 times the current setting and 1.2 times the current setting define dimensional tolerance fields for bimetal system, for steady state operation.

Figure 6.7 shows displacement x force diagrams for one bimetal at minimum current setting. Curve a, represents the displacement of one bimetal when the overload release is submitted to a current equal to 1.05 times the minimum current setting.

(a)

(b)
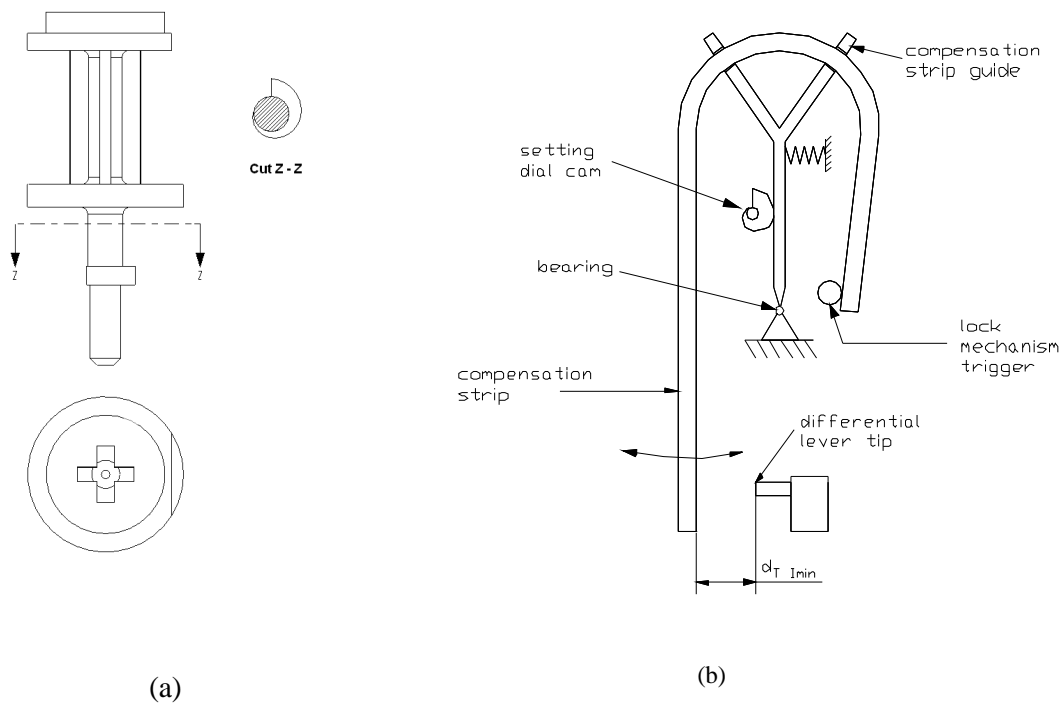
Figure 6.6 – (a) Setting dial and corresponding cam; (b) Sketch for current setting mechanism
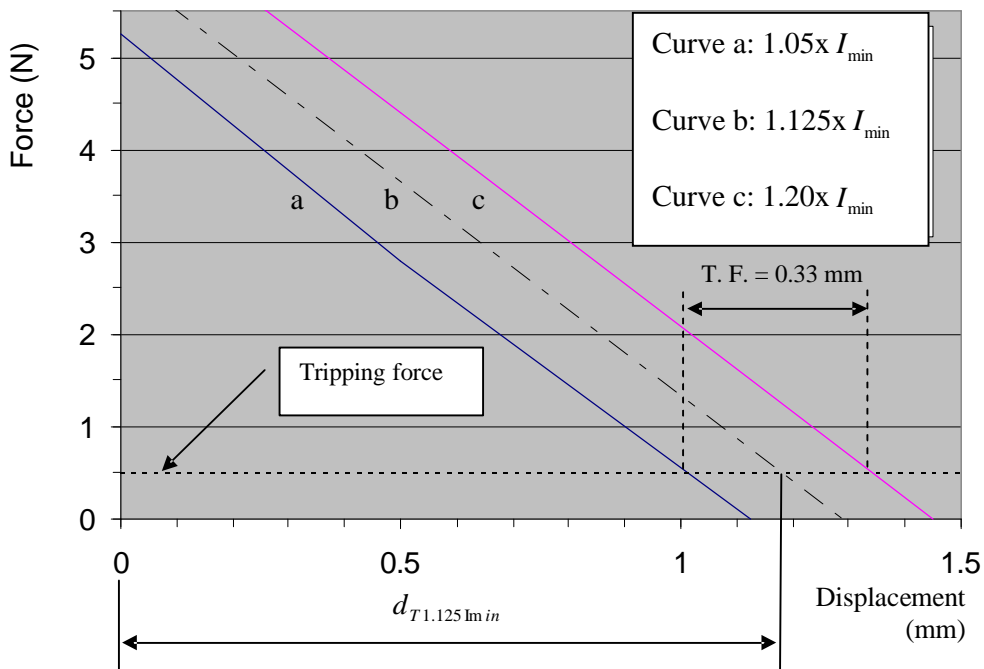
Figure 6.7 – Tolerance field (T.F.) for minimum current setting (I_{min}) /57/

Curves b and c, represent the displacement at 1.125 and 1.2 times the minimum current setting respectively.

Supposing overload release has reached steady state, tripping shall occur within the tolerance field. Parameter "$d_{T1.125\,\mathrm{Im}\,in}$" is the necessary bimetals displacement for tripping occur in the middle of the tolerance field.

It is possible to design similar displacement x force diagrams for each marked value of current scale (Figure 6.8).

According to Schulze and Fraulob /58/, bimetals displacement is proportional to the square of the applied current. As a consequence, the tolerance field increases with the increase of the current setting value (also showed at figure 6.8). Therefore, the smallest tolerance field for the overload release operation happens at minimum current setting.

Due to it, WEG decided to calibrate MPW25 overload releases at their minimum current setting (detailed at section 6.4). This text thoroughly discusses MPW25 overload releases accuracy only at their minimum current setting. It is suggested that future researches could analyse all factors that influence overload releases accuracy at other marked values of the scale.

Figure 6.9 shows a displacement x force diagram for the complete bimetal system, reported also by Fraulob and Salmoria /56/.

For preparing it, forces and displacements were measured at the differential lever tip, i.e., the objective here was to measure the three bimetals actuating simultaneously against the compensation strip.

The lines in this diagram present a smaller slope until applied forces reach approximately 1 N and a higher slope for forces higher than 1 N. It means bimetal system has different stiffness values.

According to Fraulob and Salmoria /56/ the reason for it is that when the bimetal system is submitted to operating currents, the three bimetals present different displacements. Therefore, until applied force reaches approximately 1 N, just two bimetals are actuating. For applied forces higher than 1 N three bimetals are actuating simultaneously.

The reason for this behaviour is the bimetal strip installed in the middle pole of motor protective circuit breakers present a larger displacement in comparison to the displacements presented by the other bimetal strips. Grützmacher /55/ showed middle pole bimetal strips reach higher temperature values due to higher thermal resistances for heat flowing to the environment.

As informed before, the bimetal system has to provide a tripping force equal to 0.5 N. Based on figure 6.9 is also possible to say that, the tripping force can be provided by just two bimetals actuating against the compensation strip.
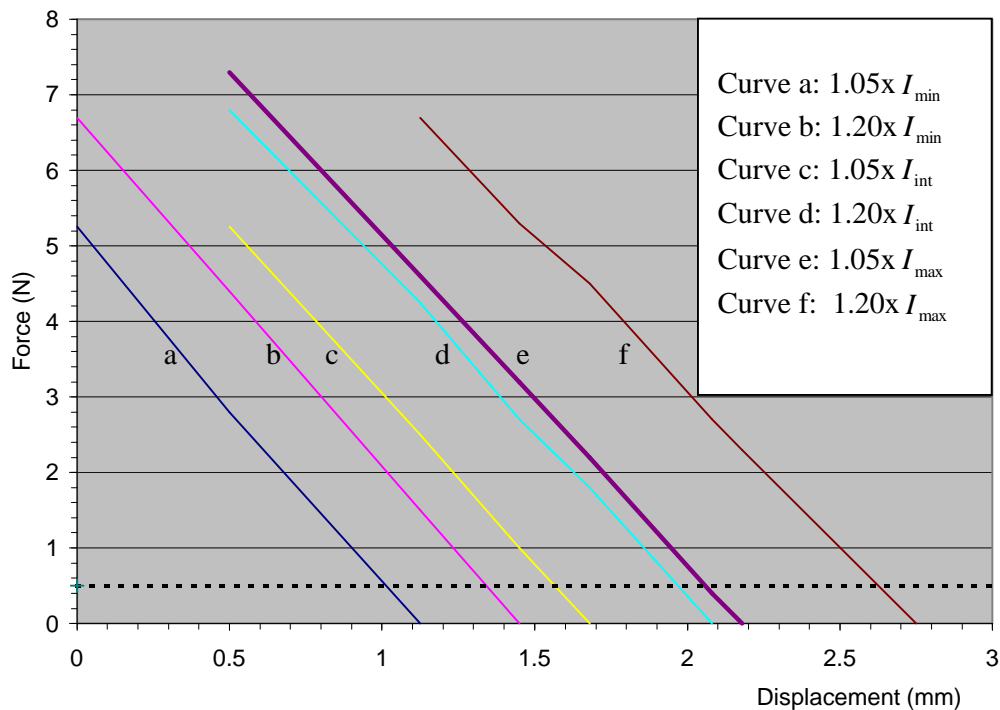
Figure 6.8 – Tolerance field for I_{min}, I_{int} and I_{max}

6.4 – Design parameters for accurate operation of MPW25's overload release

6.4.1 – Manufacturing and adjustment of overload releases

The bimetal strips are first stamped (appendix 6 details design parameters for stamped bimetal strips) and after it they are inserted in an insulating sleeve. The electric resistance wire is wound around the insulating sleeve and after it the winding is pressed between two flat surfaces in order to reach proper and uniform thermal contact to the bimetal strip (values and tolerances for resistance compactness are informed in appendix 7).

One end of the resistance winding is welded to the top of the bimetal strip. After the previous steps the part (bimetal strip + resistance winding) is LASER welded to the bimetal base (Figure 6.10). The resistance of 100 % of bimetal assemblies must be measured as indicated at figure 6.10. Appendix 7 informs tolerance fields for total resistance.
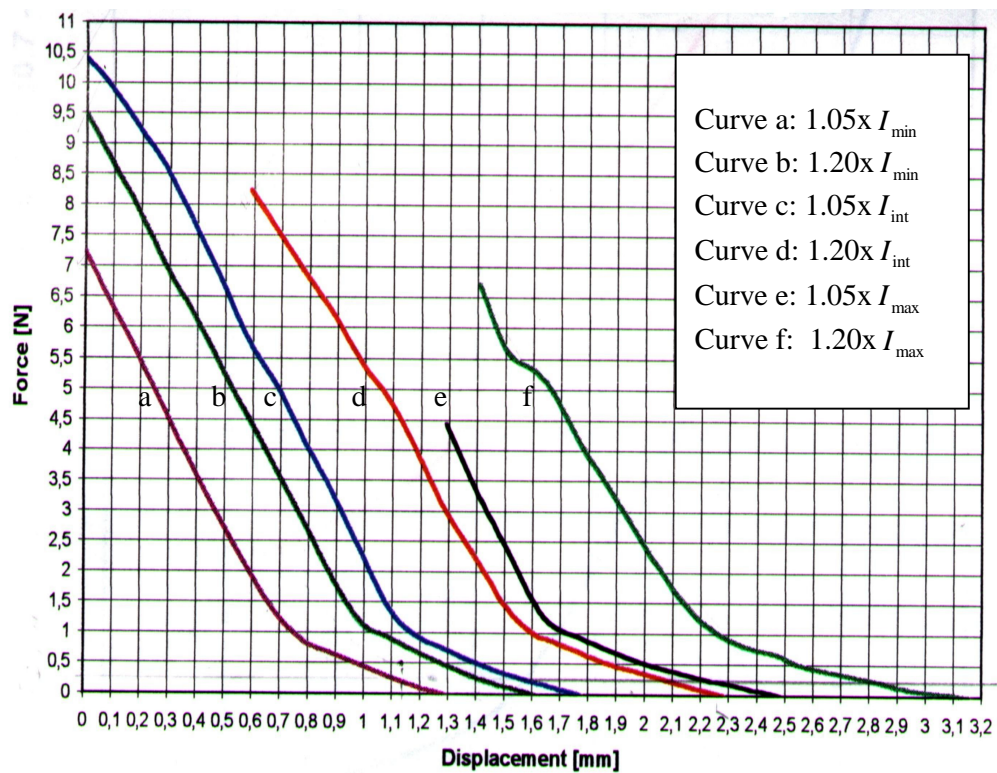
Figure 6.9 – Displacement x force diagram for the complete bimetal system /56/
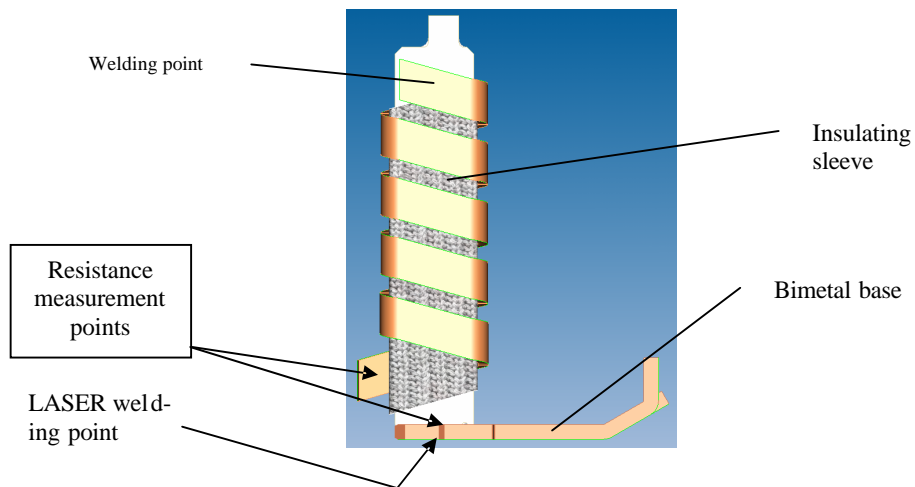
Figure 6.10 – Bimetal assembly

During the previous manufacturing steps, the bimetal strips are mechanically and thermally stressed which make their operation irregular /59/, /60/, /61/. Due to it the bimetal

assemblies are placed in an oven and submitted to three stress relieving cycles like the one showed at figure 6.11.

After the stress relieving operation the bimetal assembly is coupled to the magnetic release and complete thermo-magnetic releases are obtained (Figure 6.12).
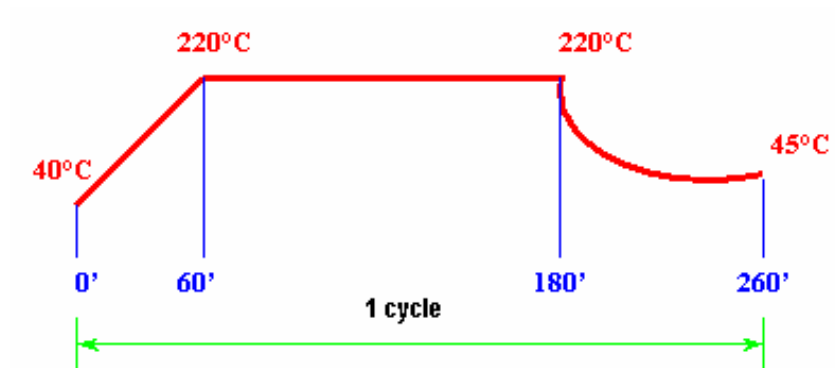
Figure 6.11 – One stress relieving cycle
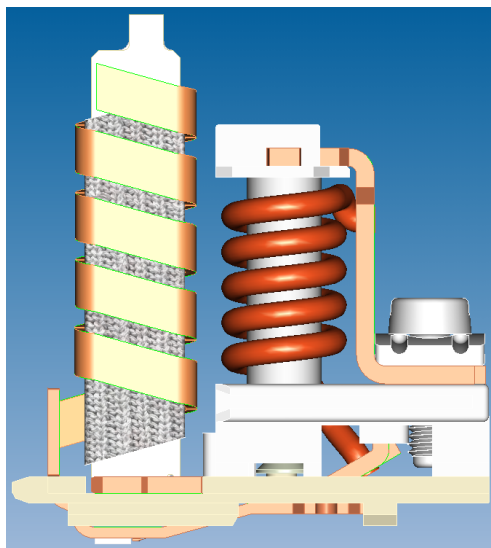
Figure 6.12 – Complete thermo-magnetic release

Then three complete thermo-magnetic releases are assembled in each MPW25 housing, one per phase (Figure 6.13).
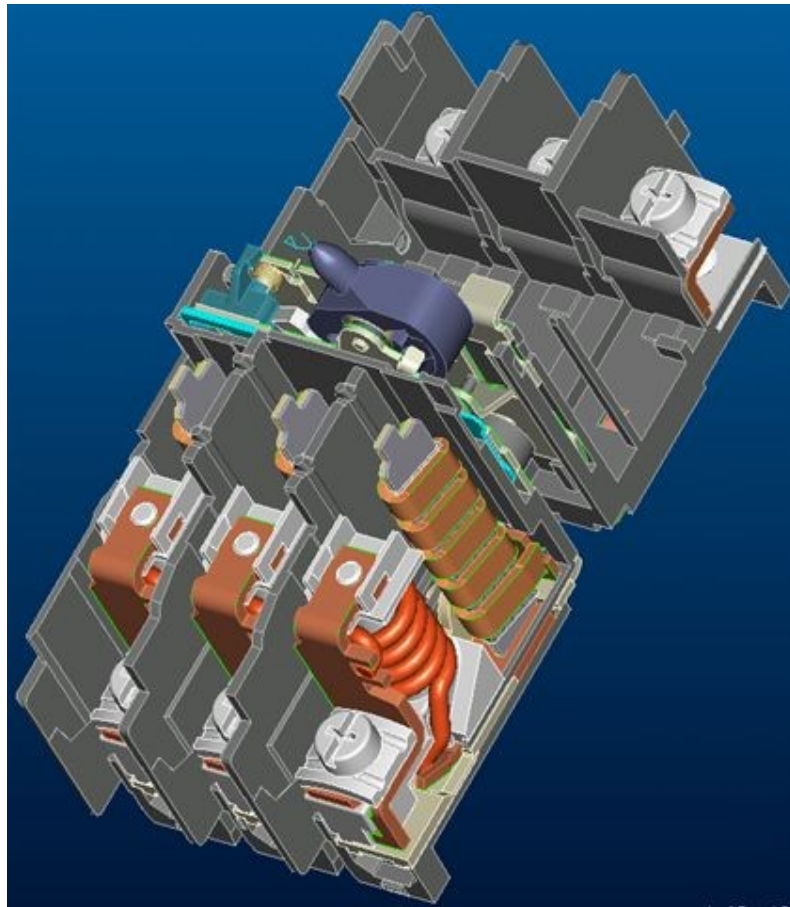
Figure 6.13 – Thermo-magnetic releases inserted in MPW25's housing

The accurate operation of the overload release requires two important conditions are fulfilled:

- All three bimetal tops should be simultaneously in touch with the tripping bar and with the differential tripping bar when the overload release has been submitted to three-phase operating current and has reached steady state, i.e., hot state operation. The overload release would present malfunction in case one bimetal top were very far from the tripping bar. Under these conditions, the overload release would operate as it was submitted to phase loss conditions. On the other hand, it was informed at section 6.3 that the middle pole bimetal strip presents a larger displacement in comparison to the other two bimetal strips (hot state operation). These conditions would lead to the need of adjusting the bimetal strip tops (in cold state) in relation to the tripping bars in a way of compensating the larger displacement of the middle pole (in hot state). It was also showed at section 6.3 that just two bimetal strips are able of pro-

viding the necessary tripping force. Considering the above mentioned conditions, and the difficulty of foreseeing the different displacements for all MPW25 current ranges, WEG decided to adjust the three bimetal tops to be simultaneously in touch to the tripping bars when the bimetal strips are in cold state, i.e., not submitted to any current. These relations are represented in figure 6.14. It is not possible to provide this adjustment by bending the bimetal strips. Such operation would re-introduce mechanical stresses to the bimetal strips.

- When setting dial is positioned as indicated in figure 6.15 and bimetal strips are in cold state, the differential lever tip must keep a "pre-set" distance from the compensation strip when the latter is clock wise rotated to the point where the lock mechanism trips (Figure 6.14). The reason for this required position for setting dial will be explained at section 6.4.2.

(1) Bimetals top
(2) Tripping bar
(3) Differential tripping bar
(4) Differential lever
(5) Compensation strip
(6) Lock trigger at tripped position
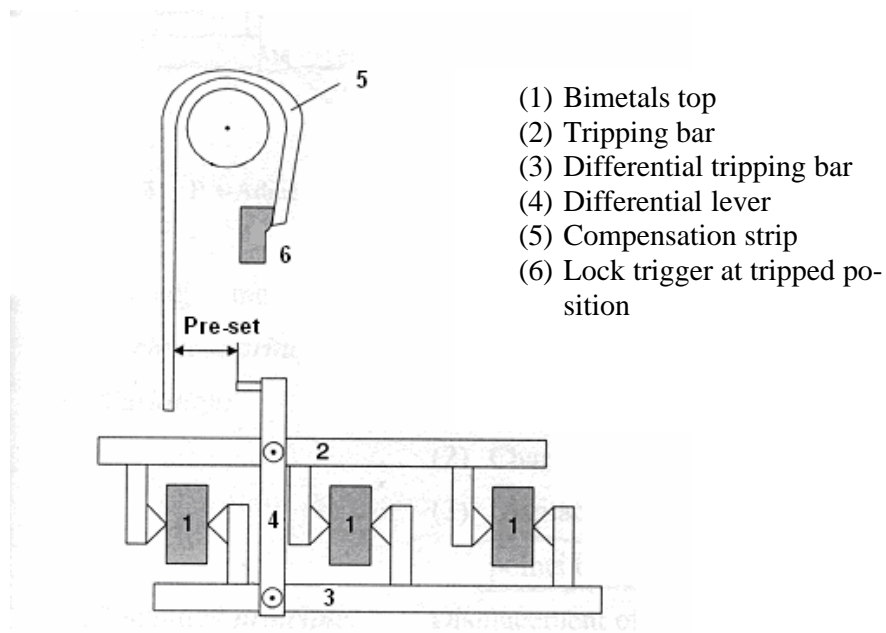
Figure 6.14 – Overload release adjustment at minimum current setting /57/, /62/

"Pre-set" distance is given by equation 6.1:

$$\Pr e - set = d_{F1.125\,\text{Im}\,in} + \Delta d \qquad (6.1)$$

Where:

$d_{F1.125\,\mathrm{Im}\,in}$ = bimetals free displacement when submitted to 1.125 times the minimum current setting (refer also to figure 6.9);

Δd = gap; necessary for calibration operation (to be detailed at section 6.4.2).
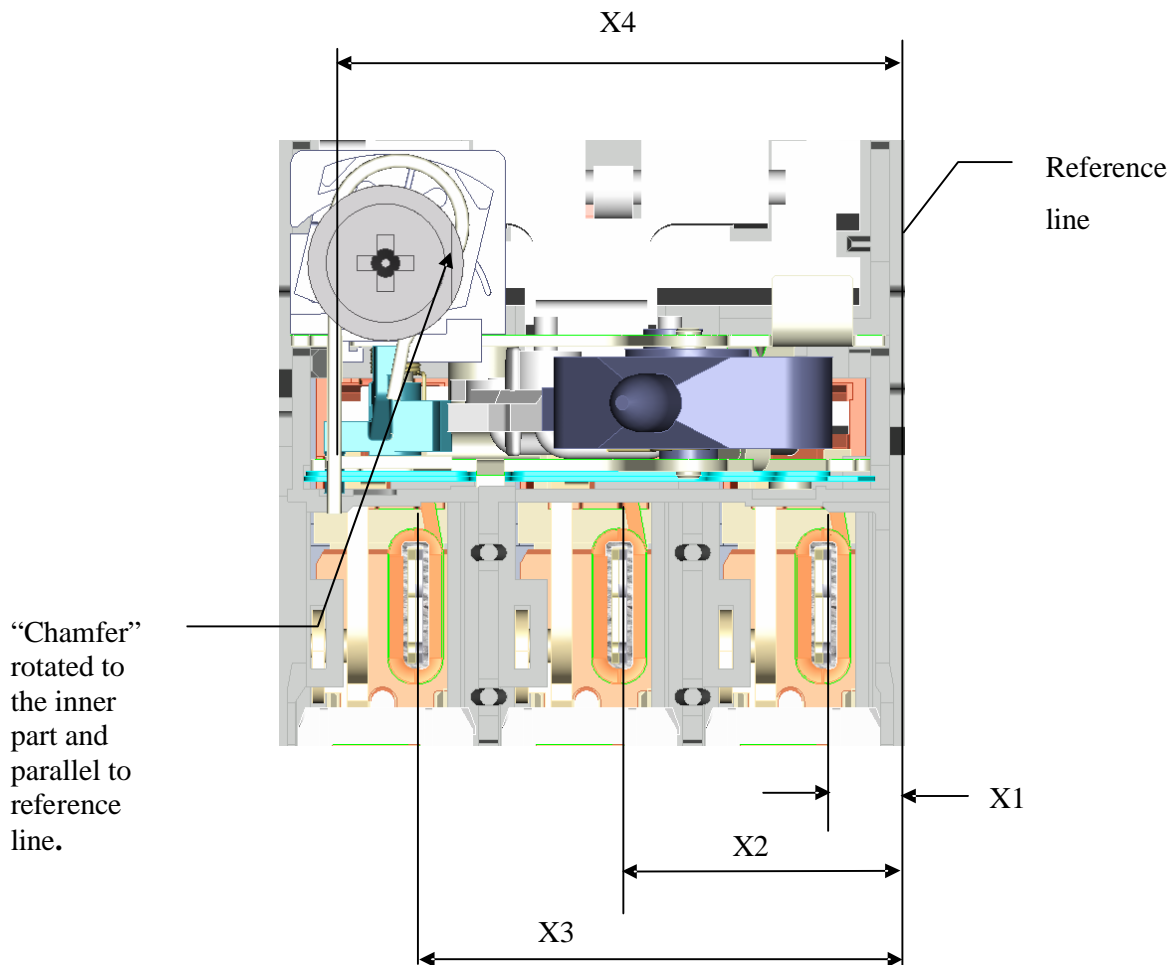
Figure 6.15 – Overload release measurement

WEG decided to use a "Pre-set" value equal to 1.3 mm, that was confirmed by practical tests.

Due to manufacturing tolerances, these conditions can be achieved only after an adjustment operation is performed for every single MPW25. It is necessary to measure the position of the three bimetal tops in relation to a reference on the housing (X1, X2, and X3). At the same operation, the compensation strip is displaced to the left up to tripping the lock mechanism. The compensation strip tripping position (X4) is also measured in relation to the same reference (Figure 6.15).

The tripping bars are supplied as a single piece for MPW25 assembly line (figure 6.16(a)). After the previously described measurements, it is necessary to cut the tripping bars (figure 6.16 (b)) in a way the two conditions presented before are fulfilled.

After the cutting operation the tripping bars and the differential lever are assembled in MPW25 like showed at figure 6.17. After this assembly stage, MPW25 cover is fit on the housing.
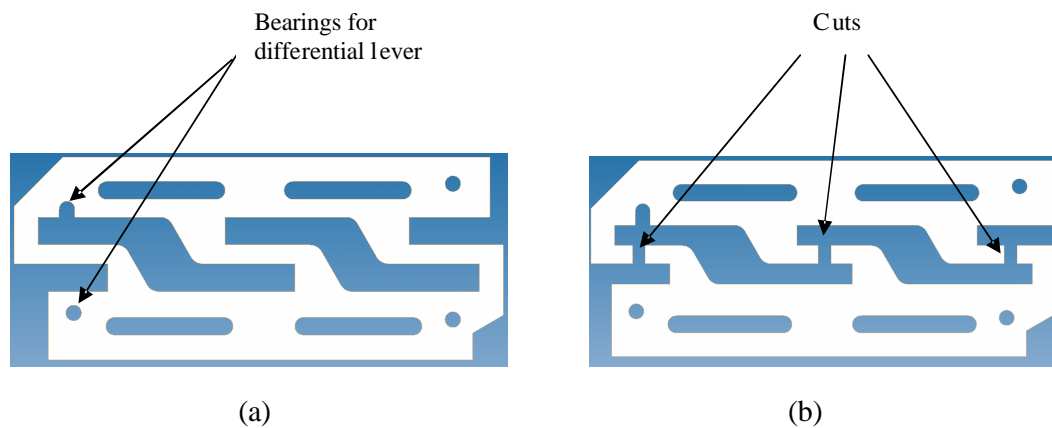
Figure 6.16 – Tripping bars: (a) as a single piece; (b) after cutting
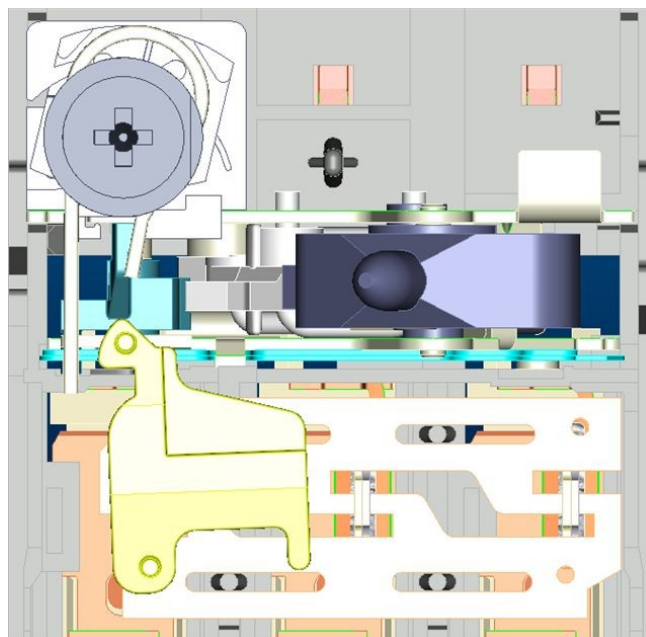
Figure 6.17 – MPW25 overload release after adjustment operation

6.4.2 – Overload release calibration

Figure 6.18 shows that the tripping distance at 1.125 times the minimum current setting $d_{T1.125\,\text{Im}\,in}$ cannot be accurately foreseen for every single device. There is a tolerance field for this parameter.

The main reasons for this tolerance field are:

- Manufacturing tolerances for total electric resistance;
-           ”   ”   for resistance winding compactness;
-           ”   ”   for bimetals stiffness;
-           ”   ”   for lock mechanism tripping forces; etc.
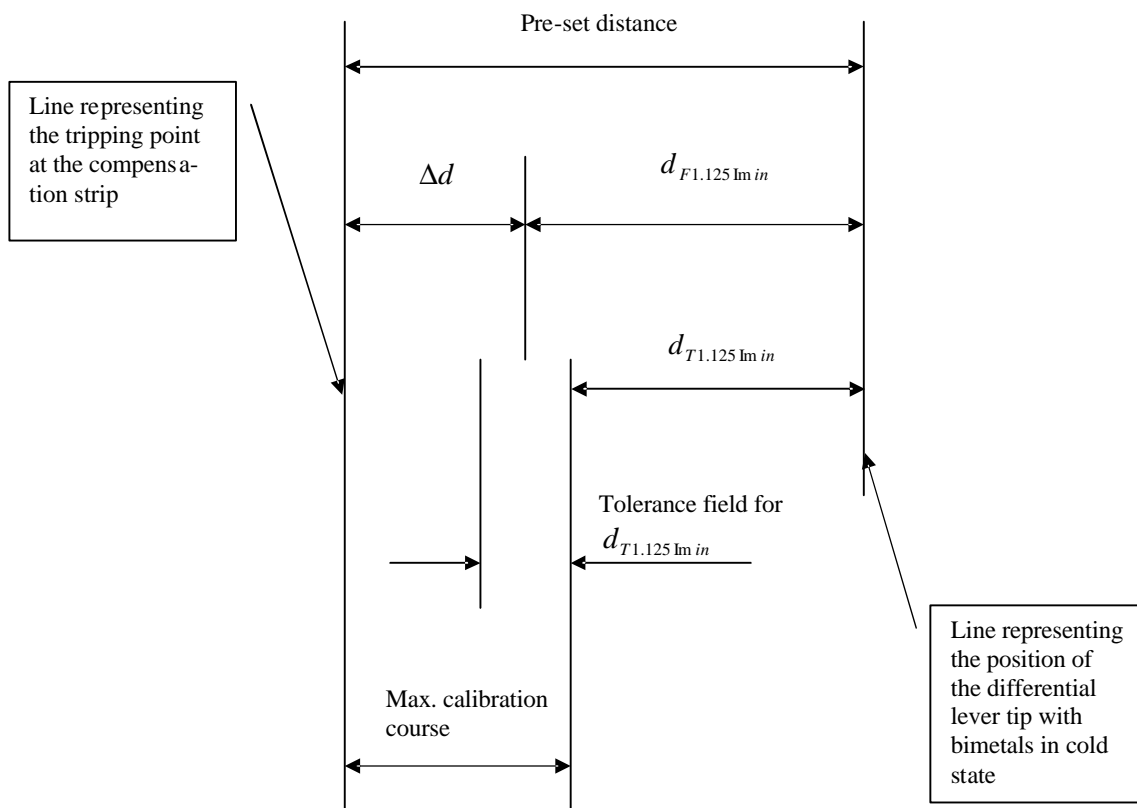
Figure 6.18 – Tolerance field representation for $d_{T1.125\,\text{Im}\,in}$

The above mentioned points explain why pre-set distance cannot be adjusted exactly equal to tripping distance when bimetals are in cold position. Therefore, it is necessary to submit each device to an additional operation, named scale calibration, with bimetals in hot conditions, i.e., with current.

Scale calibration is performed submitting each overload release to a calibration current and after a specific time the setting dial is anti-clock wise rotated moving the compensation strip until the lock mechanism trips. A small hole is drilled on the setting dial showing its exact position in relation to minimum current values previously engraved on the scale (Figure 6.1).

Figure 6.19 shows the setting dial (cut view showing only the cam) assembled together with the compensation strip guide. The setting dial is positioned as indicated at figure 6.15.

At this position, the cam has an available range equal to $a_1 + a_2$. $a_1 \sim 167°$, is used only for calibration when the setting dial is anti-clock wise rotated during manufacturing process. $a_2 \sim 113°$, is used only for current setting when the setting dial is rotated in the opposite direction, by MPW25 user. Point "A" is the start point for calibration process. The advantage of this solution is that setting angle, a_2, is always enough for current setting along the engraved scale /63/.
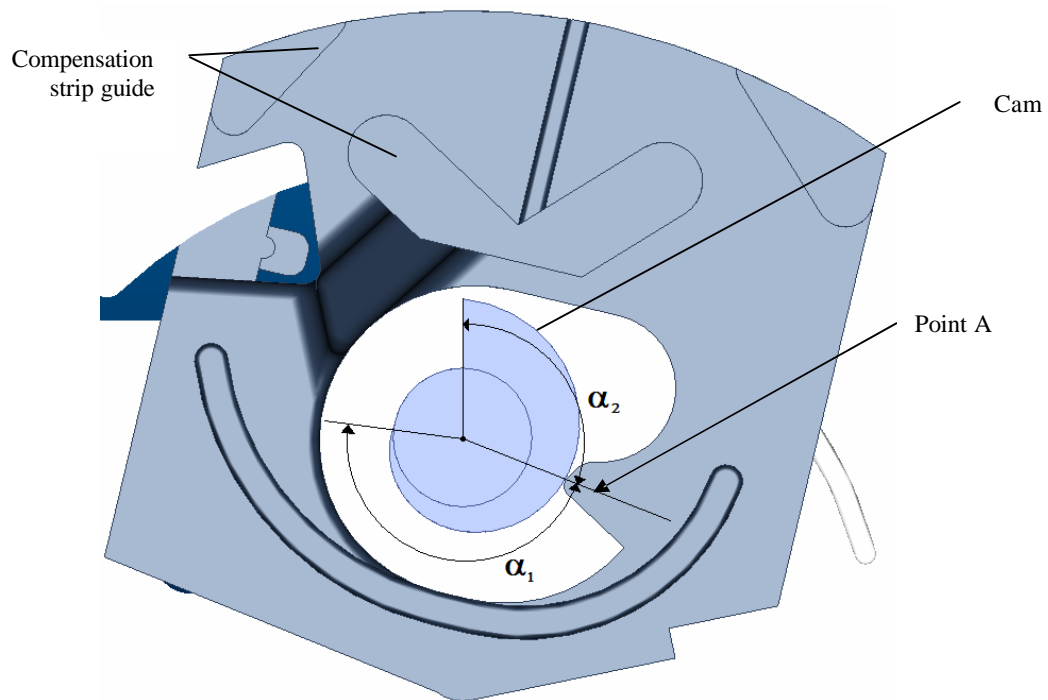
Figure 6.19 – The use of setting dial for both calibration and current setting

The calibration process can be performed in 2 different ways:

a) Static calibration: each device is loaded with 1.125 times its minimum current setting up to thermal equilibrium is reached (it takes approximately 1 hour). After it the setting dial is rotated up to tripping the lock and the setting dial is marked. This calibration procedure is normally used only for definition of engraved scale, for pre-series production or for small production quantities.

b) Dynamic calibration: This procedure is used for high production quantities and requires the use of an automatic calibration equipment in connection to a test laboratory. Each single MPW25 is submitted to a current value equal to approximately 3 times its minimum current setting. After a short time delay the setting dial is rotated up to tripping the lock and the setting dial is marked. Thermal equilibrium is not reached during dynamic calibration.

Appendix 8 presents an average current-time characteristic curve for MPW25. It shows that when the overload release is submitted to a current value equal to 3 times its current setting it will trip within approximately 30 seconds. WEG decided that reasonable production efficiency would be reached in case the whole dynamic calibration operation was performed in 50 seconds maximum.

When WEG started MPW25 pre-series production, one single sample was calibrated at 1.05 times minimum current setting (static calibration). After it the sample was submitted to 3 times the minimum current setting. It was observed the device tripped after 28 seconds. The same calibration and measurement sequence was provided for 1.125 and 1.2 times minimum current setting respectively. Tripping times at 3 times minimum current setting were 32 and 35 seconds respectively. These results were plotted as showed at figure 6.20.
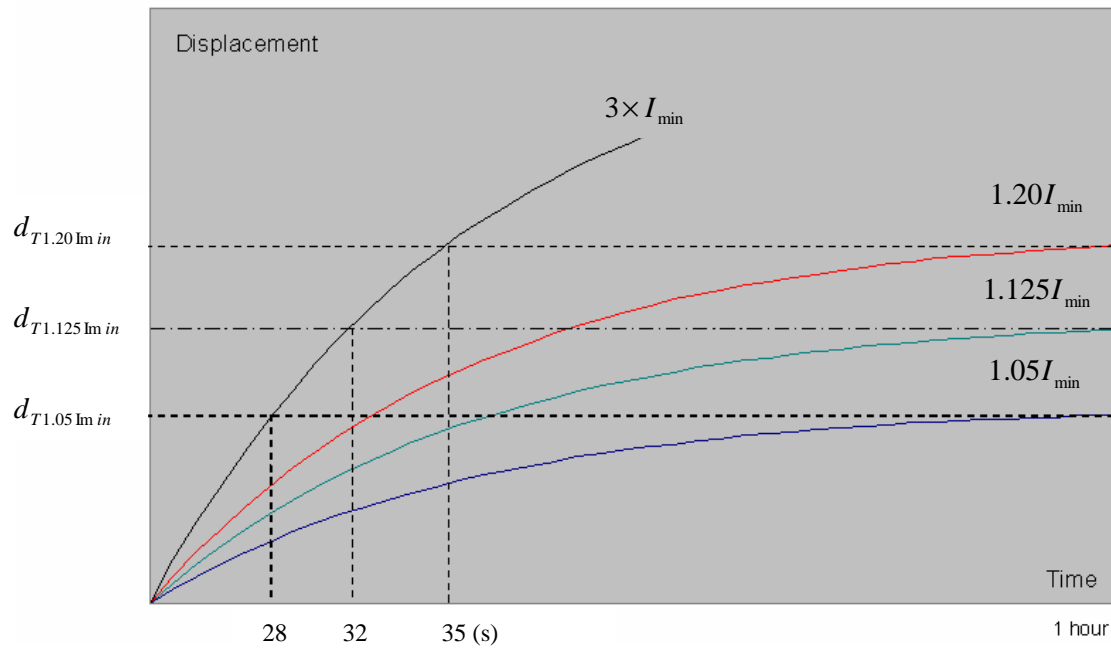
Figure 6.20 – Studies about dynamic calibration

Considering these results, a first approach for dynamic calibration was established as follows:

- Every MPW25 is submitted to 3 times its minimum current setting;
- After 32 seconds the automatic equipment starts rotating the setting dial in anti-clock wise movement, in a high speed.
  Rotation speed = 180º / 1.2 seconds;
- During the rotation MPW25 must trip. In case trip does not happen until 33.2 seconds (Figure 6.21), the device must be rejected by the automatic calibration equipment.
- Accepted devices have their setting dials marked with a drilled hole. This mark is used
  for setting the dial along MPW25 engraved scale.

Figure 6.22 shows displacement versus time curves for three different MPW25 samples when submitted to 3 times the minimum current setting. These curves are hypothetical and the main idea here is to show the distribution of tripping displacement values after overload releases have been dynamically calibrated.
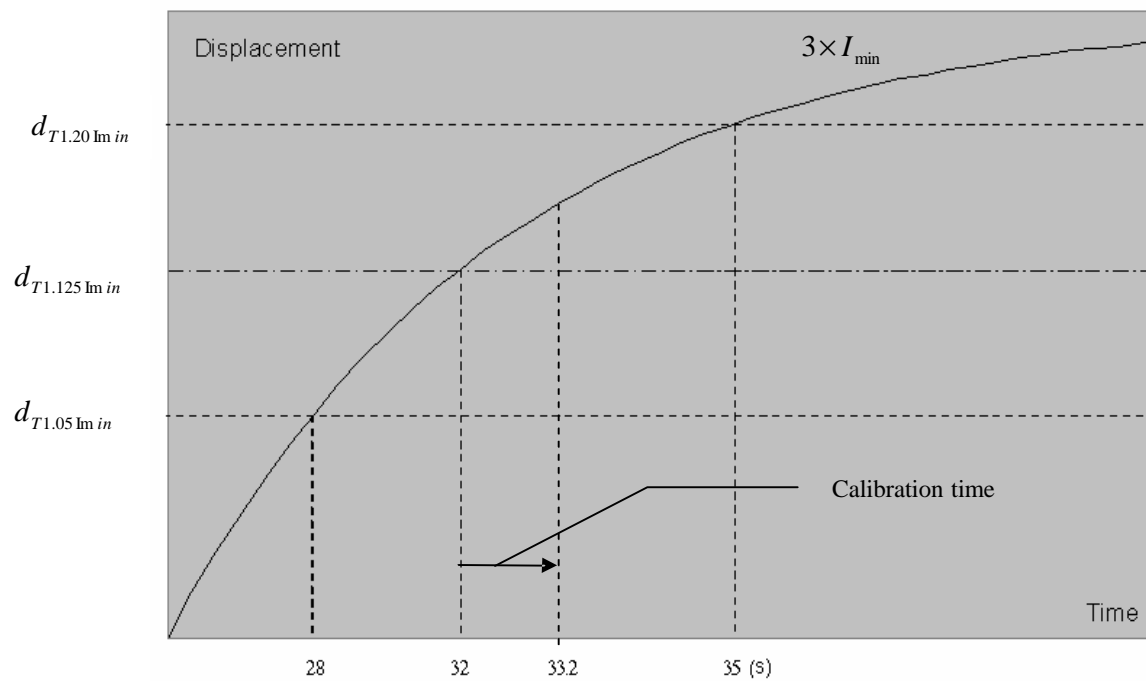
Figure 6.21 – Dynamic calibration procedure
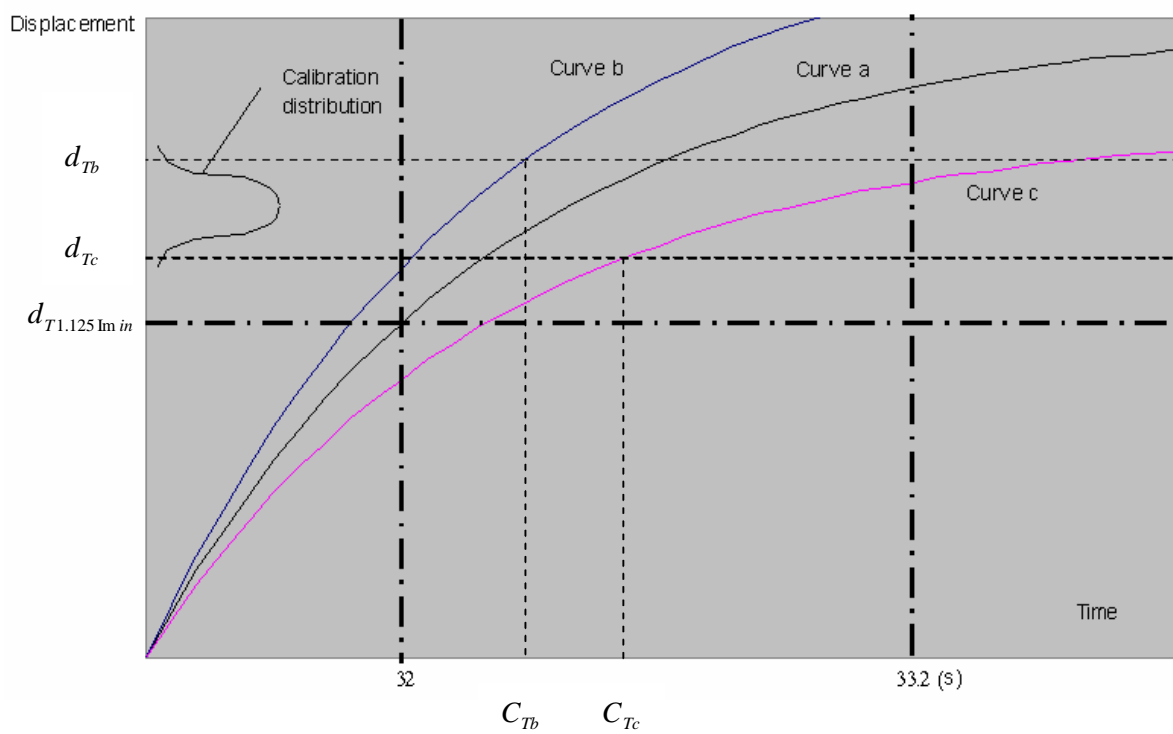
Figure 6.22 – Dynamic calibration distribution

- Curve a: device "a" (a reference sample) was calibrated at 1.125 times its minimum current setting (static calibration). When it was subsequently submitted to three times minimum current setting the device tripped after 32 seconds, i.e., it reached $d_{T1.125\,\mathrm{Im}\,in}$ in exactly 32 seconds. Curve "a" represents this "calibration" condition.

- Curve b: due to manufacturing tolerances, device "b" bimetals have a larger displacement in comparison to device "a". When submitted to the calibration procedure, at 32 seconds its displacement is larger than $d_{T1.125\,\mathrm{Im}\,in}$. At this moment, automatic calibration equipment starts rotating the setting dial until trip occurs. Therefore, bimetals tripping displacement for device "b" would be d_{Tb}. C_{Tb} is the calibration time for device "b".

- Curve c: in a similar way, device "c" bimetals have a smaller displacement in comparison to device "a". Due to it, when submitted to calibration procedure, at 32 seconds the bimetals displacement is smaller than $d_{T1.125\,\mathrm{Im}\,in}$. At this moment, automatic calibration equipment starts rotating the setting dial until trip occurs. Therefore, bimetals tripping displacement for device "c" would be d_{Tc}. C_{Tc} is the calibration time for device "c".

Supposing some additional samples were submitted to the proposed dynamic calibration process, a statistic distribution for the calibration tripping point could be observed (Figure 6.22).

Continuing the dynamic calibration studies, the complete pre-series production lot was submitted to the proposed calibration process. After this step a sample of the pre-series production lot was submitted to a current limit test (detailed at chapter 7). Figure 6.23 is a plot for the distribution of tripping currents. This distribution can be described by a mean value (for central tendency) and by a standard deviation value (for dispersion).

The plot showed the current limit distribution displaced toward the upper tolerance limit. Therefore some specimens from the lot were out of IEC 60947-4-1 limits of operation.

There are two possibilities to solve this trend to the upper tolerance limit:

- Start calibration operation earlier than 32 seconds;
- Use a calibration current multiple smaller than 3.

It was decided to re-calibrate the pre-series lot using a calibration current multiple smaller than 3 (e.g.: 2.8 x minimum current setting). After the re-calibration some samples

were submitted again to current limit tests to confirm the chosen current multiple was correct. The test results are also represented at figure 6.23.

The next lot (number 2) was provided as follows:

- Assemble 10 samples and calibrate them using the same calibration current multiple used for re-calibrating pre-series production;
- Take the samples to a test laboratory and provide current limit tests. Test results are represented at figure 6.24. Due to manufacturing tolerances, the test results distribution showed the use of previously applied calibration current multiple would lead to a lot with its current limit mean value displaced to the lower limit of operation (IEC 60947-4-1);

It was decided to calibrate the new lot using a current multiple higher than the one applied during pre-series production re-calibration. Similar conditions were observed when providing the next lots (Figure 6.24).
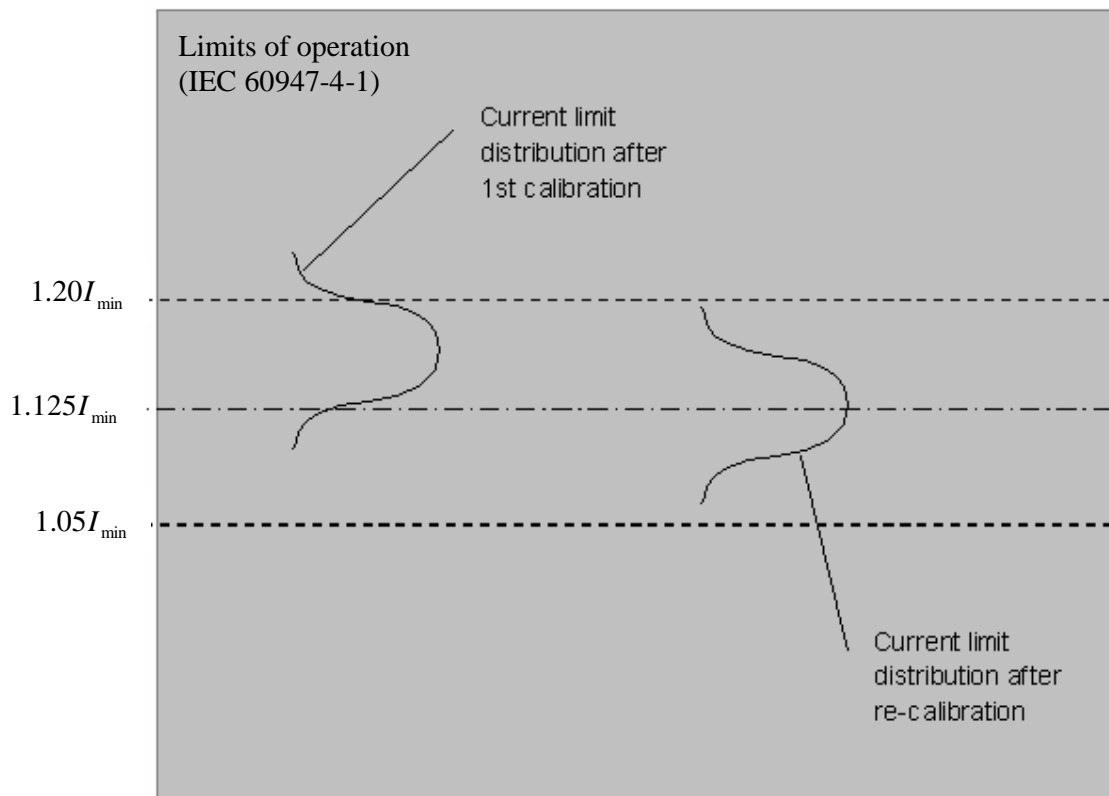
Figure 6.23 – Results for current limit test (pre-series production lot)
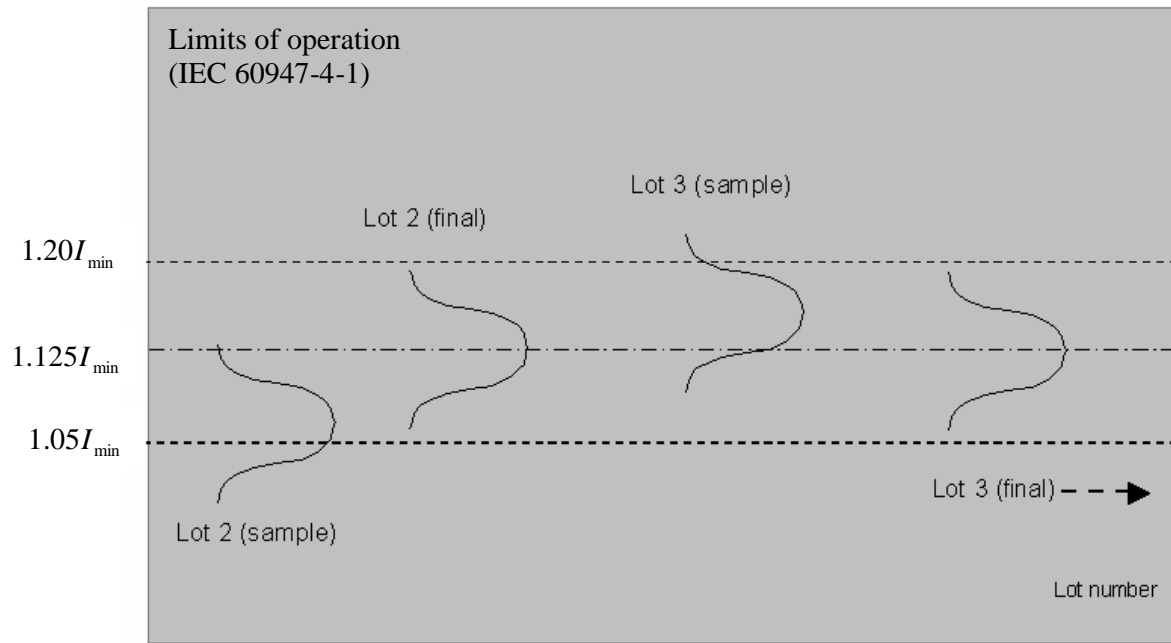
Figure 6.24 – Calibration distribution for consecutive lots (same current setting range)

Based on the previously described experience, it was finally decided to implement the following procedure for dynamic calibration:

- Before starting a new production lot, prepare 10 samples with the calibration current multiple used for producing the previous production lot for the same current setting range. The other calibration parameters were maintained unchanged: calibration starting time = 32 seconds; rotation speed = 180° / 1.2 seconds; calibration finish time = 33.2 seconds.

- Take the 10 samples to the test laboratory and submit them to an operation limit test (detailed at chapter 7). Feed back the assembly line if a new calibration current multiple is necessary. In case a new calibration current multiple is necessary, new samples are provided and forwarded to the test laboratory;

- After finding the appropriate calibration current multiple the whole production lot is assembled and calibrated. Accepted devices have their setting dials marked with a drilled hole;

- For a final quality control, a sample from the production lot is submitted to an operating limits test in the laboratory. In case the sample is rejected, the whole lot is reprocessed and submitted to a new quality inspection.

6.5 – Main conclusions for chapter 6

- MPW25 motor protective circuit breakers include all control and protection functions necessary to provide a direct-on-line manual motor starter. Overload protection is provided by a bimetallic overload release;

- MPW25 overload release must work according to the limits of operation specified by IEC 60947-4-1 at each marked value of current scale. These limits define dimensional tolerance fields for overload release tripping distances;

- The smallest tolerance field available is observed when the overload release operates at its minimum current setting. Due to it WEG decided to calibrate the overload release at its minimum current setting;

- Due to manufacturing tolerances tripping bars must be adjusted for every single MPW25. This adjustment provides both proper mechanical contact between the bimetal tops and tripping bars and the necessary pre-set distance for calibration;

- Tripping distance cannot be accurately predicted for every single overload release. Due to it every overload release must be submitted to an additional operation named scale calibration;

- Scale calibration is performed submitting the overload release to a current multiple and after a specific time the setting dial is rotated until MPW25 trips;

- There are two possible methods for scale calibration: static calibration and dynamic calibration. Dynamic calibration method is recommended for high production quantities. On the other hand the tripping point of dynamic calibrated lots may present a higher dispersion when compared to lots manufactured using the static calibration procedure.

- Dynamic calibration method requires the use of a test laboratory to assure calibration parameters are able to provide devices according to IEC 60947-4-1 limits of operation;

- On chapter 7, the actual performance of MPW25 overload releases will be measured. Obtained results will be compared to IEC 60947-4-1 requirements;

- This chapter has just discussed the accuracy of MPW25 overload release scale at minimum current setting. It is recommended the accuracy at the other points of the scale may be analysed by future researches.

CHAPTER 7

TESTS AND ANALYSIS ON MPW25'S OVERLOAD RELEASES

This chapter details test procedures used to evaluate overload releases accuracy. Actual performance of currently manufactured MPW25 is also measured and discussed. After it, possible reasons for low tripping repeatability are thoroughly analysed. Some improvements on product and process parameters are also implemented. Additional factors that may influence MPW25 performance are further discussed. Finally, the effects of these factors on tripping repeatability are analysed by an experiment.

7.1 – Test procedures for evaluating overload releases accuracy

7.1.1 – Operating limits test

These tests are performed to confirm the overload release works according to the limits of operation specified at section 5.3.2.

Overload releases shall be connected using conductors in accordance with table 7.1 for test currents corresponding to 125 % of the current setting for devices of trip class 10. The tightening torque for terminal screws shall be 2.0…2.5 Nm (according to MPW25 design parameters). Connecting conductors length shall be 1m.

Thermal overload releases with all poles energized shall be tested as stated at section 5.3.2.

The characteristics defined at section 5.3.2 shall be tested at –5 ºC, +20 ºC and + 40ºC.

Three-pole thermal overload releases energized on two poles only shall be tested as stated at section 5.3.2 on all combinations of poles and at the maximum and minimum current settings /40/.

Table 7.1 – Test conductors (copper) for test currents up to 32 A inclusive
(IEC 60.947-1, partial) /35/.

Range of test current [A]		Conductor size $[mm^2]$
> 0	≤ 8	1.0
8	12	1.5
12	15	2.5
15	20	2.5
20	25	4.0
25	32	6.0

7.1.2 – Current limit test ($I_{\lim}$)

The minimum tripping current of an overload release can be determined by a current limit test ($I_{\lim}$). It consists of submitting the overload release to increasing multiples of current setting as showed at figure 7.1.
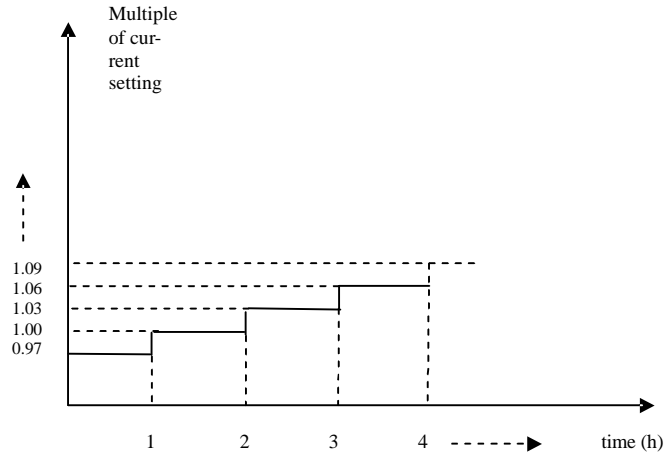
Figure 7.1 – Current limit test ($I_{\lim}$)

Each multiple of current setting is maintained until thermal equilibrium is reached (~ 1 hour for MPW25). The test sequence is interrupted when the overload release trips.

Current limit value is determined according to equation 7.1:

$$I_{\lim} = \frac{I_{trip}}{I_{setting}} - 0.03 \tag{7.1}$$

Where:

$I_{\lim}$ = current limit value [p.u.];

I_{trip} = current value that has tripped the overload release [A];

$I_{setting}$ = current value that has been set at the overload release dial [A].

Tripping repeatability of one specific device may be evaluated by repeating current limit test for three times. The overload release shall be subsequently submitted to three current ageing operations. Each current ageing operation consists of applying 7.2 times maxi-

mum current setting during 4 seconds. Finally, two additional current limit tests are performed.

A proposed measure for tripping repeatability is the range of obtained current limit values.

Electric conductors and device's terminals shall not be touched or moved during the above complete test sequence. Otherwise bimetals positions could be affected and influence test results.

It can be noticed that when an overload release is submitted to a tripping repeatability test, the minimum measurable current limit range is 0.03 p.u.

It was showed at chapter 6 that the operation of thermo-mechanical overload releases depends on different moving parts. The relative movement between these parts depends on proper clearances and is subject to the effects of friction.

Due to these considerations, it is reasonable to say that thermo-mechanical overload releases could present current limit repeatability within a range equal to ± 0.03 p.u. (or 0.06 p.u.). This current limit range (0.06 p.u.) is quite large compared to overload releases tolerance field (1.2 – 1.05 = 0.15 p.u.).

Anyway, it is proposed overload releases can be considered to have a good tripping repeatability when obtained current limit values are within a range equal to 0.06 p.u.

7.2 – Actual performance of MPW25's overload releases

As informed at section 6.4.2, a sampling from each production lot is submitted to an operating limits test, before delivering the whole batch to stocks.

Each sampling contains 5 % of the pieces from the lot.

The samples are submitted to operating limit tests at minimum, intermediary and maximum current settings. In case the samples do not trip at 1.2 times the current settings, they are additionally submitted to 1.37 times the current settings and tripping time is recorded. Table 7.2 is a summary for operating limits tests at minimum current setting for lots produced during three months.

Main conclusions obtained from table 7.2:

- MPW25 overload releases are not operating according to IEC 60947-4-1 requirements (Table 5.2, at section 5.3.2).
- The worst performance was observed on devices from current range equal to 6.3 – 10 A (signalled at Table 7.2).

Table 7.2 – Operating limit tests results on samples from assembly line

Current range (A)	Quantity of samples that operated at each multiple of current setting (%)			
	1.05xImin	1.2xImin	1.37xImin (Tp ≤3min)	1.37xImin (3 > Tp ≤ 8 min)
1.0 – 1.6	0.4	94.8	4.1	0.7
1.6 – 2.5	0.2	95.4	2.8	1.6
2.5 – 4.0	0.3	95.5	3.3	0.9
4.0 – 6.3	0.2	94.9	3.1	1.8
6.3 – 10	0.5	90.6	6.2	2.7
10 – 16	0.0	93.6	4.8	1.6
16 – 20	3.0	92.2	4.0	0.8
20 – 25	0.0	97.0	2.4	0.6

7.3 – Evaluation of MPW25's overload releases tripping repeatability

After obtaining test results reported at section 7.2 it was decided to take 10 samples of MPW25/6.3 – 10A and submit them to a tripping repeatability test.

The specimens were first submitted to four current limit tests. After it they were aged by current and submitted again by a current limit test. This current ageing/current limit test process was repeated three times.

Table 7.3 is a summary of this test sequence including the test results.

The complete test report including a picture of testing equipment is showed at appendix 9.

Table 7.3 – Test of tripping repeatability (MPW25/6.3-10)

Sample	1º	2º	3º	4º	5º	6º	7º	8º	Average	Range
1	1.21	1.21	1.15	1.15	1.18	1.15	1.18	1.15	1.17	0.06
2	1.27	1.21	1.24	1.27	1.27	1.21	1.21	1.21	1.24	0.06
3	1.27	1.15	1.09	1.09	1.12	1.12	1.15	1.12	1.14	0.18
4	1.27	1.21	1.18	1.18	1.21	1.21	1.24	1.21	1.21	0.09
5	1.30	1.21	1.15	1.15	1.21	1.21	1.21	1.18	1.20	0.15
6	1.21	1.18	1.15	1.15	1.09	1.18	1.15	1.12	1.15	0.12
7	1.27	1.27	1.18	1.24	1.21	1.24	1.24	1.21	1.23	0.09
8	1.21	1.12	1.12	1.15	1.09	1.18	1.15	1.15	1.15	0.12
9	1.18	1.12	1.15	1.15	1.09	1.18	1.15	1.18	1.15	0.09
10	1.33	1.24	1.24	1.3	1.33	1.33	1.24	1.33	1.29	0.09
7,2 * In				3 X	3 X	3 X	3 X			
Date	20-Jun	21-Jun	22-Jun	23-Jun	27-Jun	28-Jun	29-Jun	30-Jun		

Main conclusions obtained from this test: tested samples did not show a good tripping repeatability. 80% of the samples presented current limit values in a range larger than 0.06.

MPW25 of different current ranges are likely to present a similar behaviour. It is necessary to analyse the reasons for it and improve this feature.

Possible reasons for MPW25 low tripping repeatability are presented at figure 7.2:
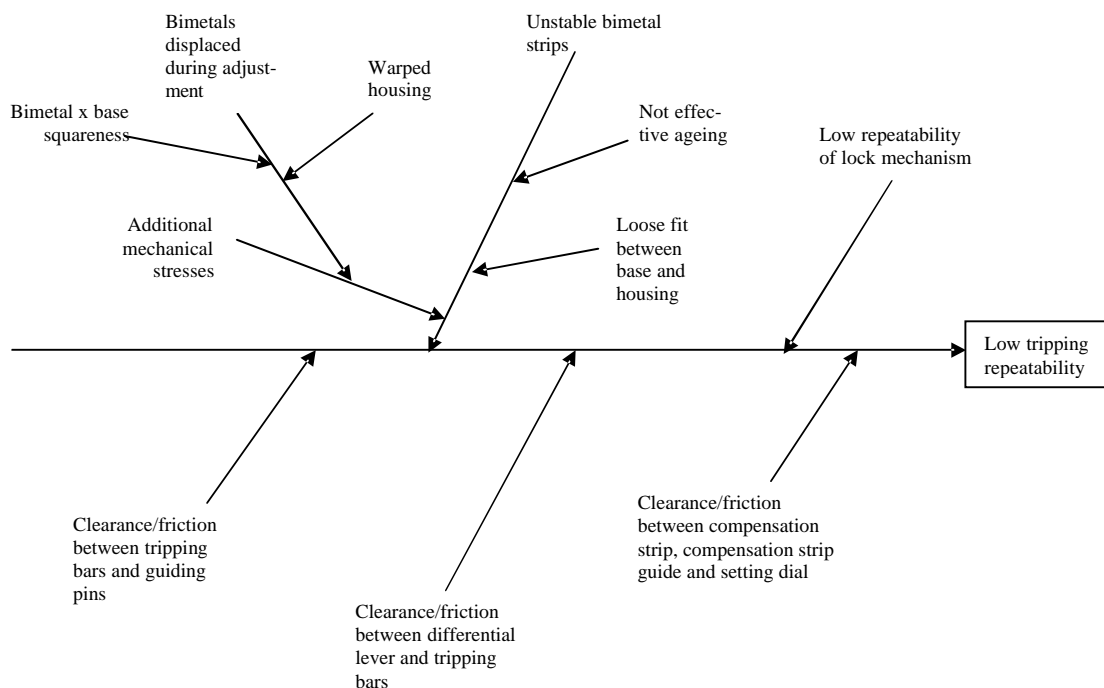
Figure 7.2 – Fish bone diagram for low tripping repeatability

7.4 – Loose fit between bimetal bases and housing

Bimetal bases and housings are mating shafts and holes respectively. Their proper fitting depends on many different dimensions.

These dimensions are showed at figures 7.3, 7.4 and 7.5.

Table 7.4 is a summary containing these dimensions, their actual measurements and fit analysis.

Column 1 shows the letter related to each dimension showed at the above-mentioned figures. When necessary, this column shows the mating dimensions.

Column 2 shows actual measurements on a similar device available in the market.

Column 3 shows MPW25 design parameters; meanwhile column 4 shows actual measurements on MPW25 parts available for the assembly line. It was observed there was a loose fit between dimension "F" (shaft) and dimension "C" (hole). Due to it, the housing

thermo-plastic mould was corrected. The new measurements for dimension "C" are showed at column 5.

It was also observed that in spite dimension "I" (shaft) is according to design parameters, the bimetal base guide is larger than dimension "C" (hole in the housing). There is a risk of housing deformation during assembly of bimetal bases into the housing.
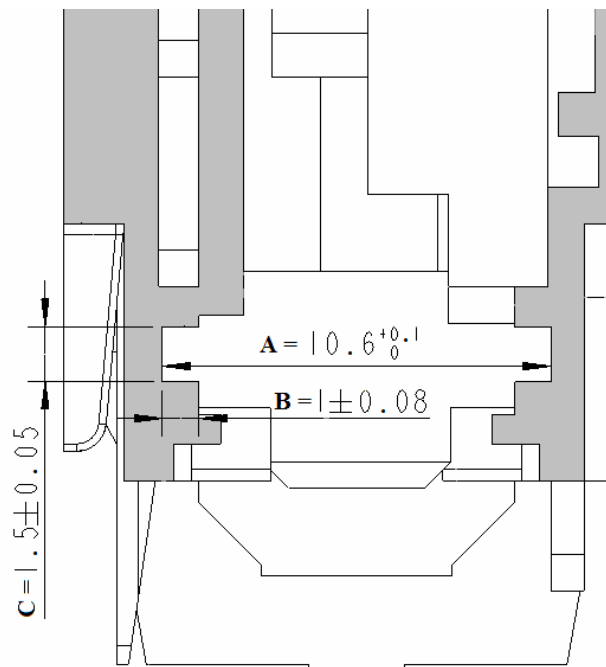
Figure 7.3 – MPW25 housing – cut view (partial).
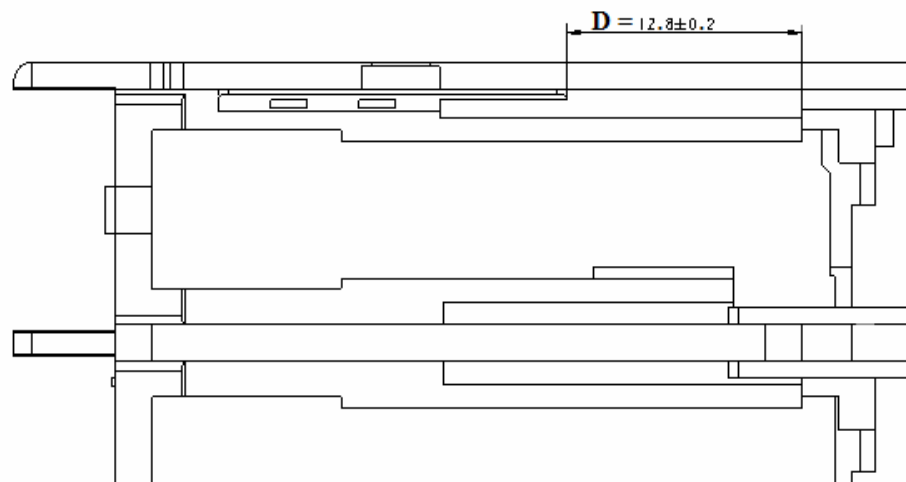
Figure 7.4 – MPW25 housing – top view (partial).
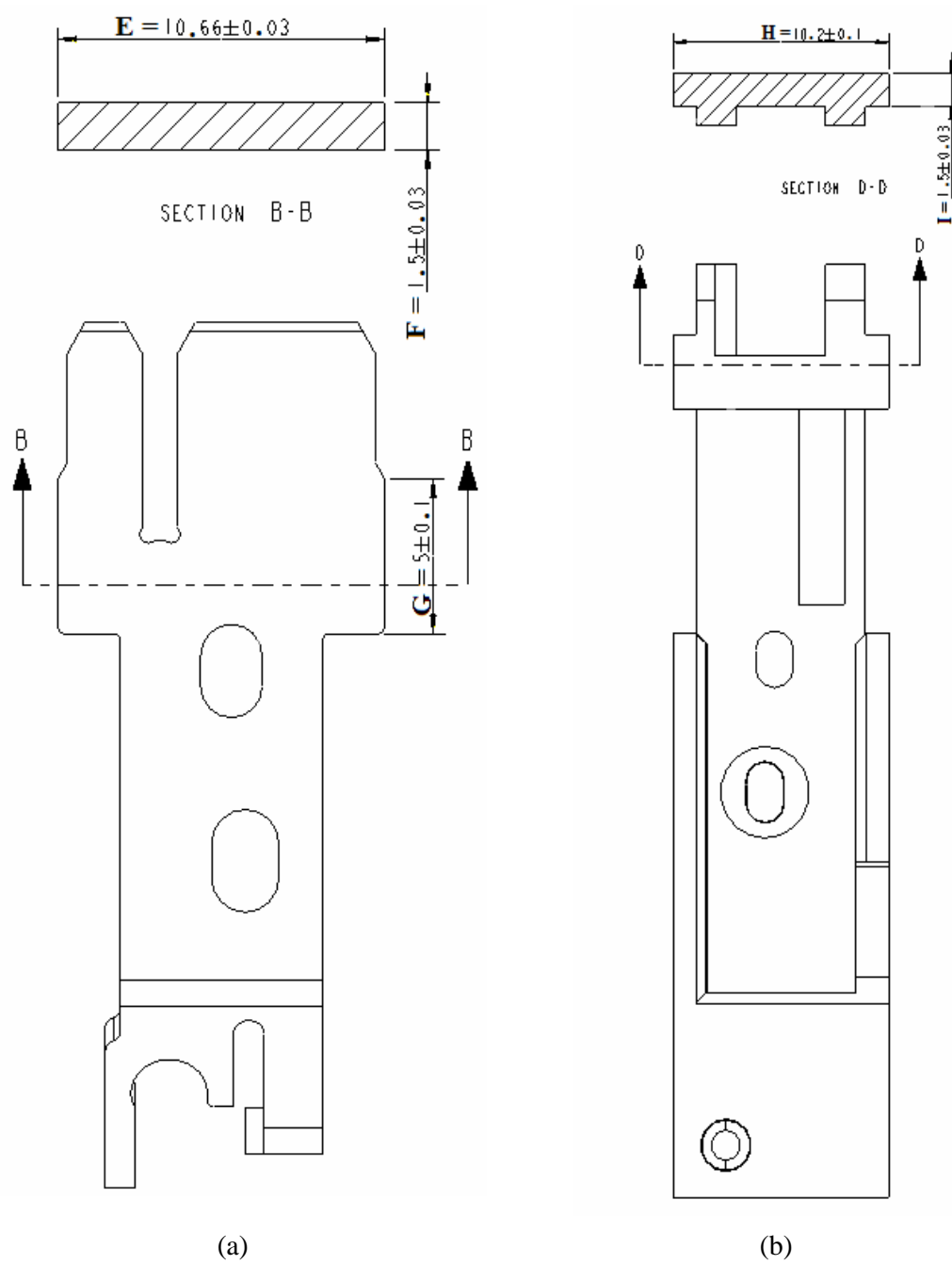
Figure 7.5 – (a) Bimetal base; (b) Contact seat. Cross section shows bimetal base guide

Table 7.4 – Bimetal base and housing: measurements and analysis

Dimension	Similar device from the market - disassembled	MPW25 design	Measurements on MPW25 parts (mm)		Remarks
			Before changing	After correction	
A (hole)	10.6	$10.6\,^{+\,0.1}_{\quad0}$	10.55, 10.54, 10.40	-	Accepted
E (shaft)	10.60	10.66 ± 0.03	10.64	-	ü
C (hole)	1.5	1.5 ± 0.05	1.59, 1.61, 1.55	1.51, 1.51, 1.50	Decided to reduce "C" to 1.45 mm
F (shaft)	1.52	1.5 ± 0.03	1.52	-	ü
B	1.0	1 ± 0.08	0.9 up to 1.06	-	Accepted
D	12.2	12.8 ± 0.2	8.5	-	Accepted
G	5.2	5 ± 0.1	5.1	-	ü
H	10.28	10.2 ± 0.1	10.21	-	ü
I	1.28	1.5 ± 0.03	1.52	-	Bimetal base guide larger than dimension C. Risk of housing deformation.

After correcting the housing (dimension "C"), two complete overload releases were submitted to an additional test to confirm bimetals stability.

Bimetals top positions were first measured. A force equal to 1.5 N (equivalent to 3 times the necessary tripping force to be provided by bimetal system) was subsequently applied on bimetal tops.

After removing the force bimetal top positions were measured again and the difference between the positions were calculated.

The maximum observed difference was 0.02 mm. This value is smaller than 7 % of bimetals tolerance field at minimum setting current. Due to these measurements the bimetal bases were considered to be stable.

The same measurement sequence was repeated after applying forces equal to 3 N and 5 N respectively. As expected, with such large forces bimetals presented a larger displacement in relation to their initial position.

A detailed test report is presented at appendix 10.

In spite of bimetal bases were considered to have become stable, it was decided to enhance the fitting between bimetal base and the housing by reducing dimension "C" to 1.45 mm.

7.5 – Application of additional mechanical stresses on bimetal strips

As explained at chapter 6 tripping bars must be cut during adjusting operation. Figure 7.6 shows available distance for cut (**Y**). It was noticed in the assembly line, some bimetal tops were so displaced that the tripping bars were cut out of the available cutting region.
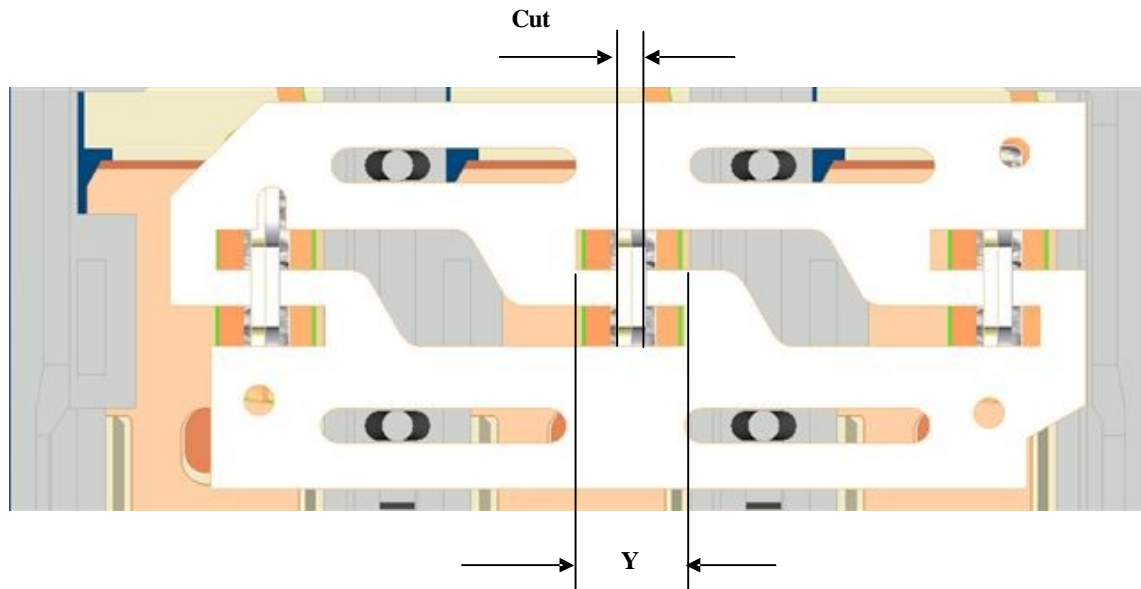
Figure 7.6 – Tripping bars: available distance for cut (**Y**)

To avoid such defective tripping bars, assembly line workers were trained to check bimetal top positions with a special template. Defective devices should be rejected. Instead of it, during this research it was observed that workers were using the template for "adjusting" bimetal tops. Such operation is likely to have been causing additional mechanical stresses on bimetal strips and therefore causing unstable operation of overload releases. This "operation" was immediately forbidden.

On the other hand, there was a suspect the high displacement of bimetal tops was caused by warped housings. To investigate it, three housings were cut according to section Z-Z as showed at figures 7.7 and 7.8.

The samples were subsequently placed in a 3D measuring machine and aligned by the line showed at figure 7.8.

Region of apparent warp

Figure 7.7 – MPW25 housing

alignment line
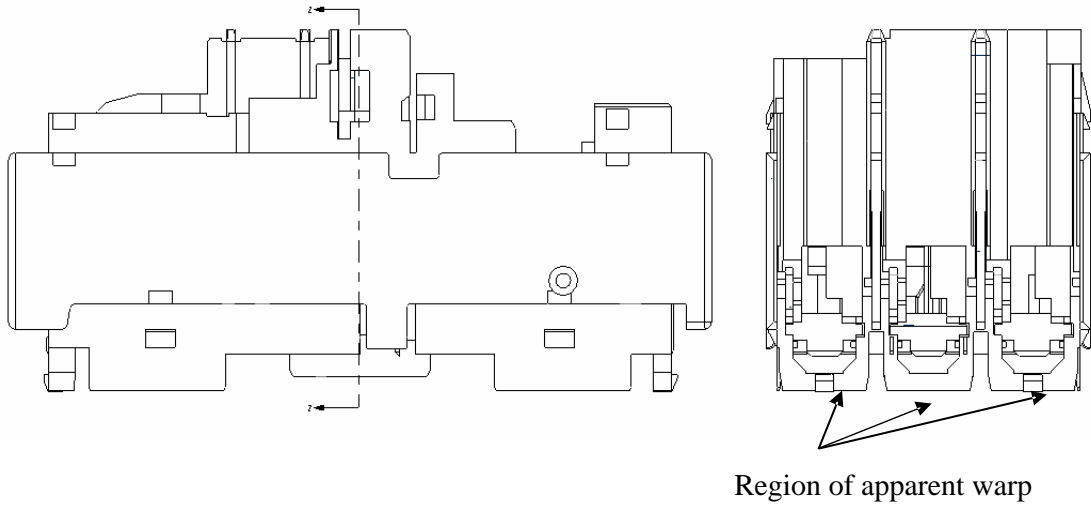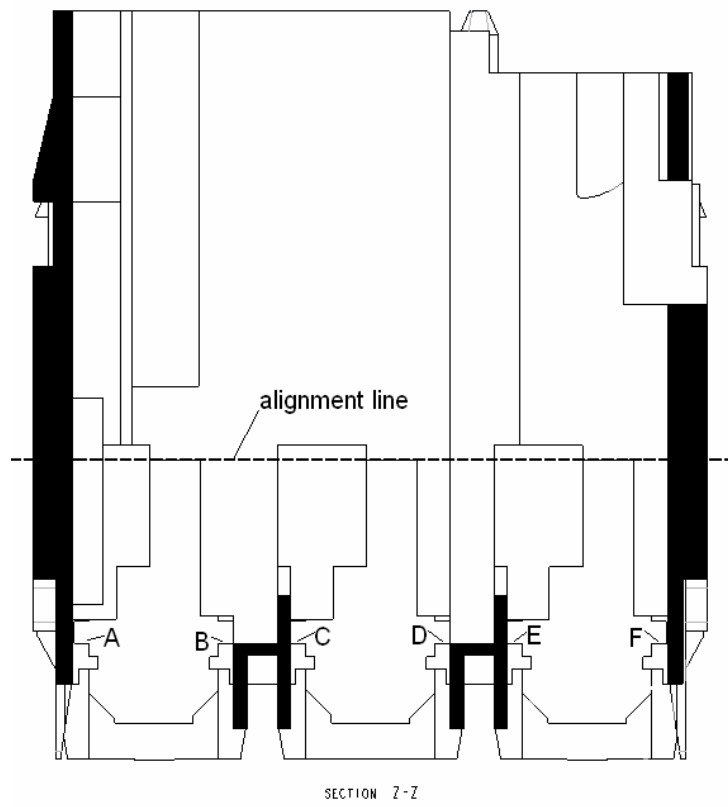
A   B   C   D   E   F

SECTION Z-Z

Figure 7.8 – MPW25 housing – section Z-Z

Surfaces A, B, C, D, E, and F are mating surfaces for bimetal bases. Surface C was used as a reference for measuring the relative position of the other bimetal bases fits. Measurement results are showed at table 7.5.

Table 7.5 – Measurement of housing warpage

Sample	Measurements [mm]					
	A	B	C (reference)	D	E	F
1	-0.01	-0.01	0.00	+ 0.03	- 0.08	-0.04
2	+ 0.01	+ 0.01	0.00	- 0.05	+ 0.07	+ 0.04
3	- 0.01	0.00	0.00	- 0.05	+ 0.05	+ 0.04

Samples 2 and 3 presented the worst warp, i.e. 0.05 mm.

Figure 7.9 represents the consequence of this warp value on bimetal top displacement.

Maximum calculated value for bimetal top displacement is 0.2 mm.

Available distance for cut: (Y) ~ 3 mm.
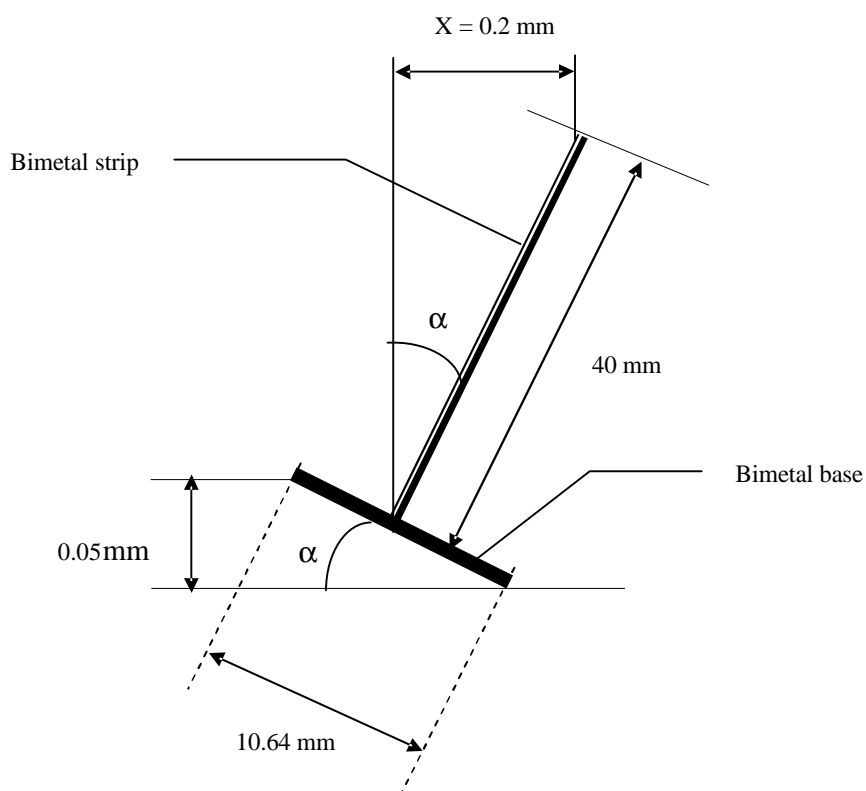
Figure 7.9 – Displacement of bimetals top for worst warp

The main conclusions here are:

- Measured housings presented a negligible warp ($X << Y$); this is not the reason for the observed excessive bimetals top displacement.
- Excessive bimetals top displacement is likely to be caused by not proper squareness between bimetal strips and their bases. This feature shall be analysed by additional researches.

7.6 – Analysis of stress relieving procedure (ageing)

Table 7.6 summarises stress relieving procedures recommended by different bimetal manufacturers.

Table 7.6 – Recommended ageing procedures

Manufacturer	Ageing temperature	Cycle	Bimetals position in the oven
Vaccumschmelze /59/	- In principle, ageing temperature should range between 250 and 450 ℃; or at least 50 ℃ above the maximum temperature of use. - Bimetals maximum allowed operating temperature should not be exceeded.	- "heating-up and particularly cooling should not take place too rapidly.	- "Parts must be so positioned that their thermal deflection is not impeded."
Kanthal /60/	- "…at least 50 ℃ above the maximum temperature of operation…ageing is seldom performed below 200 ℃." - Bimetals maximum operating temperature should not be exceeded.	- Duration: 2 – 3 hours. - In case of high demands for accuracy ageing in 2 or 3 stages is recommended	xxx
Shivalik /61/	- 50 ℃ above maximum service temperature. Minimum ageing temperature = 250 ℃. - Ageing temperature should not exceed the maximum allowed working temperature.	- Maximum heating or cooling speed = 20 ℃/min.	- "The components must be free to deflect…They should be spread out singly on the tray of the oven."

Test reports /55/ show bimetals for motor protective circuit breakers can reach a temperature rise equal to 110 ℃, when the device is submitted to 1.5 times the setting current (steady state). Of course, in normal operation this device would have tripped before reaching that temperature.

On the other hand MPW25 is designed to operate at a maximum ambient temperature equal to + 60 ºC.

Considering the above information the maximum operating temperature for MPW25 bimetals can be estimated as 170 ºC. This temperature value is far bellow the maximum operating limits presented at table 7.7.

Table 7.7 – Operation temperature limits /60/

Bimetal type		Maximum temperature of application [ºC]
TB 1577 A	/59/	450
TB 1511	/60/	400
721 Cu 5	/61/	350

Table 7.8 compares WEG's ageing method with recommended procedures presented at table 7.6:

Table 7.8 – Ageing method currently used by WEG

	Ageing temperature	Cycle	Bimetal position
Ageing procedure (based on a technology transfer agreement with AEG – Germany /64/)	220 ºC	- 3 cycles - heating speed = 3 ºC/min - Cooling speed = 2.2 ºC/min	- Spread in a tray; multiple bimetal layers. - Tray depth ~ 70 mm.
Conclusions	- According to ageing procedure recommended by Kanthal (Table 7.6)	-According to Kanthal (Table 7.6)	- Risk of impede thermal deflection (not according to table 7.6)

The main conclusion here is: the use of multiple bimetal layers can impede bimetals deflection during ageing process. This behaviour can create additional mechanical stresses in bimetals structures.

It was decided to perform an experiment for evaluating the influence of this factor on overload releases repeatability (detailed at section 7.9).

In addition to the previous analysis, the ageing oven settings were also checked. It was detected the oven temperature was set for 210 ºC instead of 220 ºC as specified at table 7.8.

After correcting this parameter, the actual temperature in the ageing oven was measured as follows:

- Eleven thermocouples were distributed inside the oven as indicated at figure 7.10. Thermocouple 10 was positioned inside the upper tray, between bimetal strips. Thermocouple 11 was positioned inside the tray located in the center of the oven, between bimetal strips;
- The oven was completely loaded with bimetals to be aged;
- The ageing cycles were started and temperatures were plotted (obtained plot is showed at appendix 11);
- Average measured temperatures are showed at table 7.9.
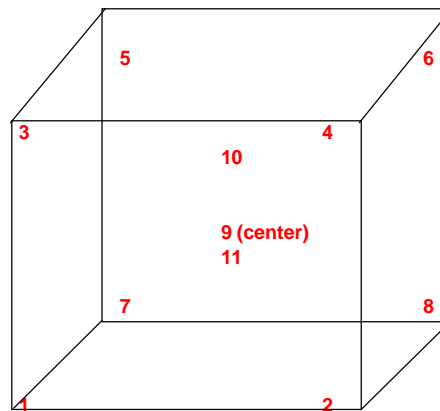
Figure 7.10 – Distribution of thermocouples inside ageing oven

Table 7.9 – Average temperatures in the oven
(during 2nd cycle)

Measured points	Average temperature [ºC]
1	222,7
2	218,2
3	218,6
4	217,7
5	221,7
6	221,3
7	223
8	224,3
9	222,6
10	221,4
11	221,3
Oven average	221,2

The main conclusions obtained from these measurements are:

- The actual temperature inside the ageing oven is equal to 221.2 ± 3.5 ºC;
- The ageing oven has a homogeneous temperature distribution;
- Heating speed = 2.9 ºC/min;
- Cooling speed = 1.9 ºC/min.

7.7 – Analysis of clearances and friction between overload releases parts

Tripping bars and respective guiding pins (Figure 7.11) were measured and analysed as showed at table 7.10.
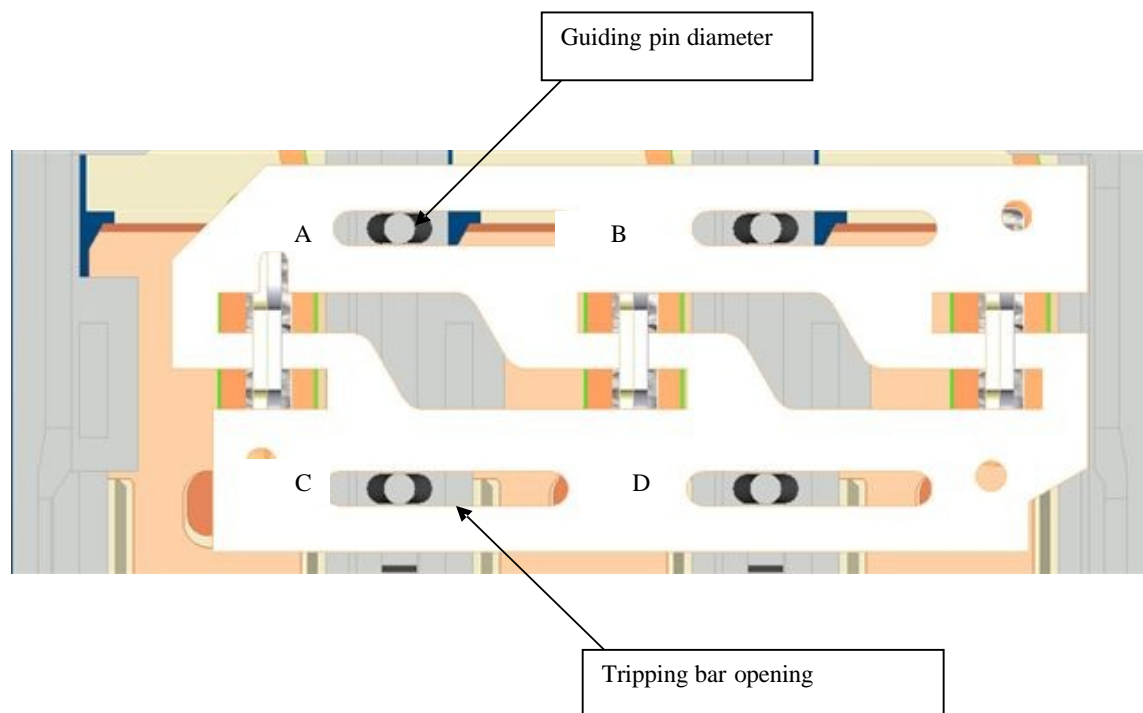
Figure 7.11 – Measuring features of tripping bars and guiding pins.

Table 7.10 – Measurements on tripping bars and guiding pins

Feature	Similar device from the market		MPW25	
	Measurements [mm]	Remarks	Measurements [mm]	Remarks
Width of tripping bars openings				
A	1.43		1.44	
B	1.44	Small burrs	1.44	Medium burrs
C	1.42		1.45	
D	1.40		1.45	
Diameter of guiding pins				
A	1.23		1.27	
B	1.22	-	1.24	-
C	1.22		1.24	
D	1.22		1.25	
Smallest clearance	0.18	-	0.17	-

Main conclusions:

- There are reasonable clearances between the different parts;
- Burrs may influence on overload release repeatability. This influence will be investigated by additional experiments.

Additionally, tripping bars bearings (Figure 7.12) and corresponding shafts at differential lever were measured and analysed as showed at table 7.11.
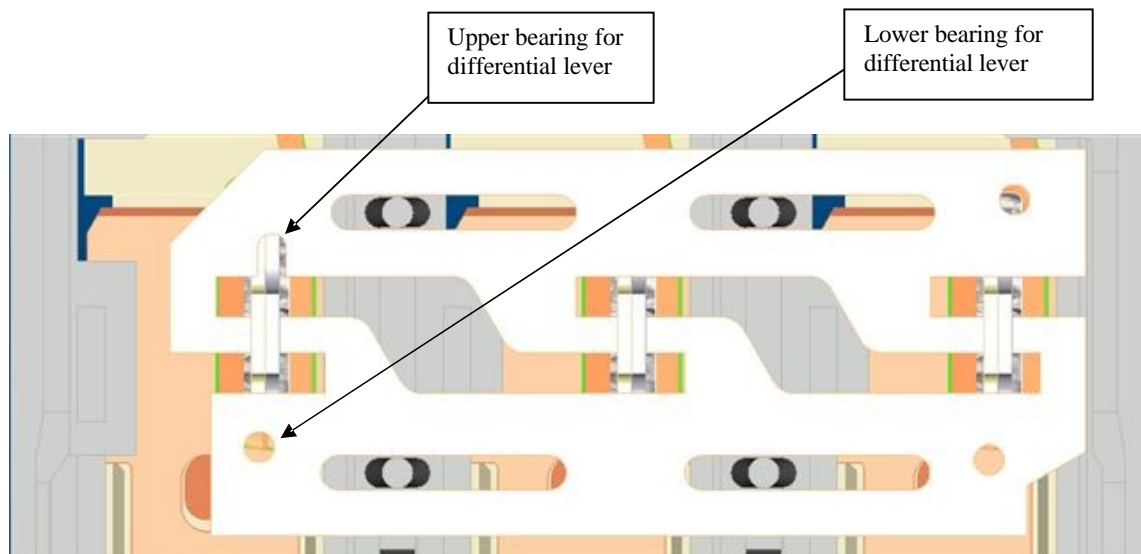
Figure 7.12 – Tripping bars bearings.

Table 7.11 – Measurements on tripping bars bearings and corresponding shafts

Feature	Similar device from the market		MPW25	
	Measurements [mm]	Remarks	Measurements [mm]	Remarks
Upper bearing diameter	1.59	-	1.06	-
Diameter of corresponding shaft at differential lever	1.43	-	1.00	-
Clearance	0.16	-	0.06	Not enough clearance
Lower bearing diameter	1.66	-	1.16	-
Diameter of corresponding shaft at differential lever	1.39	-	1.00	-
Clearance	0.27	-	0.16	-

Main conclusions: MPW25's upper bearing diameter is too small compared to the corresponding shaft at the differential lever (actual clearance value = 0.06 mm). This characteristic may influence on overload release tripping repeatability. Desirable clearance value: 0.15…0.20 mm (according to MPW25 design). It was decided to correct stamping tools for this MPW25 part.

Every manufacturing tool employed by the company has a complete measuring report showing actual dimensions for the obtained parts when the tool was approved to start regular operation. The report for tripping bar stamping tool is showed at appendix 12. Signalled values show upper bearing diameter was out of design tolerances but it was still acceptable.

Besides that, every manufactured part has a quality procedure informing which features must be inspected, by sampling, during regular production. The quality procedure for this specific part is showed at appendix 13. It can be observed a template is recommended for inspecting the lower bearing of the tripping bar. Nevertheless, it is not clear if the same procedure must be employed for inspecting the upper bearing. Main conclusion here: there is a risk this feature has not been inspected by quality personnel.

Clearances necessary for compensation bimetal operation (Figures 7.13 and 7.14) were also measured as showed at table 7.12. Actual values were considered acceptable.
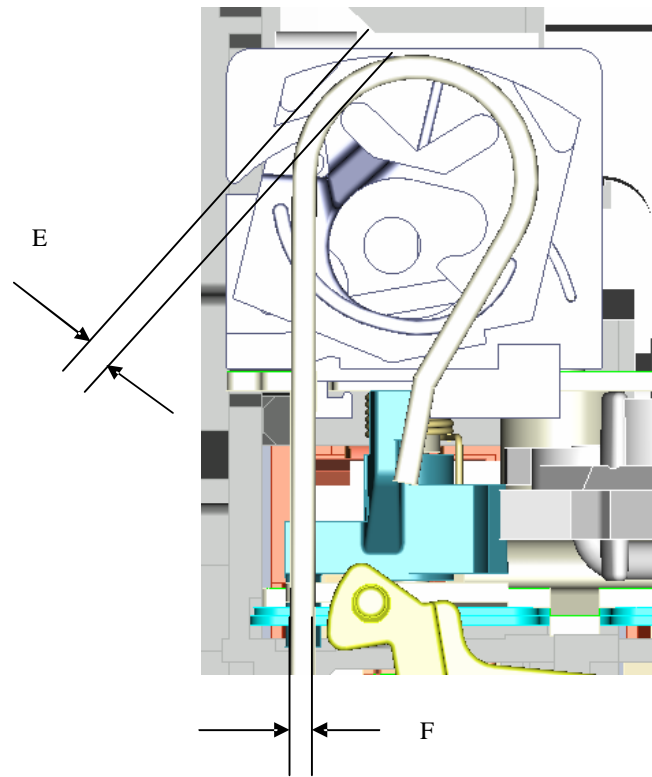
Figure 7.13 – Measuring features of compensation bimetal and its guide
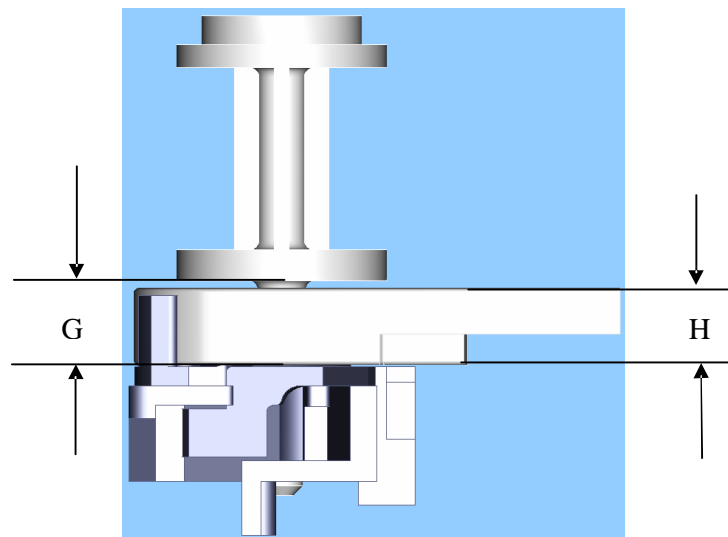
Figure 7.14 - Measuring features of complete compensation bimetal

Table 7.12 – Measurements on complete compensation bimetal

Dimension	Similar device from the market		MPW25	
	Measurements [mm]	Remarks	Measurements [mm]	Remarks
E	1.20	-	1.28	-
F	1.04	-	1.01	-
Clearance	0.16	-	0.27	-
G	4.24	-	4.25	-
H	4.06	-	4.04	-
Clearance	0.18	-	0.21	-

7.8 – Analysis of lock mechanism tripping repeatability

Three lock mechanisms had their tripping forces and tripping travels measured under the following conditions:

- Lock mechanism alone;
- Lock mechanism already assembled in MPW25 housing;
- Lock mechanism assembled in MPW25 housing with complete base assembly;
- Lock mechanism assembled in MPW25 housing with complete base assembly; tripping operation via the compensation bimetal.

Test procedures and results are detailed in appendix 14.

Table 7.13 presents a summary for tripping operation under the last testing conditions.

Main conclusions obtained from these tests: lock mechanism presents a high tripping repeatability when assembled in MPW25 housing with complete base assembly (tripping operation via the compensation bimetal).

Table 7.13 – Measurement of lock mechanism repeatability

Manual measurement at the compensation bimetal - lock mechanism in MPW 25 housing with base assembly						
Sample	1		2		3	
Measurement	Travel	Force	Travel	Force	Travel	Force
1	1.08	0.54	1.03	0.53	0.95	0.64
2	1.06	0.60	1.02	0.54	0.94	0.61
3	1.10	0.51	1.02	0.52	1.00	0.66
4	1.16	0.53	1.07	0.48	0.93	0.61
5	1.11	0.56	1.01	0.51	0.91	0.66
Average(mm)	1.10	0.55	1.03	0.51	0.95	0.64
Minimum value	1.06	0.51	1.01	0.48	0.91	0.61
Maximum value	1.16	0.60	1.07	0.54	1.00	0.66
Maximum deviation from average value (%)	5.4	9.1	3.9	5.9	5.3	4.7

7.9 – Experiments

It was decided to perform some experiments on MPW25/6.3-10 samples for validating the previous analysis.

All tested samples were prepared with the improvements summarized at table 7.14.

Besides that, the influence of two additional factors was tested: bimetals position in the ageing oven and tripping bars clearances. Each factor was tested at two different levels (Table 7.15).

Twelve samples were prepared as detailed at table 7.16.

Test results are presented at table 7.17.

Table 7.14– Summary of features to be improved on all samples to be tested

Feature	Current status	Necessary improvement	Remarks
Fit for bimetal base into the housing (Dimension C)	1.50 mm	Change to 1.45 mm	By changing the plastic mould
Bimetal base guide thickness	1.52 mm	Change to1.30 mm	By using a file.
Squareness between bimetal strip and its base	Some defective parts were detected	Select parts with good squareness for the experiments	It was forbidden to adjust bimetal strips tops.
Diameter of upper bearing at tripping bar	1.06	Change to 1.15-1.20 mm	By using a file.

Table 7.15– Summary of factors to be tested

Factor	Factors description	Levels description	
A	Ageing process	Low level (-)	Currently available ageing process (regular ageing process); thermal deflection can be impeded due to multiple bimetal layers.
		High level (+)	Thermal deflection not impeded (bimetals were hanged in the oven)
B	Tripping bars clearance	Low level (-)	Medium burrs in tripping bars clearances (regular clearance).
		High level (+)	Without burrs (eliminated with a file)

Table 7.16– Treatment combinations to be tested

Factor		Treatment combination	Number of samples (Replicates)
A	B		
-	-	A low, B low	3
+	-	A high, B low	3
-	+	A low, B low	3
+	+	A high, B high	3
		Total number of samples	12

Table 7.17 – Test results (I_{lim} on MPW25/6.3-10)

Sample	Ageing	Clearance	1st I_{lim}	2nd I_{lim}	3rd I_{lim}	7.2 I_{max} (3x)	4th I_{lim}	5th I_{lim}	Average	Range
1	Regular	Regular	1.26	1.27	1.24	-	1.24	1.24	1.25	0.03
2	Regular	Regular	1.30	1.24	1.27	-	1.24	1.27	1.26	0.06
3	Regular	Regular	1.21	1.18	1.18	-	1.24	1.21	1.20	0.06
4	Regular	No burrs	1.21	1.18	1.21	-	1.18	1.18	1.19	0.03
5	Regular	No burrs	1.27	1.24	1.24	-	1.21	1.24	1.24	0.06
6	Regular	No burrs	1.27	1.24	1.24	-	1.21	1.18	1.23	0.09
7	Hanged	Regular	1.24	1.18	1.24	-	1.18	1.18	1.20	0.06
8	Hanged	Regular	1.30	1.33	1.27	-	1.24	1.24	1.28	0.09
9	Hanged	Regular	1.30	1.33	1.30	-	1.33	1.27	1.31	0.06
10	Hanged	No burrs	1.30	1.27	1.24	-	1.24	1.21	1.25	0.09
11	Hanged	No burrs	1.21	1.18	1.21	-	1.18	1.18	1.19	0.03
12	Hanged	No burrs	1.24	1.21	1.24	-	1.21	1.21	1.22	0.03
Average			1.26							
Standard deviation			0.04							

Main conclusions obtained from the tests:

- Tested samples presented a remarkable improvement on tripping repeatability compared to test results showed at table 7.3. 75 % of tested devices showed current limit values within a range ≤ 0.06 p.u.;
- It was not noticed any important difference on tripping repeatability between all treatment combinations that have been tested;
- Improvements detailed at table 7.14 shall be implemented in the manufacturing tools and assembly line immediately;

7.10 – Evaluation of calibration process capability

Table 7.17 also shows average and standard deviation values for the first I_{lim} tests for the twelve samples.

Figure 7.15 represents the distribution of measured values (1st I_{lim} for the 12 samples) in relation to the limits of operation for overload releases (IEC 60947-4-1). This representation supposes the measured values were distributed according to a Gauss distribution.

Based on figure 7.15 it is possible to conclude that calibration process is not centralized in relation to IEC 60947-4-1 limits of operation.

Supposing the calibration process were centralized, a new representation for I_{lim} measured values could be obtained (Figure 7.16).
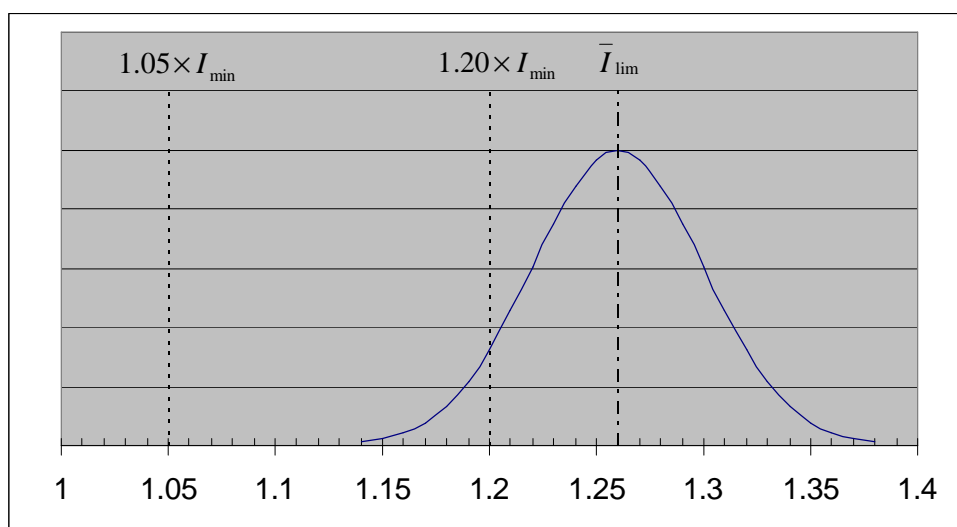
Figure 7.15 - I_{lim} distribution (for the 1st I_{lim} test sequence)
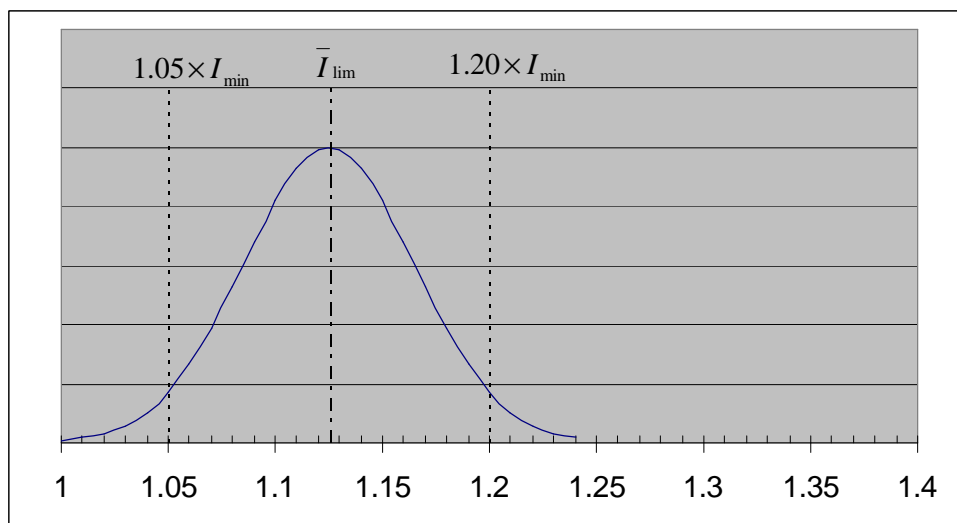
Figure 7.16 - I_{lim} distribution supposing the process has been centralized

After this centralization, calibration process capability can be calculated using equation 7.2 /65/:

$$P_p = \frac{U_L - L_L}{6 \times s} \qquad (7.2)$$

Where:

P_p = process capability index

U_L = upper limit of specifications

L_L = lower limit of specifications

s = standard deviation

Therefore, currently employed calibration process would present $P_p = 0.625$.

WEG's TBG 830 /65/ recommends that a process can be considered capable when $P_p \geq 1.33$. It can be estimated that processes with $P_p = 1.33$ are likely to produce up to 63 defective parts per million (p.p.m.).

It can be calculated that the currently employed calibration process (that presents $P_p = 0.625$) is likely to produce up to 6.2 % devices out of specification limits (or 62.000 p.p.m.).

The main conclusion here is the calibration process available in the company is not capable of meeting IEC 60947-4-1 requirements.

7.11 – Main conclusions for chapter 7

- Overload releases can be considered to present good tripping repeatability when successive current limit tests on the same sample show current limit values within a range ≤ 0.06 p.u.;

- Tests performed on samples obtained from MPW25 assembly line showed their overload releases present low tripping repeatability;

- Main causes for this performance are: a) loose fit between bimetal bases and housings; b) application of additional mechanical stresses on bimetal strips; c) upper bearing (at tripping bar) is too small. These features must be improved immediately in the assembly line;

- Available calibration process is not capable of meeting IEC 60947-4-1 specification limits. It was not possible to analyse, test and implement improvements on this feature during this research. It is recommended next researches analyse ways to improve calibration process performance.

- Currently available quality procedures were not suitable to neither prevent such failures nor correct them earlier;

- Bimetals ageing process available in the company is effective. The use of multiple layers trays does not disturb ageing process results;

- Medium burrs observed in the tripping bars clearances do not have any influence on overload releases tripping repeatability.

- A quality engineer should be hired immediately by the company. This person should not be involved on routine matters. Instead of it this specialist should be permanently analysing new products performance like it was done by this research. In case some non-conformity is found, the quality engineer should completely analyse what is happening and than make proposals for corrective actions for responsible personnel. Figure 7.17 explains the design method currently employed by WEG ACIONAMENTOS. This method is based on the concept of reverse engineering. Figure 7.18 additionally explains a proposal about a way for inserting the new quality engineer in the early stages of new products development. After the new products are launched in the market, this engineer has an important role on controlling and improving their quality.
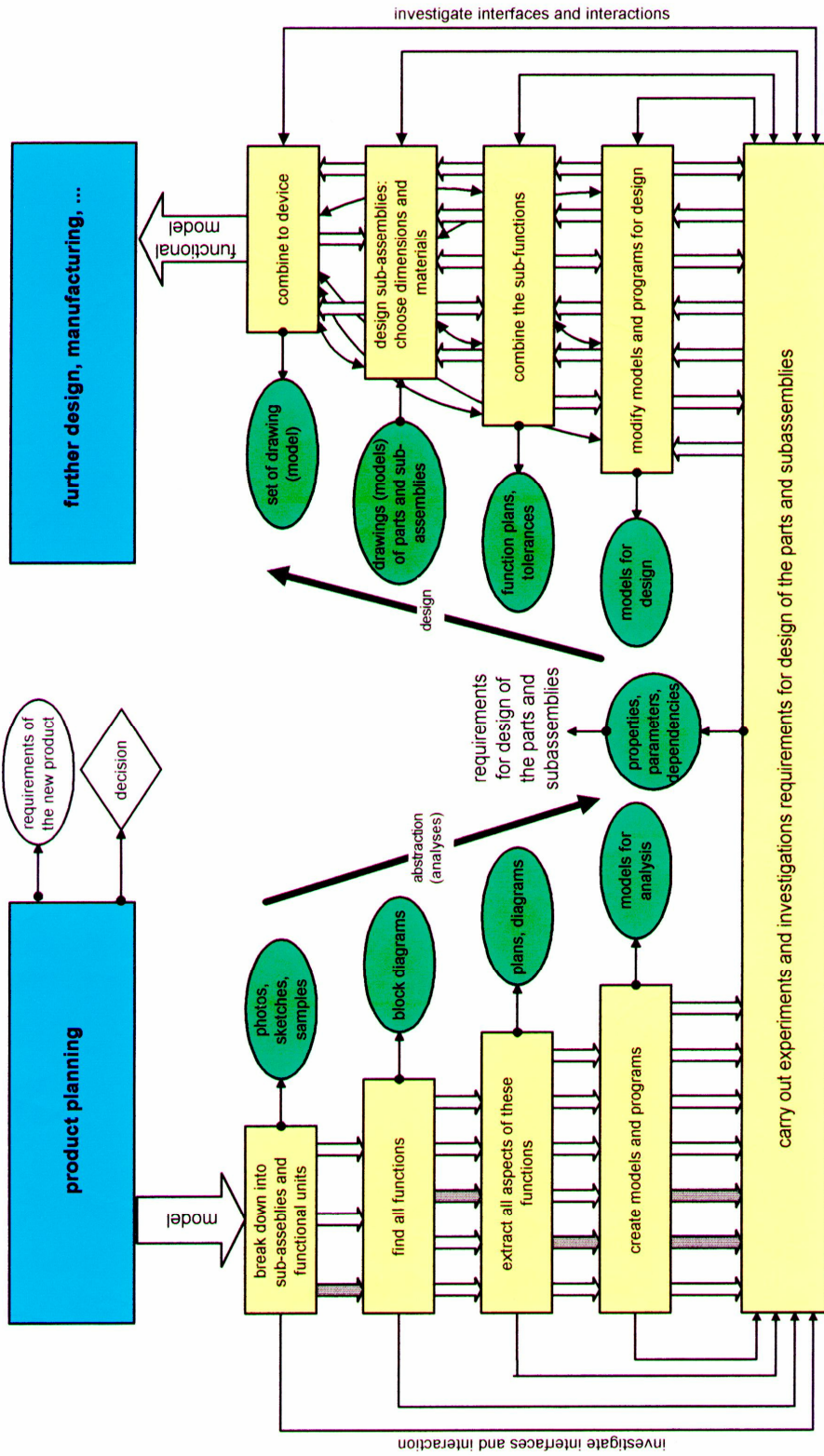
Figure 7.17 – Design method based on a pre-existing model /66/
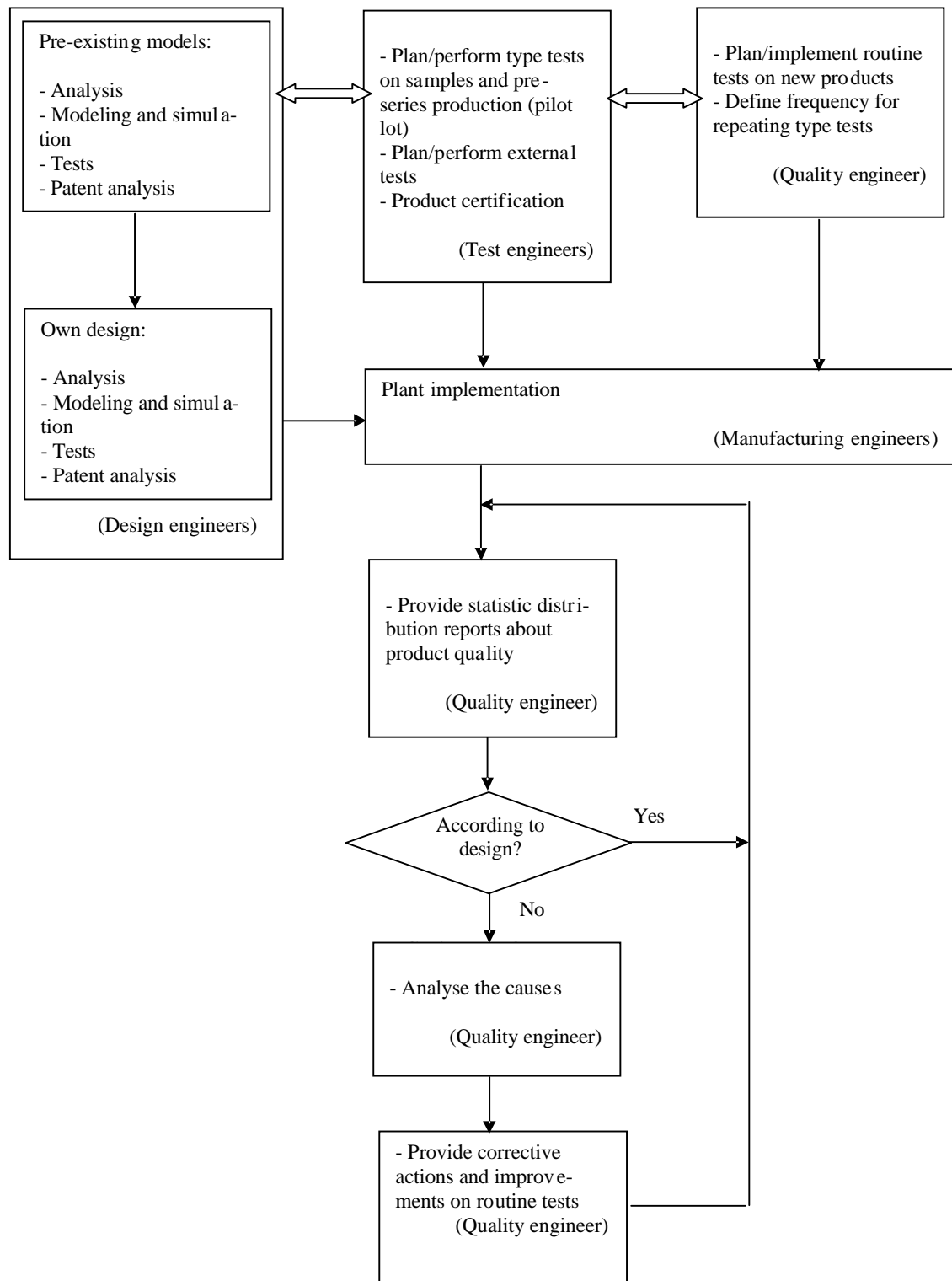
Figure 7.18 – Procedure for quality planning and quality improvement for new products

CHAPTER 8

This chapter presents the conclusions for the complete research, as well as, suggestions for future research tasks to be developed by other engineers.

8.1 – Conclusions about electric motors thermal behaviour

- This research has considered a basic thermal model for calculating thermal limit curves for electric motor windings. One 11 kW electric motor, manufactured by WEG, was subsequently submitted to overload tests. Test results showed the proposed mathematical model is valid only up to over-current values $\leq$ 1.3 times the rated current. Above this value, electric motor windings heat faster than predicted by the model. A more accurate description of temperature rise of motor windings requires the use of a better model. The new mathematical model should be validated by testing different motor sizes;

- Even though the tests have showed the proposed model has some limitations, it is possible to say that electric motors are likely to suffer a considerable decrease in their insulation system life, when they are submitted to over-current values $\geq$ 1.2 times their rated current. This behaviour explains why standards require current dependent protection devices must trip when over-current values $\geq$ 1.2 times the rated current are detected;

- Some important subjects that were not analysed here and are suggested for future researches: a) analysis of thermal behaviour and temperature rise limits for electric motors rotors; b) analysis of electric motors temperature rise when they are submitted to locked rotor conditions. Which motors are stator critical and which are rotor critical; c) analysis of temperature rise of motor windings when electric motors are submitted to phase failure operation.

8.2 – Conclusions about overload protection and MPW25's overload releases

- Classical thermo-mechanical overload relays and releases, manufactured according to IEC 60947-4-1, are able to provide proper overload protection for electric motors;

- MPW25 is a motor protective circuit breaker manufactured by WEG. Their overload releases employ the thermo-mechanical technology. This research has analysed their performance only when all poles are energized, the device is operating at minimum

current setting and is submitted to currents equal to $1.05 \times I_{min}$ and subsequently to $1.20 \times I_{min}$. This research has found the performance of MPW25 overload releases is not completely according to IEC 60947-4-1 requirements;

- MPW25 overload releases presented low tripping repeatability. Main causes for it: a) loose fit between bimetal bases and housings; b) application of additional mechanical stresses on bimetal strips; c) upper bearing (at tripping bar) is too small. These features have been already corrected. Therefore, the 1st own design by WEG ACIONAMENTOS has reached a good repeatability;

- On the other hand, it was found dynamic calibration process is not capable of meeting IEC 60947-4-1 requirements for all devices from the assembly line. Due to available time, this research was not able to analyse and improve this feature. It is necessary to, immediately, start studies for improving dynamic calibration procedures;

- It was also confirmed that bimetals ageing process, currently available at WEG, is effective;

- It is also important that future researches analyse MPW25 overload releases performance at each marked value of current scale for all limits of operation specified by IEC 60947-4-1; The same is necessary for limits of operation when the devices are energized on two poles only;

- An additional subject that was not analysed here and is suggested for future researches: the need of special settings for using IEC type overload relays and releases for protecting motors with service factor higher than 1.0;

- This text can be used as a basis for next analysis and improvements on electro-mechanical overload protection devices.

8.3 – Conclusions about quality procedures for new products development

- The company must keep the currently available procedure for approving measuring reports for each manufacturing tool. Design engineers must pay special attention before approving manufacturing tools for starting regular operation;

- The company should implement special training programs for every new product to be launched. This training program should include lectures by design engineers and manufacturing engineering personnel for all production line workers and for quality control personnel. The training program should explain main critical design features for new products performance as well as main critical features for the manufacturing

processes. With this training program, it could be expected more people would be aware about critical features of the new products and manufacturing processes. In this way the company could expect faster detection of product and process non-conformities, as well as faster and more effective corrective actions;

- Quality control personnel should pay more attention about critical features that require permanent control in the production line. Quality plans currently available at every workstation must inform all critical features that may influence on products performance. Quality control personnel must permanently improve such procedures;

- This research has also proposed some tasks for a quality engineer to be hired by the company. This person will be responsible for following up new products performance and for implementing necessary corrective actions.

REFERENCES

/1/ WEG. **Manual de Motores Elétricos.** Jaraguá do Sul, 2003.

/2/ INTERNATIONAL ELECTROTECHNICAL COMMISION. **IEC 60085 – Thermal evaluation and classification of electrical insulation** – 2nd edition. Geneva, 1984.

/3/ LATI. **UL 1446 Underwriters Laboratories Insulation system recognition.** At www.lati.com/time_lati_20/lambda_03.html

/4/ P. Leo & Co.,(B.C.) Ltd. **Electrical Insulation System Testing.** At www.pleo.com/ulsystem/eis_test.htm

/5/ Du Pont. **Technical Information – UL-Recognized 600 Volt Class Electrical Insulation Systems Based on Nomex**. 10/99.

/6/ NAILEN, R. L. **What tests of insulation's thermal life really mean.** Electrical Apparatus/March 2000.

/7/ COWERN, E. H. **The Cowern papers – Motor temperature ratings.** At www.motorsanddrives.com/cowern/motorterms4.html

/8/ CAMPBELL, B.; GALLENO, J. **Motor Life: The effects of loading, service factor and temperature rise on insulation life.** IEEE Paper No. PCIC-98-33. 1998.

/9/ COWERN, E.   H.; **Motor Temperature Ratings.** At www.baldor.com/pdf/manuals/pr2525.pdf

/10/ BONNET, A. H.; **Operating Temperature Considerations and Performance Characteristics for IEEE 841 Motors** – IEEE Transactions on Industry Applications, Vol. 37, NO.4, July/August 2001.

/11/ BERGER, F.; **Comments about Stuart's master dissertation text.** TU-Ilmenau. September 28th,2004.

/12/ INTERNATIONAL ELECTROTECHNICAL COMMISION. **IEC 60034-1 – Rotating electrical machines – Part 1: Rating and performance.** Edition 10.2. Geneva, 1999. 135p.

/13/ NATIONAL ELECTRICAL MANUFACTURERS ASSOCIATION. **NEMA MG1 – Motors and Generators**. Revision 3,2002 Interfiled. Virgínia, 1998.

/14/ THE INSTITUTE OF ELECTRICAL AND ELECTRONICS ENGINEERS, INC. **IEEE Std 118 - Standard test code for resistance measurement.** New York, 1978.

/15/ THE INSTITUTE OF ELECTRICAL AND ELECTRONICS ENGINEERS, INC. **IEEE Std 112 - Standard test procedure for polyphase induction motors and generators.** New York, 1996.

/16/ WEG. **Comparativo de Valores entre Ensaios – Motor de Indução trifásico.** Jaraguá do Sul 01/10/2003.

/17/ FITZGERALD, A.E.; KINGSLEY Jr., C.; KUSKO, A. **Máquinas elétricas.** Barueri: McGraw-Hill do Brasil, 1979. 623 p.

/18/ SIEMENS. **Seleção e aplicação de motores elétricos – Volume 1.** São Paulo: MAKRON Books do Brasil Editora Ltda, 1988. 351 p.

/19/ WEG. **TT – 96.001: Método de cálculo para estimar a elevação de temperatura dos motores de indução trifásicos sob variação de tensão e carga.** Jaraguá do Sul, 1996. 101 p.

/20/ VALENZUELA, M.A.; VERBAKEL, P.V.; ROOKS, J.A. **Thermal evaluation for applying TEFC induction motors on short-time and intermittent duty cycles.** IEEE Transactions on industry applications, Vol. 39, NO. 1, January/February 2003.

/21/ FAREG, S.F.; BARTHELD, R.G.; MAY, W.E. **Electronically enhanced low voltage motor protection and control.** IEEE Transactions on industry applications, Vol. 30, NO. 3, May/June 1994.

/22/ ROCWELL Automation. **Optimising plant production and operation through motor protection.** Publication 193-2.15. May 1997.

/23/ MARTIN, C.A. **Dinâmica de Sistemas.** Florianópolis: Apostila UFSC – EMC – GRUCON – LHW, 2003.

/24/ SHEARER, J.L.; MURPHY, A.T.; RICHARDSON, H. H. **Introduction to system dynamics.** Massachusetts: Addison-Wesley Publishing Company, 1967. 420 p.

/25/ KREITH, F. **Princípios da transmissão de calor.** São Paulo: Edgard Blücher, 1977. 550 p.

/26/ NAILEN, R.L. **Is there such a thing as a 'standard thermal limit curve'?** Electrical Apparatus (Magazine), June 2001. 6 p.

/27/ SILVEIRA, S.B. **Elevação de temperatura em motores com sobrecarga.** Jaraguá do Sul. 3 p

/28/ BOOTHMAN, D.; ELGAR, E.; REHDER, R.; WOODDALL, R.; **Thermal tracking – A rational approach to motor protection** – IEEE Paper No. T 74 029.5. 1973.

/29/ INTERNATIONAL ELECTROTECHNICAL COMMISION. **IEC 60034-11 – Rotating electrical machines – Part 11: Built-in thermal protection.** First edition. Geneva, 1978. 31 p.

/30/ GONÇALEZ, F.; STUART, R. Jr. Tecnologia de desenvolvimento de dispositivos elétricos de baixa tensão. **WEG em revista,** Jaraguá do Sul, n. 28, p. 13-15, mai./jun. 2004.

/31/ SCHNEIDER ELECTRIC. **Guide to motor control and protection.** www.schneider.co.uk/booklets.

/32/ GROUPE SCHNEIDER. **Electrical installation guide – According to IEC International Standards.** July 1996.

/33/ ROCWELL Automation. **"Coordinated" motor circuit protection.** Publication 193-2.10. July 1995.

/34/ INTERNATIONAL ELECTROTECHNICAL COMMISION. **IEC 60204-1 – Safety of machinery – Electrical equipment of machines – Part 1: General requirements** Fourth edition. Geneva, 1997. 183 p.

/35/ INTERNATIONAL ELECTROTECHNICAL COMMISION. **IEC 60947-1 – Low-voltage switchgear and controlgear – Part 1: General rules.** Edition 3.2. Geneva, 2001. 337 p.

/36/ SIEMENS. **Switching, protection and distribution in low-voltage networks.** 2nd edition. Erlangen: Publicis MCD Verlag, 1994.

/37/ MOELLER. **Wiring manual - Automation and power distribution.** 1st edition. Bonn, 1997.

/38/ NATIONAL FIRE PROTECTION ASSOCIATION. **National Electrical Code (NEC).** 1999 Edition. Quincy, MA.

/39/ INTERNATIONAL ELECTROTECHNICAL COMMISION. **IEC 60079-14 Electrical apparatus for explosive gas atmospheres – Part 14: Electrical installations in hazardous areas (other than mines).** Third edition. Geneva, 2002.

/40/ INTERNATIONAL ELECTROTECHNICAL COMMISION. **IEC 60947-4-1 – Low-voltage switchgear and controlgear – Part 4-1: Contactors and motor-starters – Electromechanical contactors and motor-startes.** Second edition. Geneva, 2000.

/41/ THE INSTITUTE OF ELECTRICAL AND ELECTRONICS ENGINEERS, INC. **ANSI/IEEE C37.96 American National Standard – guide for ac motor protection**. New York, 1988.

/42/ SIEMENS. **Manual de baja tension.** 2ª Edición. Amberg/Erlangen: Publicis MCD Verlag, 2000.

/43/ MOELLER. **Main Catalogue – Industrial Switchgear.** Bonn, 2001/2002.

/44/ SCHNEIDER ELECTRIC. **Konponenten der Steuerungs und Automatisierungstechnik.** Ratingen, April 1999.

/45/ SIEMENS. **Low-voltage controlgear, switchgear and systems – Catalog NS K . 2000.** Erlangen.

/46/ WEG. **Contatores e relés de sobrecarga (catálogo).** Jaraguá do Sul, 2004.

/47/ WEG. **Disjuntor motor MPW25 (catálogo).** Jaraguá do Sul, 2004.

/48/ ALLEN-BRADLEY. **Advantages of eutectic alloy overload relays.** Publication 592-2.4.1. Milwaukee, October 1989.

/49/ HEINRICH, S. **Conceptional design of a miniaturized electronic overload relay.** 2002. 119 p. Dissertation thesis (Diplomingenieur) – Fakultät Elektrotechnik, Technische Universität Dresden.

/50/ SIEMENS. **Sirius solid-state overload relays.** www.siemens.com

/51/TEXAS INSTRUMENTS. **Klixon Thermistors: 10BA Series.** At www.ti.com/snc/products/controls/motor-thermistor-10ba.htm

/52/TEXAS INSTRUMENTS. **Klixon 2AM, 3AM and 4AM series of ac on-winding motor protection.** At www.ti.com/snc/products/controls/motor-2am.html

/53/ PICO TECHNOLOGY LIMITED. **PT100 Platinum resistance thermometers.** At www.picotech.com/applications/pt100.html.

/54/ Texas Instruments. **Klixon Phenolic motor protectors.** At www.ti.com/snc/products/controls/motor-phenolics.html

/55/ GRÜTZMACHER, E. **Análise e modelamento de disparadores bimetálicos de sobre-carga de disjuntores-motores de baixa tensão.** 2003. 155 p. Master dissertation. Universidade Federal de Santa Catarina.

/56/ FRAULOB, S. ; SALMORIA, R. **Necessary measurements of bimetal systems.** 2000. Internal report for WEG.

/57/ FRAULOB, S. **Adjustment of thermal bimetal releases.** 2000. 111 p. Dissertation thesis (Diplomingenieur) – Fakultät Elektrotechnik, Technische Universität Dresden.

/58/ FRAULOB, S.; SCHULZE, L. **Bimetal system: relation between current and displacement.** 1998. Fakultät Elektrotechnik, Technische Universität Dresden.

/59/ VACUUMSCHMELZE GMBH. **Thermostat metal – Vacoflex®. Clickflex®.** Hanau, 1984.

/60/ BULTEN-KANTHAL AB. **The Kanthal thermostatic bimetal handbook.** 1975.

/61/ SHIVALIK BIMETAL CONTROLS LTD. **Shivalik thermostatic bimetals handbook.** New Delhi.

/62/ SIEMENS AG. Hartinger, P.; Scholle. F.; Wied, P. **Justierverfahren für thermische überlastauslöser.** Int. Cl. H01H71/74. DE 19619295 A1. May 13th 96, November 20th 97.

/63/ SIEMENS AKTIENGESELLSCHAFT. Flieder, F.; Hartinger, P.; Weidner, G. **Justierverfahren für thermische überlastauslöser.** Int. Cl. H01H71/74, H01H83/22. EP 0 833 357 A2. September 16th 97, April 1st 98.

/64/ WEG. **TOP - 413 Tratamento térmico de componentes de RW.** 7ª Edição. Jaraguá do Sul, 2003.

/65/ WEG. **TBG - 830 Avaliação da capacidade de processo.** 1ª Edição. Jaraguá do Sul, 2002.

/66/ MATTHES, E.; SCHULZE, L. **Method for design with pre-existing model.** Dresden, 1998.

APPENDICES

APPENDIX 1
SOME DEFINITIONS ACCORDING TO NEMA MG1 /13/

1 - Medium (integral) machine

Is a machine (a) where the centerline of shaft to bottom of feet ranges from 3.5" (88,9 mm) up to 17" (431,8 mm); i.e. frame size; and

(b) "having a continuous rating up to and including the information" below (table I):

TABLE I

Synchronous speed	Motor Hp
1201 - 3600	500 Hp
901-1200	350 Hp
21-900	250 Hp

Remark: The definitions for small and large machines will not be presented here. As a simplification, all machines smaller or larger than the above definition will be considered either a small or a large machine.

2 - Service factor (SF) – AC motors

"Is a multiplier which, when applied to the rated horsepower, indicates a permissible horsepower loading which may be carried under" specified conditions.

According to part 14.37: "When the voltage and frequency are maintained at the value specified on the nameplate, the motor may be overloaded up to the horsepower obtained by multiplying the rated horsepower by the service factor shown on the nameplate… A motor operating continuously at any service factor greater than 1 will have a reduced life expectancy compared to operating at its rated nameplate horsepower. Insulation life and bearing life are reduced by the service factor load."

Nema MG 1 is even more clear about life reduction at Section III – Large machines, part 20.7.3.2: "Operation at the temperature–rise values given…for a 1.15-service factor load causes the motor insulation to age thermally at approximately twice the rate that occurs at the temperature rise value given…for a motor with a 1.0 service-factor load;"
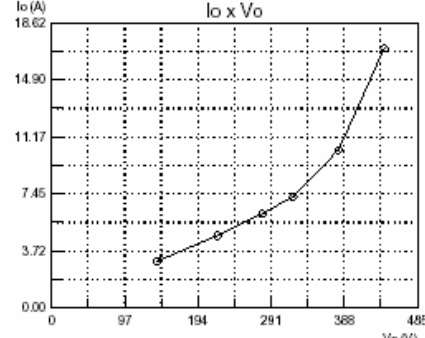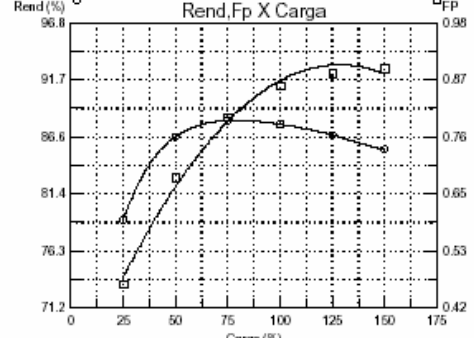
3 – Thermal protector

"A thermal protector is a protective device for assembly as an integral part of the machine and which, when properly applied, protects the machine against dangerous over-heating due to overload and, in a motor, failure to start.

Note – The thermal protector may consist of one or more temperature sensing elements integral with the machine and a control device external to the machine."

4 – Thermally protected

"The words "thermally protected" appearing on the nameplate of a motor indicate that the motor is provided with a thermal protector."

			N°: BG70604-1
WEG	**Comparativo de Valores de Ensaio** Motor de Indução Trifásico		Data: 05/04/2004

IDENTIFICAÇÃO

Potência: 15 cv	Pol: 4 polos	Tensão: 380 V
Frequência: 60 Hz	Rotação: 1755 rpm	Corrente: 22.8 A
Grau Proteção: IP55	Isolamento: B	FS: 1.15
Modelo: 132M 022003	Categoria: N	Item: 00410
Cod. Vendas: 1BTEIFIIXX01504OZ		
EB: 6991.6451	Dt. Ensaio: 10/02/2003	

		DIRETO	IEC	NEMA	D. Placa	TAB. VALORES
N O M I N A L	Ia (A) Pa (W) Cos Ø N (%) Pj1 (W) Pj2 (W) Ps (W) Ptot (W) RPM	22.28 12584.81 0.858 87.72 633.04 296.34 102.28 1544.90 1754	22.21 12541.20 0.858 88.03 630.20 295.01 62.71 1501.15 1754	22.28 12588.21 0.858 87.70 627.79 297.77 109.35 1548.15 1754	22.80 0.830 88.50 1755	22.75 0.830 88.50 1755
5 0 %	Ia (A) Cos Ø N (%) RPM	14.28 0.678 86.65 1778	14.30 0.678 86.46 1778	14.29 0.678 86.59 1778		0.680 86.80
7 5 %	Ia (A) Cos Ø N (%) RPM	17.94 0.796 88.07 1767	17.93 0.796 88.10 1767	17.94 0.797 88.01 1767	0.00	0.800 88.20
1 2 5 %	Ia (A) Cos Ø N (%) RPM	27.31 0.883 86.69 1740	27.14 0.883 87.27 1741	27.30 0.883 86.70 1740		

T E M P E R	Desv. I Max.(%) RPM Inicio RPM fim Rquente (20°C) T. Amb. DT. Mancal DT. Carc. DT. Bobina CTA	0.22 1763 1755 0.82661 27.20 -27.20 40.85 75.24 1.60	V A Z I O	U (V) I (A) Po (W) Pmec (W) Pfe (W) Cos Ø Pjo (W) Rfria (20°C)	380 10.28 650.93 116.32 396.92 0.096 137.69 0.64203	B L O Q	Pab (kW) kVA/cv Cp/Cn Cmax/Cn Ip/In Ip (A) R1 (Ohm) R2 (Ohm) X1+X2(Ohm)	66.20 7.68 2.28 3.04 7.68 175.05 0.850000 0.590262 0.959815

(Temp. rise of motor windings — DT. Bobina: 75.24)

Características do Ensaio	Gama : 0.9967	Correção do Dinamômetro : -0.002294

Io x Vo

Rend,Fp X Carga

PARECER TÉCNICO

Executado: Vanio Souza de Jesus	Verificado:

APPENDIX 3

		Nr.:
	WEG	Date: 27/3/2004 10:15:19

PERFORMANCE CURVES RELATED TO RATED OUTPUT
Three-phase Induction Motor - Squirrel Cage - Rotor de Gaiola (ING)
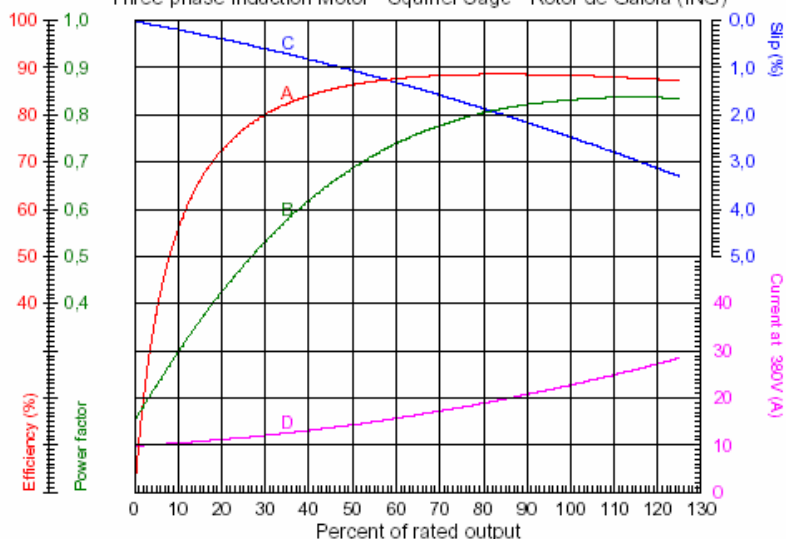
Customer	: WEG
Product line	: IP55 Motors

Output	: 11 kW	II/In	: 8,3
Frame	: 132M	Duty cycle	: S1
Rated speed	: 1755	Service factor	: 1,15
Frequency	: 60 Hz	Category	: ---
Rated voltage	: 380 V	Locked rotor torque	: 230 %
Insulation class	: F	Max torque	: 280 %
Rated current	: 22,8 A		

Optional:

Performance sheet obtained from www.weg.com.br; electronic data sheet.

Performer: STUART	Checked:

APPENDIX 4

SOME DEFINITIONS ACCORDING TO IEC 60034-11 /29/

1 – Built-in thermal protection

"The protection of certain parts of a rotating electrical machine against excessive temperature" is provided by a "thermally sensitive device incorporated within the machine."

2 – Thermal protection system

"A system intended to ensure the built-in thermal protection" either by means of a thermal detector or a thermal protector.

3 – Thermal detector

A device, "sensitive to temperature only, which will initiate a switching function in a control system when its temperature reaches a predetermined point."

4 – Thermal protector

A device, "sensitive to machine temperature and current, which carries the machine current, and which, when its temperature reaches a predetermined value, will switch off the supply to the machine."

5 – Thermal overload with slow variation

"The variation of the temperature of the protected part is sufficiently slow for the temperature of the thermal detector or protector to follow without appreciable delay."

This kind of overload may be caused by many reasons including "gradually increasing mechanical overloads."

APPENDIX 5

THERMAL TIME CONSTANTS FOR ELECTRIC MOTORS
(SOURCE:WEG MOTORES)

Motor Frame (According to IEC)	Thermal time constant for heating - t_h (in minutes)			
	2 poles	4 poles	6 poles	8 poles
63	9.36	12.96	14.47	
71	9.81	14.01	16.34	17.83
80	12.21	14.78	18.19	18.84
90	13.58	16.56	18.73	21.85
100	16.08	17.52	20.03	23.11
112	16.69	18.93	21.97	23.33
132	18.97	20.64	23.71	30.37
160	21.83	23.41	27.99	34.11
180	24.58	25.22	32.27	40.48
200	29.76	30.72	35.01	39.68
225	34.37	33.12	41.11	39.69
250	36.03	34.89	42.65	43.68
280	40.45	39.69	48.51	49.94
315	45.32	43.41	50.26	59.07
355	57.30	56.18	66.26	67.29

APPENDIX 6

Espessura : 1.10 +/-0.03 mm

42,8±0,1

41,4

(1,4)

0,2

R0,3 XXXX   XXXX   XXXX

0,2

1,4

3,2

R0,8

1,5

8

R1

3,4

45° X 0,7

Arestas sem rebarba

07

NOTA :

xxxx conforme tabela abaixo :

Dimensões a 20 °C

NOTA :

Tolerâncias gerais conforme norma ISO 2768
dimensionais grau m
forma e posição grau H

Faixa de corrente [A]	Código DIN 1715	Código VACOFLEX	Código SHIVALIK
0,10-0,16 a 4,0-6,3	TB 1577 A	2036	206-1
6,3-10 a 10-16	TB 1511	2036 S 11	206Cu11
16-20 a 20-25	---	- - -	721 Cu 5

Tabela 1

Consulte o programa de controle de documentos para obter a versão atualizada.

247	C3	Acrescentada nota sobre arestas sem rebarba	Ricardo	Pachtmann	Ivo	05/04/2004	07
169/03	Tabela 1	Adicionado códigos Shivalik faixas 11,10 a 16 A.	Rubens	Ricardo	Ivo	16/12/2003	06
RLM	LOC	RESUMO DAS MODIFICAÇÕES	EXECUTADO	VERIFICADO	LIBERADO	DATA	IND

EXECUTADO	Ridi	TRAT. :		PESO : 2,960 g	
VERIFICADO	Aleo	REVESTIMENTO:			
LIBERADO	Ivo				
DATA LIBER	12-Apr-01	MATERIAL : Especificado de acordo com a faixa de corrente (ver tabela 1)		ESC : 3:1	

Bimetal / MPW25

10.0301.07

WEG

Cópia impressa é considerada "CÓPIA NÃO CONTROLADA"

APPENDIX 7

Faixa de Corrente	Número de espiras	Passo [mm]	Dimensões do fio [mm]	Material	RESISTENCIA (conf. nota 1) Valor médio	Campo de tol.	Resistência [Ω/m] Tol. ± 4 %	Compactação [mm] Tol. ± 0.04
0,10 a 0,16	67	0.41	Ø 0.2	CrAl 22-24 5	42,98 Ω	41,26 - 44,70 Ω	33,42	2.9
0,16 a 0,25	51	0.61	Ø0.25	NiCr 70 30	17,7 Ω	16,9 - 18,4 Ω	23,99	3
0,25 a 0,40	46	0.90	Ø 0.4	CrAl 20 4	9,6 Ω	9,18 - 9,94 Ω	9.938	3.1
0,40 a 0,63	32	1.22	Ø 0.55	CrAl 20 4	3,80 Ω	3,62 - 3,92 Ω	5.290	3.5
0,63 a 1,00	22	1.55	Ø 0.7	CrAl 20 4	1,56 Ω	1,5 - 1,63 Ω	3.309	3.3
1,00 a 1,60	18	1.82	Ø 0.63	CuNi 44	614 mΩ	589,2 - 638,3 mΩ	1.620	3.2
1,60 a 2,5	8	4.33	Ø 0.75	CuNi 44	207,2 mΩ	198,9 - 215,5 mΩ	1.109	3.4
2,5 a 4,0	6	4.88	2.5 x 0.3	CuNi 44	88,14 mΩ	84,6 - 91,6 mΩ	0.650	3.2
4,0 a 6,3	7	4.10	3 x 0.75	CuNi 44	38,04 mΩ	36,5 - 39,6 mΩ	0.233	3.6
6,3 a 10	5	6.27	2.8 x 0.76	CuNi23Mn	18.8 mΩ	18,08 - 19,6 mΩ	0.149	3.65
10 a 16	7	6	3.29 X 0.87	CuNi 6	6,61 mΩ	6,34 - 6,87 mΩ	0.037	3.8
16 a 20	4	8	3.4 x 0.8	CuNi 2	1,85 mΩ	1,78 - 1,93 mΩ	0.0188	3.8
20 a 25	4	8	3.3 x 0.8	CuNi 1	1.31 mΩ	1,26 - 1,36 mΩ	0,00982	3.8

Nota 1:
Pontos de medição
(O bimetal já está
soldado com a base
e com o fio de
aquecimento)

Dimensões dos bimetais
conf. desenho n° 10.0301.##

Dimensões dos isolantes
conf. desenho n° 10.0304.##

Isolante usado para bimetais
bobinados com tiras de resistência
Faixas de 1,6...2,5 A até 20...25 A

Isolante usado para bimetais
bobinados com fio de resistência
Faixas de 0,1...0,16 A até 1,0...1,6 A

Região de solda

NOTA:
Estas vistas mostram a região onde
deve ser soldada a resistência de aquecimento

Especificação de bobinagem do fio de aquecimento / WMW25

	Atualizado valores de resistência (conf. nota 1)		Rubens	Ricardo	Ivo
			EXECUTADO	VERIFICADO	LIBERADO
PNP		RESUMO DAS MODIFICAÇÕES			
EXECUTADO	Ridi	TRATAMENTO:			
VERIFICADO		REVESTIMENTO:			
LIBERADO		MATERIAL : Conforme tabela acima			
DATA LIBER	18-Sep-03				

ESC. : 3:2

10.0303.11

APPENDIX 8

Curva Característica Tempo-Corrente do MPW25 Classe 10

Disjuntor Motor MPW25 Classe 10
Temp. Amb.: 20°C

A Curva Característica Tempo-Corrente foi determinada de acordo com a IEC 60947.
Esta Curva Característica Tempo-Corrente se aplica ao estado frio. Em temperatura normal de operação os tempos de atuação do disparador térmico são reduzidos para aproximadamente 25% do valor dado. Em condições normais, os três pólos devem ser carregados. Os três contatos principais devem ser ligados em série para carga CC ou monofásica.
As características do disparador eletromagnético de curto-circuito se aplicam para as frequências de 50/60Hz.
As características apresentadas são valores médios para o disjuntor-motor MPW25.

APPENDIX 9

	Relatório de Ensaio	N° .: 128/04
		Página:1 de 2
Produto:	**MPW25-10A**	Data: 05/07/2004

Objetivo:
Realizar ensaio para verificar a repetibilidade de corrente limite.

SOLICITANTE:	*Engenharia de Produtos*

AMOSTRAS		
DESCRIÇÃO	**ORIGEM**	**OBSERVAÇÕES**
MPW25-10A	*Expedição*	As amostras foram solicitadas na expedição para realização de ensaio.

" Os resultados deste relatório se referem somente as amost ras ensaiadas/analisadas".

" The test results refer about test samples ".

NORMAS		
NÚMERO	*REVISÃO*	*CAPÍTULO*
sem norma	-	-

Procedimentos de ensaio:

O ensaio consiste em aplicar múltiplos de corrente até o desarme do disjuntor. As amostras devem ser dispostas em posição de funcionamento, com os pólos alimentados em série junto com as demais amostras. Os múltiplos de corrente aumentam 3% x In a cada hora, até que a peça atue pelo térmico.

EQUIPAMENTOS / EQUIPAMENTS		
DESCRIÇÃO:	*CÓDIGO*	*Calibração:*
Fonte variável de corrente Multímetro Fluke 179 Alicate de Corrente 80i	21319 21132	10/2004 7/2004

CONCLUSÃO:
As amostras ensaiadas não apresentaram repetibilidade na corrente limite.

EXECUÇÃO:	*APROVAÇÃO / SOLICITAÇÃO:*
César Schaefer Laboratório P & D	*Reinaldo Stuart Jr* Gerente Dep. Técnico

"REPRODUÇÕES DESTE DOCUMENTO SÓ TEM VALIDADE SE FOREM INTEGRAIS."

"WEG, Transf ormando energia em soluções" - "WEG, Transforming solutions into energy"

APPENDIX 9
(Continuation)

![WEG logo] Transformando energia em soluções	Relatório de Ensaio		N° .: 128/04
			Página:2 de 2
Produto:	**MPW25-10A**		Data: 05/07/2004

1) Dados do ensaio:

	1ºILim	2ºILim	3ºILim	4ºILim	5ºILim	6ºILim	7ºILim	8ºILim
1	1,24	1,24	1,18	1,18	1,21	1,18	1,21	1,18
2	1,30	1,24	1,27	1,30	1,30	1,24	1,24	1,24
3	1,30	1,18	1,12	1,12	1,15	1,15	1,18	1,15
4	1,30	1,24	1,21	1,21	1,24	1,24	1,27	1,24
5	1,33	1,24	1,18	1,18	1,24	1,24	1,24	1,21
6	1,24	1,21	1,18	1,18	1,12	1,21	1,18	1,15
7	1,30	1,30	1,21	1,27	1,24	1,27	1,27	1,24
8	1,24	1,15	1,15	1,18	1,12	1,21	1,18	1,18
9	1,21	1,15	1,18	1,18	1,12	1,21	1,18	1,21
10	1,36	1,27	1,27	1,33	1,36	1,36	1,30	1,36
7,2 * In				3 X	3 X	3 X	3 X	
Data:	20/jun	21/jun	22/jun	23/jun	27/jun	28/jun	29/jun	30/jun

2)Corrente limite das amostras

	1º	2º	3º	4º	5º	6º	7º	8º
1	1,21	1,21	1,15	1,15	1,18	1,15	1,18	1,15
2	1,27	1,21	1,24	1,27	1,27	1,21	1,21	1,21
3	1,27	1,15	1,09	1,09	1,12	1,12	1,15	1,12
4	1,27	1,21	1,18	1,18	1,21	1,21	1,24	1,21
5	1,30	1,21	1,15	1,15	1,21	1,21	1,21	1,18
6	1,21	1,18	1,15	1,15	1,09	1,18	1,15	1,12
7	1,27	1,27	1,18	1,24	1,21	1,24	1,24	1,21
8	1,21	1,12	1,12	1,15	1,09	1,18	1,15	1,15
9	1,18	1,12	1,15	1,15	1,09	1,18	1,15	1,18
10	1,33	1,24	1,24	1,3	1,33	1,33	1,24	1,33
7,2 * In				3 X	3 X	3 X	3 X	
Data:	20/jun	21/jun	22/jun	23/jun	27/jun	28/jun	29/jun	30/jun

Obs.: Gráficos em anexo

APPENDIX 9
(Continuation)

Test report number 128/04 – Picture of test facility

APPENDIX 10

WEG	RELATÓRIO DE ENSAIO	No. 0
		Folha: 1 de 3
Produto:MPW25	Tipo:Conjunto termo magnético	Data emissão:17/09/04

OBJETIVO:A medição visa comparar a posição dos bimetais em relação a um ponto de referência antes e depois de um deflexão, simulada com uma célula de carga.

SOLICITANTE: Reinaldo Stuart Junior

AMOSTRAS

DESCRIÇÃO	ORIGEM	OBS.

" Os resultados deste relatório se referem somente as amostras ensaiadas/analisadas".

NORMAS

NÚMERO	REVISÃO	CAPÍTULO

ENSAIOS/ ANÁLISES PRELIMINARES

EQUIPAMENTOS/ INSTRUMENTOS UTILIZADOS

DESCRIÇÃO	CÓDIGO	VALIDADE DA CALIBRAÇÃO
MMC 3D MITUTOYO BRT - M507	3180	jul/05
Célula de Carga IMADA DPS-110R	9408	jul/05

CONCLUSÃO:

EXECUÇÃO	APROVAÇÃO
Deivt Tomaselli- Qualidade	Ridi Luiz Salmória - Chefe da Qualidade

"REPRODUÇÕES DESTE DOCUMENTO SÓ TEM VALIDADE SE FOREM INTEGRAIS."

"WEG, Transformando energia em soluções"

APPENDIX 10
(Continuation)

				No. 0
WEG	**RELATÓRIO DE ENSAIO**			Folha: 2 de 3
Produto:MPW25		Tipo:Conjunto termo magnético		Data emissão:17/09/04

RESULTADOS ENCONTRADOS

	Amostra 1			Amostra 2		
	bimetal 1	bimetal 2	bimetal 3	bimetal 1	bimetal 2	bimetal 3
Posição inicial (Pi)	39,22	24,76	10,38	39,95	24,88	10,29
Posiçao após F1,5N	39,20	24,75	10,37	39,94	24,86	10,29
Deslocamento da Pi	**0,02**	**0,01**	**0,01**	**0,01**	**0,02**	**0,00**
Posiçao após 1º F3,0N	39,20	24,74	10,37	39,93	24,86	10,28
Deslocamento da Pi	**0,02**	**0,02**	**0,01**	**0,02**	**0,03**	**0,01**
Posiçao após 2º F3,0N	39,19	24,74	10,36	39,93	24,85	10,27
Deslocamento da Pi	**0,03**	**0,02**	**0,02**	**0,02**	**0,03**	**0,02**
Posiçao após 3º F3,0N	39,19	24,74	10,36	39,93	24,86	10,27
Deslocamento da Pi	**0,03**	**0,03**	**0,02**	**0,02**	**0,03**	**0,02**
Posição após 1º F5,0N	39,18	24,72	10,35	39,90	24,85	10,27
Deslocamento da Pi	**0,04**	**0,04**	**0,03**	**0,04**	**0,03**	**0,03**
Posição após 2º F5,0N	39,17	24,61	10,35	39,90	24,82	10,25
Deslocamento da Pi	**0,05**	**0,16**	**0,03**	**0,05**	**0,06**	**0,04**
Posição após 3º F5,0N	39,16	24,72	10,35	39,90	24,82	10,26
Deslocamento da Pi	**0,06**	**0,05**	**0,03**	**0,05**	**0,06**	**0,04**

A posição dos bimetais é resulatado da média de cinco medições.

Deivt Tomaselli- Qualidade	Ridi Luiz Salmória - Chefe da Qualidade

"WEG, Transform ando energia em soluções"

APPENDIX 10
(Continuation)

![WEG] RELATÓRIO DE ENSAIO		No. 0
		Folha: 3 de 3
Produto:MPW25	Tipo:Conjunto termo magnético	Data emissão:17/09/04

ANEXO 1 - ESQUEMA DE MEDIÇÃO

Deivt Tomaselli- Qualidade	Ridi Luiz Salmória - Chefe da Qualidade

"REPRODUÇÕES DESTE DOCUMENTO SÓ TEM VALIDADE SE FOREM INTEGRAIS."

"WEG, Transformando energia em soluções"

APPENDIX 11

APPENDIX 12

ШЕО		**RELATÓRIO METROLÓGICO**				N°: 231		
						Item: 10.0104		

Descrição: ATUADORES DESLIZANTES DIFERENCIAIS /MPW25   Data: 03/07/02

Material: Código: Utilização: MPW 25 Folha: 01/02

Ferramenta: N° Cavidades: 01 Fornecedor: Revisão: 00
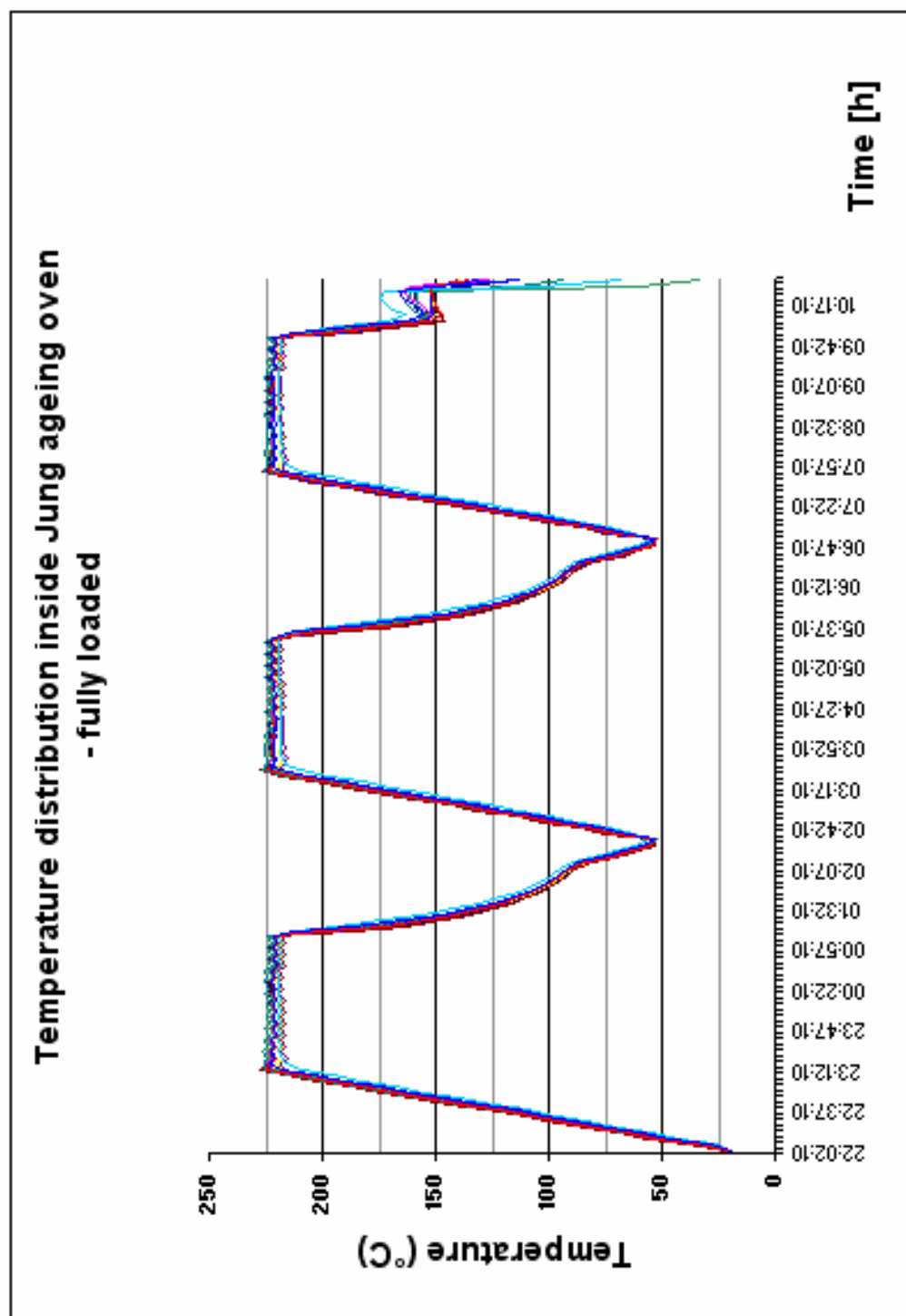
Seq.	Quadr.	Especificado	Valor encontrado por peça/cavidade 1					CQ C	CQ NC	Solcit. A	Solcit. R
1		4 ± 0,1	4,07					X			
2		32 ± 0,1	32,01					X			
3		1	1,02					X			
4		2,5	2,53					X			
5		1,9	1,96					X			
6		32,5 ± 0,1	32,54					X			
7		15,2	15,24					X			
8		25,9	25,93					X			
9		21,7	21,68					X			
10		17,1	17,15					X			
11		12	11,98					X			
12		7,7	7,62					X			
13		3	3,07					X			
14		8,3	8,16					X			
15		1,4	1,45					X			
16		3,7	3,66					X			
17		3,7	3,70						X		
18		1,2 ± 0,05	1,12						X		
19		120°	120					X			
20		R1	1,00					X			
21		0,5	0,50					X			
22		1,8	1,88					X			
23		Ø 1,2 ± 0,05	1,18					X			
24		3,1	3,14					X			
25		2,6	2,53					X			
26		5,9	5,86					X			
27		8,3	8,18					X			
28		16,8	16,73					X			

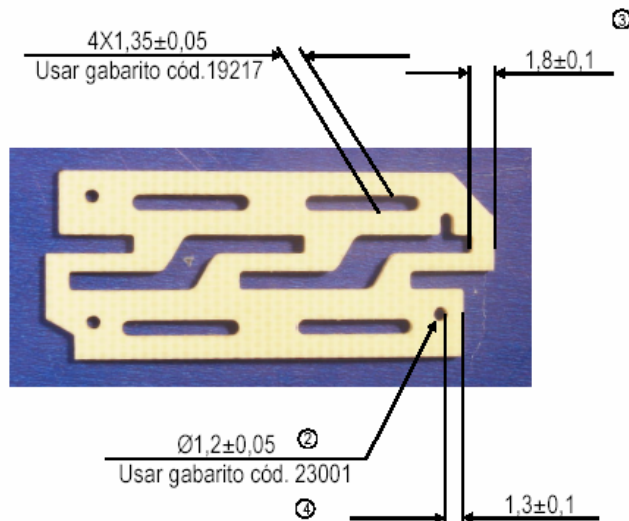| Seção da Qualidade		Laudo do Solicitante		Aprovado:	X
Executante: Matias P.S.		Nome: Jose A. Sç: Qualidade		Reprovado:	
Data: 03/07/02 Visto:		Data: 4/7/2 Visto:			

MOD. 0630-1
Rev. 12/99

"TRANSFORMANDO ENERGIA EM SOLUÇÕES".

APPENDIX 13

Verificar 1 peça a cada 400 golpes
Rebarba máxima 0,08mm

Esta peça deve ser liberada pelo Controle de Qualidade
1,8±0,1 e 1,3±0,1 medir no microscópio

③

4X1,35±0,05
Usar gabarito cód.19217

1,8±0,1

Ø1,2±0,05 ②
Usar gabarito cód. 23001

④

1,3±0,1

10.0104

	1. Manchas		5. Empenamento		9. Sujeira		1. Aceitável conforme plano
	2. Quebras		6. Linha de fluxo		10. Peças Misturadas		2. Não afeta a qualidade do produto
	3. Deformações		7. Queima		11. Falhas de injeção		3. Afeta a qualidade do produto
	4. Rebarbas		8. Rechupe		12. Trincas		obs: Aceitar c/ 0 defeito / Rejeitar c/ 1 defeito

Liber.	José	05/04/02	Alterado código do calibrador / Era 19216	14/09/04		4
Verif.	Irineu	05/04/02	Acrescentada cota 1,8±0,1	14/11/02	José	3
			Acrescentado gabarito	16/09/02	José	2
			Criação do Plano	05/04/02	José	1
		Data	Resumo das modificações	Data	Liberação	

| Esc. | Descrição: Atuadores deslizantes diferenciais / MPW 25 | |
| % | Código do Item: 6700.0274 | |

Plano de Controle

Código: 4082.0432

APPENDIX 14

⊞⊟⊟	Test report	Nr.
		Page: 01 of 04
Product: Lock mechanism	Type:MPW25	Date of issue:Sep 24, 04

OBJECTIVE: Measurement of lock mechanism repeatability.

SAMPLES

DESCRIPTION	Source	OBS.
Lock mechanism employed at MPW25	Assembly line	3 samples

Standard

Number	REVISION	CHAPTER

PRELIMINARY ANALYSIS

EQUIPMENT/ USED INSTRUMENTS

DESCRIPTION	CODE	VALIDITY OF THE CALIBRATION
Dynamomerter	9408	july/2005
Digital scale	9406	july/2005
Automatic measuring device available at assembly line	-	-

CONCLUSION:

Test inspector	APPROVAL
Deivt Tomaselli- Quality	Ridi Luiz Salmória - Head of the Quality

"W EG, Transforming energy into solutions "

APPENDIX 14
(Continuation)

ꟻ WEG	Test report		Nr.
			Page: 02 of 04
Product: Lock mechanism		Type:MPW25	Date of issue:Sep 24, 04

1 - Measurement with Automatic device						
Sample	1		2		3	
Measurement	Travel	Force	Travel	Force	Travel	Force
1	0.35	1.06	0.40	1.23	0.48	0.88
2	0.34	1.05	0.40	1.08	0.47	0.86
3	0.37	1.00	0.37	1.02	0.47	0.86
4	0.36	1.03	0.39	1.02	0.47	0.85
5	0.35	1.06	0.41	0.95	0.44	0.86
Average(mm)	0.35	1.04	0.39	1.06	0.47	0.86
Minimum value	0.34	1.00	0.37	0.95	0.44	0.85
Maximum value	0.37	1.06	0.41	1.23	0.48	0.88
Maximum deviation from average value(%)	5.7	3.8	5.1	16.0	6.4	2.3

Tolerances Force = $0,95^{\pm0,35}$ N

Travel = $0,6^{\pm0,2}$ mm

Conclusions: a) Travel: samples 1 and 2 do not operated according to design parameters.
b) Force: all tested samples operated according to design parameters;
sample 2 showed a lower repeatability when compared to the other samples.

2 - Manual measurement - lock mechanism in MPW25 housing						
Sample	1		2		3	
Measurement	Travel	Force	Travel	Force	Travel	Force
1	0.50	1.04	0.55	0.82	0.61	0.85
2	0.51	1.09	0.48	0.98	0.56	0.80
3	0.51	0.99	0.57	0.86	0.56	0.78
4	0.51	0.97	0.48	1.10	0.58	0.83
5	0.50	1.03	0.55	0.85	0.54	0.86
Average(mm)	0.51	1.02	0.53	0.92	0.57	0.82
Minimum value	0.50	0.97	0.48	0.82	0.54	0.78
Maximum value	0.51	1.09	0.57	1.10	0.61	0.86
Maximum deviation from average value(%)	1.9	6.9	9.4	19.6	7.0	4.9

Force = $0,95^{\pm0,35}$ N

Tolerance Travel = $0,6^{\pm0,2}$ mm

Conclusions: samples 1,2 and 3 operated according to design parameters after they were
assembled in their corresponding housings.

"REPRODUCTIONS OF THIS DOCUMENT ALONE HAVE VALIDITY WILL BE INTEGRAL."

"WEG, Transformi ng energy into solutions "

158

APPENDIX 14
(Continuation)

WEG	Test report		Nr.
			Page: 03 of 04
Product: lock mechanism		Type:MPW25	Date of issue:Sep 24, 04

3 - Manual measurement -
lock mechanism in MPW25 housing and base assembly

Sample	1		2		3	
Measurement	Travel	Force	Travel	Force	Travel	Force
1	0.74	0.72	0.61	0.73	0.66	0.72
2	0.74	0.71	0.60	0.74	0.63	0.72
3	0.74	0.69	0.62	0.67	0.61	0.74
4	0.73	0.71	0.62	0.69	0.62	0.70
5	0.74	0.70	0.63	0.71	0.60	0.74
Average(mm)	0.74	0.70	0.62	0.71	0.62	0.72
Minimum value	0.73	0.69	0.60	0.67	0.60	0.70
Maximum value	0.74	0.72	0.63	0.74	0.66	0.74
Maximum deviation from average value(%)	1.3	2.8	3.2	5.6	6.4	2.8

Force = $0,95^{\pm0,35}$N
Tolerance Travel = $0,6^{\pm0,2}$mm

Conclusions: a) samples 1,2 and 3 operated according to design parameters after they were
assembled in their corresponding housings and base assemblies.
b) Samples presented a significant improvement on tripping repeatability under
this assembly condition.

4 - Manual measurement at the compensation bimetal - lock mechanism in
MPW25 housing and base assembly

Sample	1		2		3	
Measurement	Travel	Force	Travel	Force	Travel	Force
1	1.08	0.54	1.03	0.53	0.95	0.64
2	1.06	0.60	1.02	0.54	0.94	0.61
3	1.10	0.51	1.02	0.52	1.00	0.66
4	1.16	0.53	1.07	0.48	0.93	0.61
5	1.11	0.56	1.01	0.51	0.91	0.66
Average(mm)	1.10	0.55	1.03	0.51	0.95	0.64
Minimum value	1.06	0.51	1.01	0.48	0.91	0.61
Maximum value	1.16	0.60	1.07	0.54	1.00	0.66
Maximum deviation from average value(%)	5.4	9.1	3.9	5.9	5.3	4.7

Conclusions: tested samples pr esented a high tripping repeatability when completely
assembled and operated via the compensation bimetal.

"REPRODUÇÕES DESTE DOCUMENTO SÓ TEM VALIDADE SE FOREM INTEGRAIS."
"WEG, T ransforming energy into solutions "

**APPENDIX 14
(Continuation)**

![WEG]	Test report	Nr.
		Page: 04 of 04
Product: Lock mechanism	Type:MPW25	Date of issue:Sep 24, 04

Automatic equipment available at the assembly line

Equipment for manual measurement

"REPRODUÇÕES DESTE DOCUMENTO SÓ TEM VALIDADE SE FOREM INTEGRAIS."

"WEG, Tr ansforming energy into solutions "

Livros Grátis

(http://www.livrosgratis.com.br)

Milhares de Livros para Download:

Baixar livros de Administração
Baixar livros de Agronomia
Baixar livros de Arquitetura
Baixar livros de Artes
Baixar livros de Astronomia
Baixar livros de Biologia Geral
Baixar livros de Ciência da Computação
Baixar livros de Ciência da Informação
Baixar livros de Ciência Política
Baixar livros de Ciências da Saúde
Baixar livros de Comunicação
Baixar livros do Conselho Nacional de Educação - CNE
Baixar livros de Defesa civil
Baixar livros de Direito
Baixar livros de Direitos humanos
Baixar livros de Economia
Baixar livros de Economia Doméstica
Baixar livros de Educação
Baixar livros de Educação - Trânsito
Baixar livros de Educação Física
Baixar livros de Engenharia Aeroespacial
Baixar livros de Farmácia
Baixar livros de Filosofia
Baixar livros de Física
Baixar livros de Geociências
Baixar livros de Geografia
Baixar livros de História
Baixar livros de Línguas